2015

DUNE AND COASTAL EVOLUTION IN ISLA SALAMANCA NATIONAL PARK, COLOMBIA

Juan Felipe Gómez
Student, gome7540@mylaurier.ca

DUNE AND COASTAL EVOLUTION IN ISLA SALAMANCA NATIONAL PARK, COLOMBIA

by

Juan Felipe Gómez Velásquez
Bachelor of Science-Geology**,** Universidad Nacional de Colombia

THESIS
Submitted to the Faculty of Arts/Department of Geography and Environmental Studies
in partial fulfillment of the requirements for
Degree of Master of Science

Wilfrid Laurier University
Winter 2015

ABSTRACT

This project analyzes natural variables influencing the coastal and dune evolution in Isla Salamanca National Park (ISNP), a biosphere reserve and Ramsar site located in Colombia, on the Caribbean coast. Since at least the early 1950s, the park has been affected by eroding trends along most of the shoreline. Particularly, most modern dunes are located close to the coastline, forming scarped dunes regularly affected by storm wave-action.

The trends through time of rain, bathymetry and coastline changes during the last six decades were studied through statistical analysis, mapping of landscape features, and satellite images and historical aerial photograph interpretation. Once these trends were identified, six vegetation transects were developed over dunes located in areas under contrasting morphodynamic regimes: moderate erosion rates (east area), high erosion rates (central area), and accretion (west area).

The findings of this work indicate that those dunes located at the east extreme and central areas of ISNP are scarped and impeded dunes fixed in position by an abundant vegetation cover. In contrast, mobile embryo dunes, either without vegetation or covered only by vegetation species that can thrive under sand burial, are common at the west end of the study site, a sector where accretive processes have been occurring over the last six decades. This findings contribute to understanding the morphodynamics producing the accelerated coastal retreat taking place in ISNP, thereby providing useful data to support sound decisions for the management of the coastal zone in this National Park.

Acknowledgements

This project was conducted with the support of many colleagues and friends, both in Canada and Colombia. In the following pages, I will do my best to acknowledge most, if not all, of them.

Since the very beginning, even before becoming a grad student at Wilfrid Laurier University, Dr. Mary-Louise Byrne has encouraged me to translate my initial ideas into the actual project that became this thesis. I deeply appreciate all her support and encouragement in helping move my work and ideas forward.

I would also like to express my gratitude to my other committee member, Dr. James Hamilton, for his receptiveness to my questions about tropical landscapes, advice and guidance along this project.

Although the thesis has drifted into other topics, the starting ideas and suggestions came from Colombian geologists Blanca Oliva Posada and José Henry Carvajal, who were interested in standardizing a methodology and a legend for mapping coastal landforms in the Colombian Caribbean. I extend my gratitude to them and to all the geologists who worked with me in Invemar from 2010-2011. Somehow, all your advice and cheerfulness are included here. Special thanks to Willian Henao, who dealt with all the bureaucracy in Colombia to obtain aerial photographs for this study.

Since we met as undergraduate students in Medellín, my wife, Luisa Fernanda Ramírez, has been a source of inspiration and motivation for projects in both academia and life. During the field work for this thesis, I could not have asked for better company. A tireless field assistant,

she withstood the high temperatures and thorny vegetation of Isla Salamanca, patiently collecting and classifying plant species across the dunes. This work is hers, too. Thanks for always being there, *caramelo escaso*.

I have been very fortunate to meet Dr. Robin Davidson-Arnott, Professor Emeritus, Department of Geography, University of Guelph. In the last few years, he gave not only meaningful advice to improve my work but also his friendship, which is even more valuable.

In the midst of globalization and competitiveness, working on environmental issues can seem quixotic. However, the existence of organizations such as Rufford, dedicated to supporting research for nature conservation projects in the developing world, is encouraging. I am deeply grateful for the funding I received from Rufford Foundation; without their support my field work, which is one of the main components of this research, would not have been possible. Also, the Geoeye Foundation generously provided recent high resolution satellite images from the study site, which were very useful for analyzing coastal and landforms patterns.

Evaristo Rada, a resident of Tasajera, took a break from his daily job selling sodas in a booth near the study site to join our field activities. I appreciate that his positive attitude and permanent enthusiasm were contagious.

As a student of the joint program in Geography, I was an assiduous visitor of the writing centers at Wilfrid Laurier University and University of Waterloo. In particular, I had many appointments with Mary Janet McPherson and Jane Russwurm, attentive listeners who helped me find the proper words and grammar to polish my manuscript. Through reading the drafts

together, we were able to walk around Isla Salamanca a few times. Thank you both for improving this work and for your positive energy.

At Wilfrid Laurier, I want to extend my gratitude to Grant Simpson, Jo-Anne Horton, and Pam Schaus, who were always keen to assist when required.

After reading the proposal, University of Waterloo PhD candidate Cristóbal Pizarro, shed light on the importance of including the surrounding communities of the study site. I appreciate the time that he took to read and make suggestions during the initial phase of this work.

I would also like to thank PhD candidate Heidi Karst, engineer Julio Bohórquez,geologist David Morales, and José Ortiz for their professional assistance. Thanks also to Alvaro Cogollo, who aided in plant identification.

I cannot end without mentioning how grateful I am for having such a wonderful and loving family in Colombia. From my inner circle, my mom, Luz Helena, my sister, Diana, and my aunts, Melva and Amparo, have permanently provided support.

To my parents,

who showed me the Caribbean Sea and Isla Salamanca for the first time.

TABLE OF CONTENTS

Chapter 1 Introduction 1

1.1 Objectives 3

1.2 SITE DESCRIPTION 5

1.2.1 Climate 13

1.2.1.1 Precipitation 14

1.2.1.2 Wind 15

1.2.2 Oceanography Parameters 17

1.2.2.1 Tides 17

1.2.2.2 Waves and Littoral Drift 17

1.2.2.3 Sea Level Changes in the Holocene 18

1.2.3 Geologic context 21

1.2.4 Vegetation 25

Chapter 2 Methods 28

2.1 CLIMATE 29

2.2 COAStline CHANGES 31

2.3 BATHYMETRY 34

2.4 DUNE PROFILES AND VEGETATION SURVEYS 37

2.5 GEOMORPHOLOGY 40

Chapter 3 Results 43

3.1 Climate 43
3.1.1 Annual Precipitation 43
3.1.2 Wind 47
3.2 coastline changes 50
3.2.1 Coastlines Error Assessment 52
3.3 BATHYMETRY CHANGES 55
3.3.1 Error Assessment 56
3.3.2 Bathymetry Changes Assessment 57
3.4 DUNE EVOLUTION 61
3.4.1 Vegetation on Surveyed Dunes 63
3.5 GEOMORPHOLOGY 69
3.5.1 Mapping Landscapes/Geomorphology Map 70
3.5.1.1 Beaches 72
3.5.1.2 Lagoons 74
3.5.1.3 Floodplains 77
3.5.1.4 Salt flats 78
3.5.1.5 Beach Ridge Plains 78
3.5.1.6 Dunes 79
Chapter 4 Discussion 82
4.1 Coastline and Bathymetry changes 83

4.2 VEGETATION on dunes 88

4.3 GEOMORPHOLOGY 93

4.4 final Discussion 97

Chapter 5 Conclusions 101

Chapter 6 Recommendations 104

Chapter 7 References 113

LIST OF TABLES

Table 1. Summary statistics for a regression analysis of the relationship between mean annual precipitation and time for the weather station at Santa Marta 44

Table 2. Summary statistics for a regression analysis of the relationship between annual precipitation and time for the weather station at Barranquilla 44

Table 3. Summary statistics to test for normality of annual precipitation for the weather stations at Santa Marta and Barranquilla. 45

Table 4. Test results for the original and modified Mann-Kendall tests to assess data correlation 46

Table 5. Summary statistics for a regression analysis of the relationship between wind velocity and time for the weather station at Santa Marta 48

Table 6. Summary statistics to test for normality of wind data taken in Santa Marta. 49

Table 7. Test results for the original and modified Mann-Kendall tests to assess wind data correlation 49

Table 8. Location of surveyed dunes 52

Table 9. Parameters used in the determination of uncertainty for a HWL proxy 52

Table 10. Parameters for spherical and Gaussian models 55

Table 11. Comparison of the outcomes for the spherical and Gaussian semivariograms ..... interpolation models after deleting known deep values from the 2012 survey 56

Table 12. Matrix of Sørensen similarity index and Diversity Index (Italic) 69

LIST OF FIGURES

Figure 1. Area of study along the shoreline of Isla Salamanca National Park.....8

Figure 2. Bathymetry map published in 1944 9

Figure 3. Mouth of the Magdalena River and study site as pictured in map published in 1803.....10

Figure 4. Mouth of the Magdalena River and study site as pictured in a map from 1817..... 10

Figure 5. Shore protection measures installed at the 20th km. 12

Figure 6. Average monthly rainfall between 1965-2012. 15

Figure 7. Wind rose made for data taken hourly at Santa Marta airport..... 16

Figure 8. Schematic diagram showing barrier island evolution. 19

Figure 9. Tectonic setting of Colombia 23

Figure 10. Geological units in the surrounding area of the study site..... 25

Figure 11. Interlinked variables analyzed for the study site 28

Figure 12. Empirical semivariogram resulting from the 1938 depth contours map. 37

Figure 13. 1 m² quadrat to identify and quantify vegetation and topographic profile 39

Figure 14. Representation of space and time scales phenomena in coastal systems 41

Figure 15. Yearly total rainfall at Santa Marta and Barranquilla. 47

Figure 16. Variability of the yearly SOI index for the period 1951-2012. 47

Figure 17. Wind events of over 6 m/s from 1981 to 2012 48

Figure 18. Coastline position changes along Isla Salamanca since the early 1950s. 54

Figure 19. Assessment of bathymetric changes between 1938 and 2012 59

Figure 20. Bathymetric contours from the 20th km to the Magdalena River 60

Figure 21. Stabilized dunes at the 20th km and overwash channels direction.....63

Figure 22. Dunes where topographic profiles and vegetation transects were made. 64

Figure 23. Vegetation cover per m^2 (%) along Dune 1 65

Figure 24. Vegetation cover per m^2 (%) along Dune 2 65

Figure 25. Vegetation cover per m^2 (%) along Dune 3 66

Figure 26. Vegetation cover per m^2 (%) along Dune 4 66

Figure 27. Vegetation cover (%) per m^2 along Dune 5 67

Figure 28. Vegetation cover (%) per m^2 along Dune 6 67

Figure 29. Nested hierarchic sequence of landforms 71

Figure 30. Washover fans as observed West of Dune 4..... 73

Figure 31. Oblique aerial views of El Torno Lagoon..... 76

Figure 32. Spit on the west side of the former inlet of the Ciénaga Grande de Santa Marta as pictured on aerial photograph taken in 1953.....77

Figure 33. Geomorphology Map 81

Abbreviations

AOR	Average of Rates
APSL	Above Present Sea Level
BP	Before Present (where present is 1950 AD)
CGSM	Ciénaga Grande de Santa Marta
DSAS	Digital Shoreline Analysis System
ENSO	El Niño-Southern Oscillation
EPR	End Point Rates
HWL	High Water Line
IDEAM	Instituto de Hidrología, Meteorología y Estudios Ambientales de Colombia
IGAC	Instituto Geográfico Agustín Codazzi
IHO	International Hydrographic Organization
IPCC	Intergovernmental Panel on Climate Change
ISNP	Isla Salamanca National Park
ITCZ	Inter-tropical Convergence Zone
ka	kilo anna (thousands of years)
LIA	Little Ice Age
m	metre
Ma	mega anna (millions of years)
NOAA	National Oceanographic and Atmospheric Administration
RFS	Romeral Fault System
RMSE	Root Mean Square Error
SLR	Sea Level Rise

SMBF	Santa Marta Bucaramanga Fault
SNSM	Sierra Nevada de Santa Marta
USGS	United States Geological Survey

Chapter 1 Introduction

Coastal areas are one of the most highly dynamic environments in nature. Changes to the coastal zone may be either due to clearly defined cycles such as seasons or tides, with fairly predictable results, or due to phenomena with less regular periodicity like earthquakes, hurricanes or storms. To add to the variety of natural forces affecting coastal dynamics, human-induced modifications to the coastal system may trigger drastic changes in short time periods. Therefore, understanding the present coastal configuration requires recognizing that different processes within coastal systems operate at different time scales (Murray-Wallace and Woodroffe, 2014). Ideally, short-term (days, seasons, years), intermediate-term (decades, half centuries) and long-term (centuries, millennia) morphological changes must be considered to interpret current coastal configurations as well as the interplay between erosive and depositional processes.

Pilkey and Cooper (2004) observed that most of the coastlines in the world are in a state of erosion with more than 70% of beach-fringed shorelines around the world having a recessional trend (Bird, 1985). There is growing consensus about global warming, which is expected to produce a global sea-level rise as result from sea-water expansion and accelerated melting of land-based ice (Murray-Wallace and Woodroffe, 2014). Under this climate change scenario where even the most conservative projections published developed by the Intergovernmental Panel on Climate Change (IPCC) forecast a sea level rise ranging between

0.28 to 0.61 m (Church et al., 2013), or of about 0.8 m (Pfeffer et al., 2008) by 2100, further coastal retreat worldwide is expected in the intermediate-term.

Adding to global warming, other factors locally influencing current coastline retreating trends are subsidence (Milliman and Haq, 1996), either landward or seaward from the coastline, and sediment starvation of the coastal zone as consequence of human practices including but not limited to damming or altering river channels, and sand mining in streambeds. In general, any engineering structure trapping the sediment that otherwise would be delivered to the coast is detrimental for the coastal system. Therefore, understanding the factors driving past and present day coastal changes in order to decipher the history of coastal evolution is of paramount importance to effectively manage coastal areas.

Notwithstanding the existing variety of potential causes associated with worldwide erosive coastal processes, discerning and weighting the influence of each factor affecting a specific area is not straightforward. For instance, even though it has been recognized that current coastal erosion processes worldwide are somewhat driven by global warming and rising sea levels (Zhang et al., 2004), it is not always possible to isolate the impact of Sea Level Rise (SLR) on shoreline retreat (Pilkey and Cooper, 2004). Nonetheless, there are strong signs that about one hundred years ago a global sea level rise began anew, likely as an early response to global warming (Pilkey and Fraser, 2003); thus, both eustatic changes−that is, global changes in the absolute water-surface levels (Pethick, 1988)−and local SLR are recognized as important agents in coastal erosion, especially on coastal plains at low elevation (Pilkey and Cooper, 2004).

The Colombian Caribbean coast has not been an exception to the worldwide coastal retreat phenomenon, resulting in drastic changes in most of its coastlines over the last decades as

a result of the combined effect of anthropogenic and climate elements (Correa et al., 2005). The present research, located in Isla Salamanca National Park (ISNP or the park hereafter), Colombia, examines an example of landscape changes resulting from anthropogenic and natural disturbances that are commonplace on the Colombian Caribbean. Even though the study site is protected by government regulations established for National Natural Parks, the once pristine ecosystem has been modified by human activities carried out in the vicinity, such as dredging to facilitate harbor operations, modifications to river channels, and building roads and causeways. In this regard, while coastal erosion is far from being a new phenomenon in the area, having been documented since the early 1970s (von Erffa, 1972), until now, no study has focused on the effect of coastal erosion and evolution on the discontinuous fringe of dunes existing landward from the modern shoreline.

Despite the obvious interactions between beaches and dunes, they are in fact quite distinct ecosystems, the beach/surf zone being marine wave-driven, whereas the dunes are terrestrial wind-controlled (McLachlan and Brown, 2006). In addition to the unique vegetation and fauna of the dunes themselves, a well-developed dune ridge on the modern coast is important for protecting wetlands and buffering the effects of beach erosion during storms (Nordstrom, 2008). Hence, understanding dune evolution as well as the variables that affect dune movement are essential to developing a management plan for protecting and somewhat restoring not only the dunes themselves, but also the habitats of the hinterland zones.

1.1 OBJECTIVES

Characterizing dunes, beaches, and vegetation within the park and explaining their evolution requires consideration of the interplay between the variables that act in the coastal

zone, notably the rates of shoreline change, longshore sand transport, and the effects of changes in the wind and precipitation regime. Accordingly, the specific objectives associated with this aim are:

a) To quantify shoreline change from 1953 to 2013 and its relation to dune movement.

b) To assess changes in the nearshore bathymetry based on a comparison of two historical bathymetric charts published in 1944 and 2012.

c) To determine historical changes in the wind and precipitation regime, if any, that might affect coastal dune dynamics.

d) To characterize the form and vegetation patterns for at least three coastal dunes under different morphodynamic environments within the park.

f) To analyze the rates of movement for certain coastal dunes.

g) To point out strategies to somewhat restore the dune-beach system.

Overall, this project looks at understanding the recent coastal evolution of Isla Salamanca in order to provide a detailed analysis of the study area that will enable policy makers to make informed decisions when designing future managing plans. Yet, the recommendations of this work are meaningful for other areas on the Colombian Caribbean coast affected by similar processes to those taking place in ISNP.

This thesis is organized into six chapters. The present chapter, in addition to the objectives, provides background for the research, including a description of the study site and its physical setting. Chapter two describes the methods for data collection and processing involved

in this research. It is divided between office work and field work, the former focusing on aerial photographs and satellite imagery processing to evaluate coastal and geomorphology changes, and the latter on describing the beach transects that were collected during the field trips. Chapter three, the results section, assesses the coastal and bathymetry changes over time, and compares the vegetation associated with some of the local dunes. In addition there is a trend analysis for the variability of rain and wind. Finally, within Chapter three, there is an analysis of different approaches for mapping landforms and the proposed hierarchy mapping systems as they relate to the coastal geomorphology of the study site. Chapter four contrasts previous research work with findings from this project, and ends with a discussion of dune evolution and vegetation cover. Finally, Chapters five and six provide conclusions and recommendations so that management strategies and best practices to protect the beach-dune system and nearby habitats may be defined.

1.2 SITE DESCRIPTION

The study site, known as Isla de Salamanca, belongs to the National Park system of Colombia. Specifically, the study site extends 60 km along the shoreline eastward from the Magdalena River mouth, bordered on the north by the Caribbean Sea, while its southern border, on the coastal hinterland, is defined by a system of lagoons and wetlands that are crossed by a highway built in the 1950s. This road connects the nearby cities of Barranquilla to the west and Santa Marta to the east (Figure 1).

Given the fauna, flora, the importance of the area for both resident and migratory birds, and unusual scenic features (lagoons, dunes, mangroves), the site together with the surrounding

wetlands, was originally declared a National Park, called the Isla Salamanca Road Park, in 1965. It was later also designated a Ramsar site and Biosphere Reserve, in 1998 and 2000, respectively.

The Magdalena River, the largest fluvial system in Colombia, has had a strong influence on the landscape in the study site. During the colonial times[1] the first large human-made modification to this area took place. An artificial channel about 117 km long was built in an abandoned river mouth (Alvarado, 2005) in order to link the inland territories with the city of Cartagena (located 100 km southwest of Barranquilla). This channel, named *Canal del Dique*, was finished in 1650 (some modifications were completed afterwards), and since then it has been flowing into the Cartagena Bay.

Later, channel modification activities associated with the port facilities development at the Magdalena River mouth began in 1925 (Rico, 1967) and included building two levees along each side of the river that confined the fluvial system to the river channel. These activities have altered the otherwise natural distribution of sediment. Load measurements between 1972 and 1998 taken in the most downstream station located before the Magdalena River flows into the Caribbean (Calamar station), yielded an annual sediment load of 144×10^6 t/yr (Restrepo et al., 2006; Restrepo and López, 2008), and a specific sediment load upstream of Calamar of 559 $t/km^2/yr$, representing the highest sediment load along the Caribbean and Atlantic coast of South America (Restrepo and Kjerfve, 2000).

Currently, the delta mouth ends in an offshore canyon with a steep slope, having an axis with an average gradient of about 40 m/km. Since these canyons (also called valleys) extend to

[1] The area of Santa Marta was settled by the Spaniards from 1526 on, gradually replacing the indigenous population, which was destroyed by 1600 (Wiedemann, 1973).

the base of the slope (Shepard and Dill, 1966), most of the Magdalena sediments are being delivered through these canyons over the continental slope, beyond the continental shelf (Restrepo and López, 2008). On a regional scale, bathymetric charts released by the Colombian and the United Kingdom's Royal Navy (Figure 2), indicate that the platform becomes wider east from the Magdalena River mouth, an area that was directly supplied with sediment by a former Magdalena River mouth that lasted until the 1920s (von Erffa, 1972).

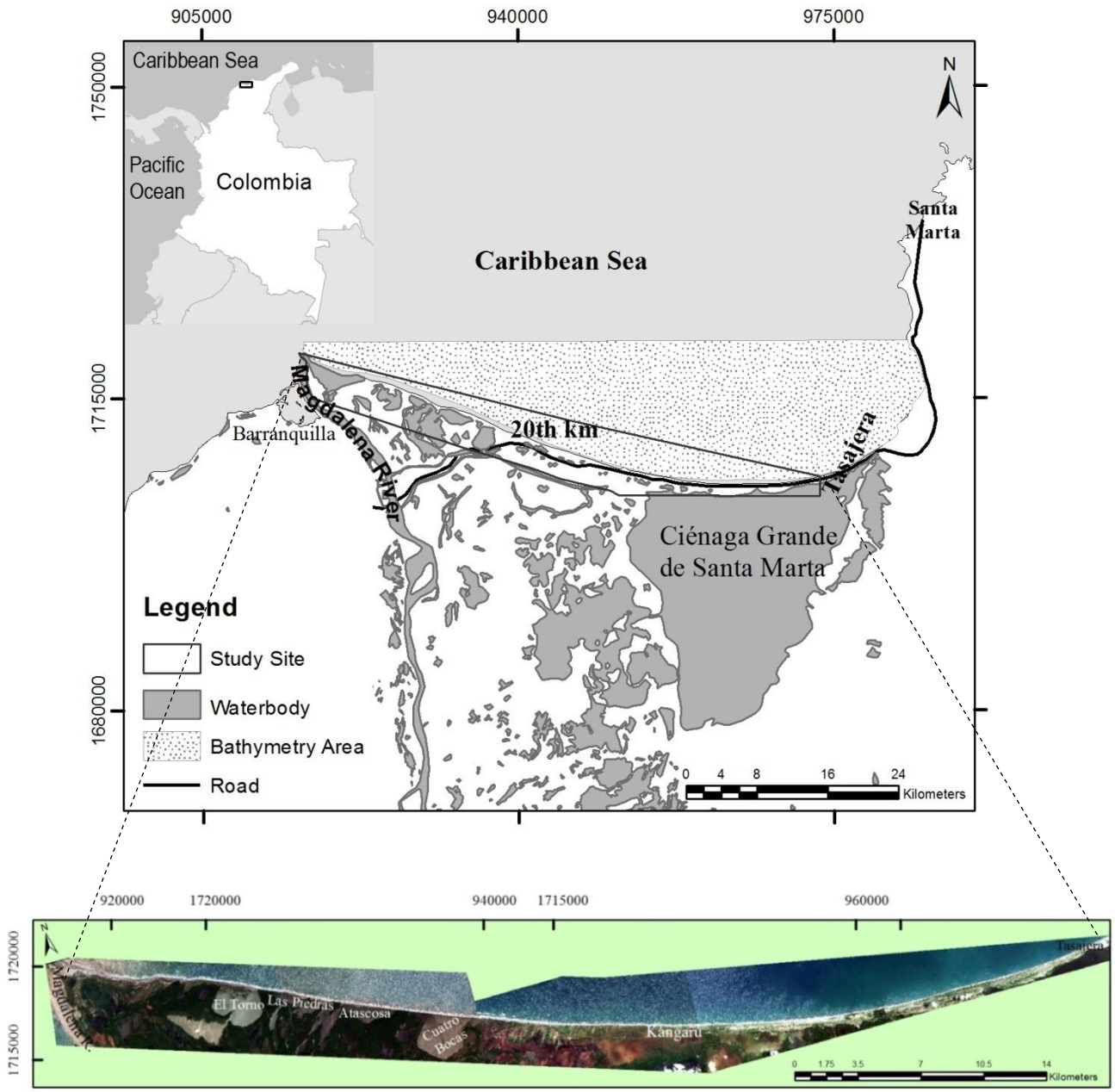

Figure 1. Area of study along the shoreline of Isla Salamanca National Park. The inset on the upper left is showing the location of the park within Colombia.

Maps from colonial times dating back to 1803, show that is now Isla Salamanca as a series of small islands (i.e., deltaic islands) surrounded by the former multi-distributary channel pattern of the Magdalena River (Figures 3 and 4). Before the port construction, the river wandered between Punta Sabanilla to the west (outside the site of study), and Los Gómez

lighthouse to the east, (Von Erffa, 1972), having a branch that flowed into La Atascosa lagoon (Figure 1).

A precise description of the east sector of the former Magdalena River delta was given by a consulting company working for the port design first phases: ". . . the area between the high lands near Santa Marta and the Magdalena River has been gradually filled as a delta of the Magdalena River. This delta was intersected by the various eastern mouths of the Magdalena. As the channels of these mouths gradually became filled the coastal sands built a long spit to the west from the Santa Marta hills, which is known as the island of Salamanca." (McKenney Black and Steward Engineers, 1921).

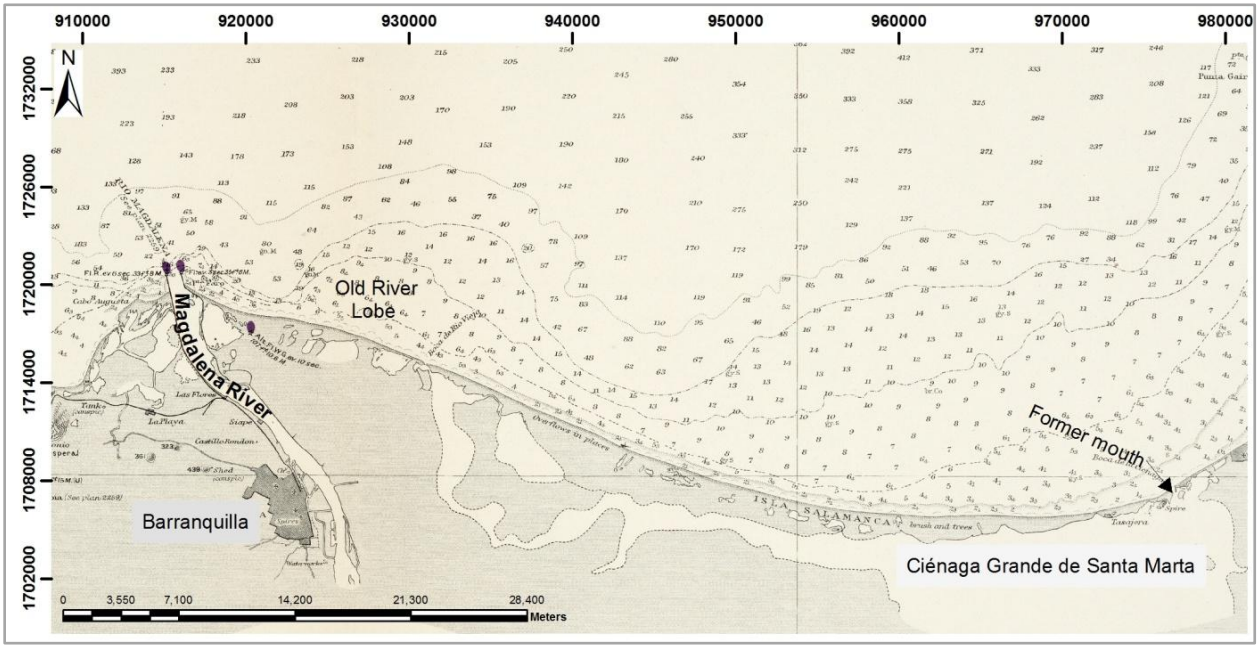

Figure 2. Bathymetry map published in 1944 (Modified from a chart published by the Hydrographic Office of the United Kingdom's Royal Navy).

Figure 3. The mouth of the Magdalena River and study site as pictured in map published in 1803 (no survey date given) (Source: IGAC, 1977).

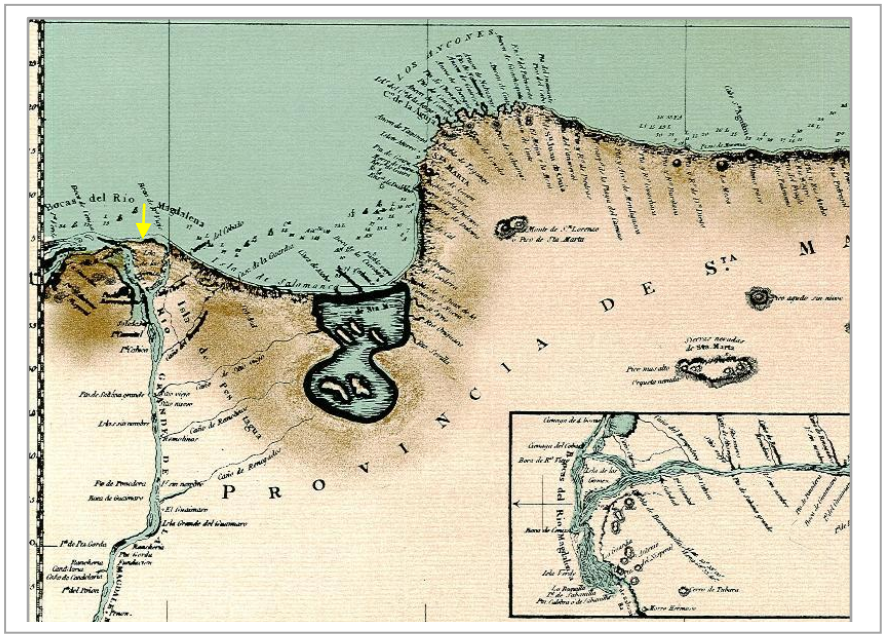

Figure 4. The mouth of the Magdalena River and study site as pictured in a map from 1817. The yellow arrow points to the former Isla Los Gómez (a detail of the river mouth is given on the right bottom) (Source: Acevedo, 1971).

In fact, based on Figures 3 and 4, it is evident that during the early nineteenth-century the river flowed through several winding mouths directly into the study area, providing a large supply of sediment. It is known that this condition, in conjunction with shallow embayments, favours barrier development across rivers mouths (Stutz and Pilkey, 2011). In contrast with Figure 3, charts published after the 1840s (e.g., Chart of the Republic of Nueva Granada published by Mosquera in 1849), show Isla Salamanca as a relatively continuous barrier spit extending westward from the inlet of the extensive lagoon of the Ciénaga Grande de Santa Marta (hereafter CGSM) (Figure 1). Shepard (1973) noticed that depressions such as CGSM are common on the margins of the largest deltas in the world.

Albeit located outside the study site, another remarkable human-induced change affecting the area was done as part of the Barranquilla-Santa Marta road construction, when the mouth of Ciénaga Grande de Santa Marta was moved west from its former location (Figure 2) to its current location, between the villages of Pueblo Viejo and Isla Rosario (von Erffa, 1972), located northeast from the study site. Furthermore, the road itself, which was partially constructed over inland parabolic dunes as well as using sand from these dunes (Angulo, 1978), constitutes a causeway and barrier not just for the sea-lagoon water interchange, but also for wind-transported sediments. In 2011, a breakwater was installed at a site known as either the 19th kilometre or the 20th kilometre (the 0 km is located at the outskirts of Barranquilla), a site where high erosion rates are endangering highway stability (see Figure 1 for the 20th km location). Since this structure has been unsuccessful so far in terms of sediment accumulation, a groin made with sandbags was installed between January and May, 2014 (Figure 5).

The drastic changes that have occurred at the Isla Salamanca coastline over a period

of less than 60 years, added to the value of its natural resources, relative ease of access, its changing dune landscape and scenery, and restricted human activities within the park (e.g., no farms, developments, or docks inside the area) makes this a particularly interesting study site. Moreover, in spite of the sparse distribution of dunes on the Colombian Caribbean, the study of these features in the park may contribute to understanding past climates and coastal evolution processes.

Figure 5. Shore protection measures installed at the 20th km. a,b,c. Breakwater made with panels of reinforced concrete (Photos taken in April, 2011 by author). d Sandbags installed to trap sediment (Photo taken from the road toward the northeast on May 28th, 2014 by Cristóbal Pizarro).

1.2.1 Climate

Climate patterns in the Colombian Caribbean are driven by the position of the Inter-tropical Convergence Zone (ITCZ), which, when it resides at its southernmost position (0°-5°S), produces dry and windy conditions, whereas the rainy season occurs when the ITCZ moves northward over the southwestern Caribbean. This seasonal pattern is weakened during strong phases of El Niño Southern Oscillations (ENSO), a major forcing mechanism of climatic and hydrologic anomalies. Long-term rainfall analysis confirms that El Niño events are associated with negative rainfall anomalies and La Niña with positive anomalies in northern South America (Poveda and Mesa, 1997).

In South America, longer term, drier conditions such as during the Little Ice Age (approximately between 550 and 200 years ago; hereafter LIA), have been related to the southward shift of the ITCZ (Haug et al., 2001). Allegedly, past changes in the livelihood of aboriginal cultures located in Tasajera (Figure 1) and Palmira (settlement located 2.4 km east of Tasajera) from an agriculture tradition to hunting and gathering practices have been related to a decrease in rainfall and loss of soils (Angulo, 1978). Aside from climate conditions, Angulo (1978) proposed that indigenous tribes were established in Isla Salamanca during the fifth century A.D.

Based on the Martonne index (i.e., the ratio between annual average precipitation and annual average temperature), the whole study area is classified as semiarid, with average annual temperatures ranging between 25° and 30°C (Villegas et al., 2006), rainfall less than 800 mm/year, and a potential evapotranspiration of 1,900 mm (Ensminger, 1997). Given the relevance of rain and wind conditions for dune evolution and vegetation establishment over the

dunes, those variables are detailed below. The rain and wind data analyzed were collected by the Institute of Hydrology, Meteorology, and Environmental Studies (IDEAM for its acronym in Spanish) at the weather stations located in the airports of Barranquilla and Santa Marta (see Figure 10 for location of these airports).

1.2.1.1 Precipitation

In terms of seasonal time scales, rainfall in Isla Salamanca, like in central and western Colombia, experiences a bimodal cycle of precipitation, having one peak in May and another in October. Regardless of its relative short east-west length (60 km), the study site is affected by an east-west decreasing gradient in rainfall. As a result, when comparing rainfall data from the weather station located in Santa Marta, east of the study site, with data from the station located in Barranquilla, west of the study site, this east-west gradient becomes apparent (Figure 6). Even though these stations are outside the study site, they were used for the rain analysis because in contrast to those stations located in the study site (i.e., Tasajera and Los Cocos), Barranquilla and Santa Marta stations have longer data records and no missing data. Annual average precipitation at the Barranquilla airport is 760 mm and at the Santa Marta airport it is 400 mm (Figure 6).

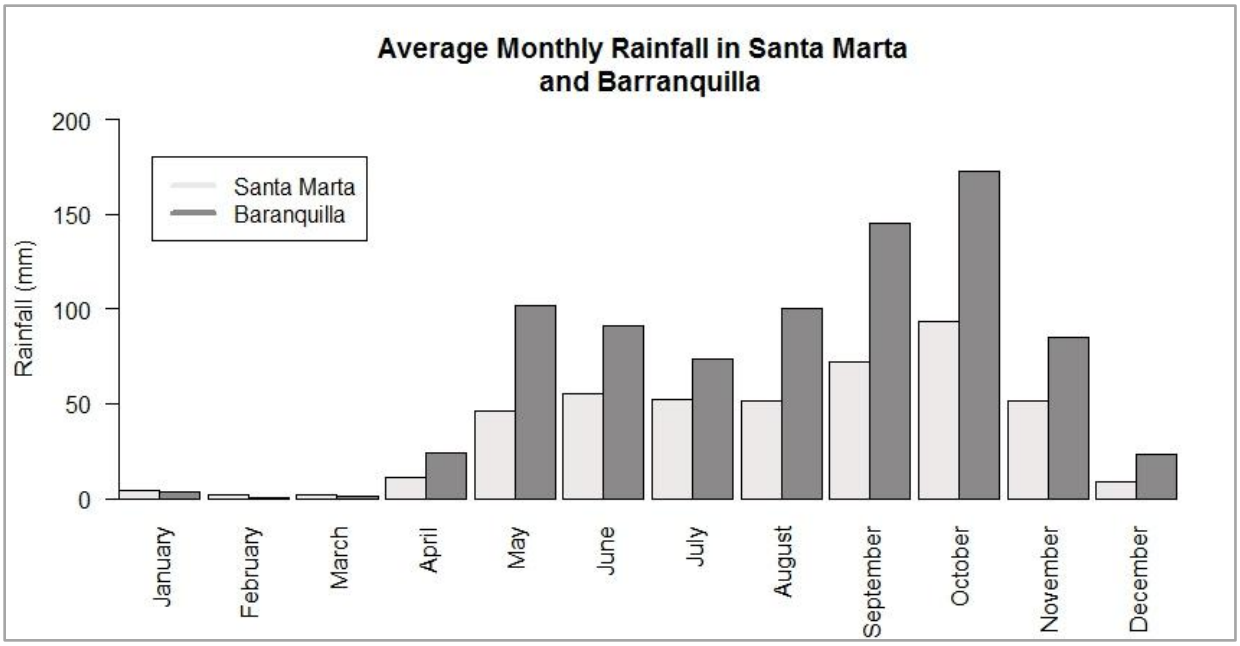

Figure 6. Average monthly rainfall between 1965-2012 (Source: created by the author from data collected by IDEAM).

1.2.1.2 Wind

During the dry season, from mid-December through April, the Northerly and Northeasterly trade winds are dominant. They blow particularly steadily during the day, whereas northerly winds may weaken during the night, enabling seaward winds to dominate instead. During the humid season the northern winds are much less strong and steady (Wiedemann, 1973). Given the east-west coastline alignment of the park, northerly and northeasterly winds approach the coastline at high angles (e.g., close to perpendicular with respect to the coastline), helping promote sediment movement and transport inland.

Despite the lack of wind-velocity and sand-transportation data for the study site, dune formation and consequently sand transportation indicates that wind speeds reach values of over 6 m/s, the threshold value for dry sand to be transported by wind (Nickling and Neuman, 1999;

Davidson-Arnott, 2010; Heathfield and Walker, 2011). Nonetheless, variables such as the presence of moisture and surface crusting (Nickling and Neuman, 1999; Heathfield and Walker, 2011), the fetch length (Delgado-Fernandez, 2010), surface roughness caused by factors such as vegetation (Nickling, 1994), local slope, and water-table elevation, may greatly affect the minimum value at which sand movement is initiated. Nevertheless, in accordance with wind data collected from 1981 to 2012 at the weather station at the airport in Santa Marta, wind speeds, particularly those coming from the North and Northeast, may reach speeds of over 8.7 m/s (Figure 7).

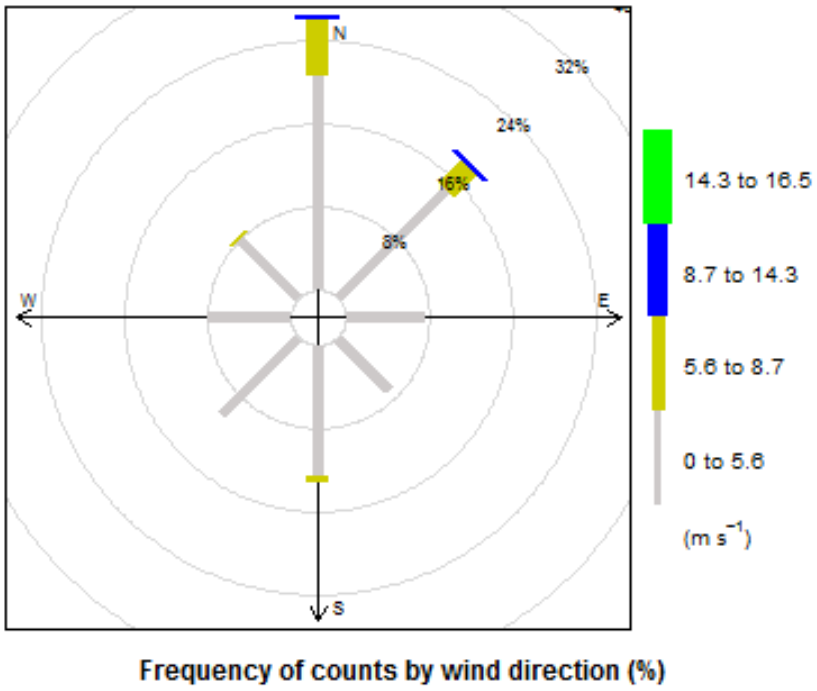

Figure 7. Wind rose made for data taken hourly at Santa Marta airport weather station from 1981-2012. Wind rose created using Openair package (Source: modified by the author from data yielded by IDEAM).

1.2.2 Oceanography Parameters

1.2.2.1 Tides

In the Magdalena Delta, the tide is a mixed, primarily diurnal type (Restrepo and López, 2008). Múnera et al. (2003), after measuring nine tidal cycles during 48-hour intervals in the channel connecting the ocean with the Ciénaga Grande de Santa Marta (CGSM), correlated this information with data from the tide gauge in Cartagena, finding a maximum tidal range value of 0.35 m. This small tidal range, added to the north-northeast predominant wind direction along the barrier, produces a microtidal, wave-dominated regime characterized by a predominantly westward longshore transport driven by northeast trade winds (Restrepo and López, 2008).

In research to assess SLR on the Caribbean based on numerical and instrumental data, the latter including historical gauge records, Losada et al. (2013) reported an overall sea–level rising trend for the deep waters of the Caribbean Sea of about 2 mm/year from 1950 to 2010.

1.2.2.2 Waves and Littoral Drift

Beaches and dunes composed of well-sorted sands and straightened by wave activity are evidence of wave-dominant processes. Measurements of average swell waves based on observations taken nearby the Magdalena Delta for the period 1963-2000 indicate that the predominant direction of swell waves comes from the northeast, with average heights of 2.3 ± 1.2 m, and significant and maximum heights of 5.1 and 9.0 m, respectively (Restrepo and López, 2008).

According to field observations of sediments accumulated on the east side of human-made structures such as a groin and a breakwater built in 2011, just 4.5 km east of the eastern border of the study area, wave-driven longshore transport–as opposed to cross-shore transport–seems to be the dominant mechanism by which sediment moves into and through the system from east to west at Isla Salamanca. Seasonal or local drift reversals from this longshore trend arise from changes in the wave-direction driven by winds coming from the northwest, or from inlet openings locally affecting the predominant wave approach.

1.2.2.3 Sea Level Changes in the Holocene

Curray (1964) related progradation versus retrogradation of a coast to the rate of Sea Level Rise (SLR), stating that for tectonically stable margins the coast retreats in most SLR scenarios unless a high rate of sediment deposition offsets this tendency.

Worldwide, during the early Holocene−the past 11,500 years−eustatic sea level rise occurred rapidly and slowed in the mid-Holocene, attaining present levels by ~7 ka BP (Murray-Wallace and Woodroofe, 2014), and changing little during the late Holocene in comparison to the whole Quaternary, a period that started 2.59 Ma BP. Many modern barrier island systems initially formed at this time as sea level rise slowed and approached present-day sea level (Stutz and Pilkey, 2011) (Figure 8).

It has been suggested that in the Caribbean Sea, instead of a Holocene highstand, a gradual but ongoing rise has taken place up to present (Murray-Wallace and Woodroffe, 2014). While eustatic sea level has changed little globally during the late Holocene, relative sea level change has varied regionally due to the influence of vertical neotectonic, glacio-eustatic and

hydro-isostatic crustal movement, as well dynamic redistribution of oceanic water mass (Woodroffe, 2003).

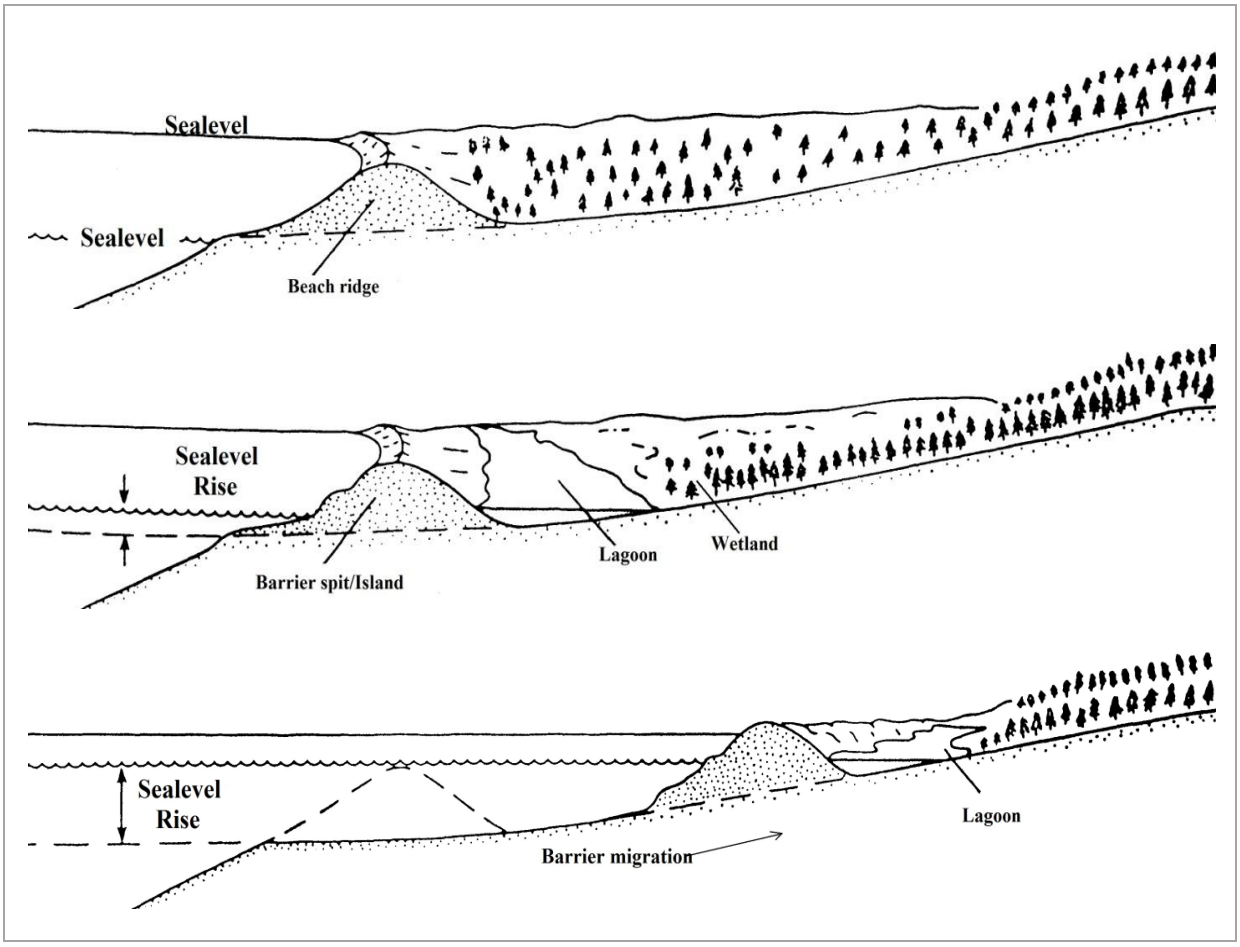

Figure 8. Schematic diagram showing barrier island evolution (top-down) under a sea level rise scenario. The upper diagram represents the conditions during the early Holocene, when sea level was about 50 metres lower than present (After Dolan and Lins, 1987).

The CGSM lagoon genesis has been related to a marine transgression that began about 2300 years B.P. (Wiedemann, 1973). Two carbon-14 samples from archeological sites at the coastal town of Tasajera at the east border of study site are dated at 1450 ± 110 and 1100 ± 105 B.P. Additionally, organic matter samples taken from the CGSM bottom, have been dated at ages ranging between 1920 ± 65 and 2430 ± 85 B.P. (Wiedemann, 1973). The above ages are in

accordance with dates obtained from archeological material left by aboriginal inhabitants that provided ages between 1615 ± 100 B.P. and 1000 ± 105 B.P. for the areas known as Los Jagüeyes and Tasajera, respectively (Figure 1); that is, after the Holocene highstand ranging between 2 and 3 m Above Present Sea Level (APSL) that has been dated for the Colombian Caribbean between 2460 and 2700 years B.P. (Robertson and Martínez, 1999). Accordingly, the formation of Isla Salamanca has been estimated to have occurred around 2000 years ago (Angulo, 1978).

In accordance, Tinley (1985) stated that many of present day coastal forms and dune characteristics result from modified or reworked features inherited from the past climatic and sea level oscillations. In fact, initiation of transgressive sheets and dunefields have been attributed to mechanisms such as climate change, sea level change, foredune desestabilization, shoreline erosion, disturbance or destruction of the vegetation cover, and the coalescence of parabolic dunes (Hesp, 2013).

Aside from global sea level changes, there are many factors that may induce local changes in sea level. Specifically, relative sea level changes may be produced by subsidence over either the coastal fringe or the shelf surface. This is particularly the case along large deltas with deep-sea fans containing large volumes of sediments (Emery, 1977), where simple gravity loading is a contributory mechanism for subsidence (Bott, 1979). This may be complemented by autocompaction−the process by which peat at a certain depths will compact itself due to the weight of the overlying peat (McKee et al., 2007)−in areas occupied by mangroves. Both conditions, a former delta and mangrove forests, are found in the study area.

1.2.3 Geologic context

Because of its position in the northwestern corner of South America, the Colombian Caribbean continental margin is affected by the interaction of the Caribbean, South America and Nazca plates, all of which converge or slip past one another at different angles and speeds (Paris et al., 2000; Ordóñez, 2008) (Figure 9). This tectonic control results in contrasting trends in the structures associated with the deformation front that stretches out along the Venezuelan and Colombian Caribbean. This front has an east-west direction west from the Magdalena Delta, and northeast to north-south trends southwest from the Magdalena Delta (Vernette, 1986).

Deep seismicity, magmatism and volcanism, are all common features present in the Western and Central ranges of Colombia associated with the Nazca plate high-angle subduction. Contrastingly, the southeastward subduction of the Caribbean Plate beneath the northwestern margin of South America is a nonmagmatic (shallow) process (Kellogg et al., 1983), associated with low seismicity (Paris et al., 2000). Nonetheless, active faults such as the Santa Marta-Bucaramanga Fault system (SMBF) may trigger earthquakes affecting the Colombian Caribbean. Idárraga and Romero (2010), based on the displacement of Quaternary deposits studied in an outcrop located 20 km southeast from the eastern boundary of the study site, stated that this section of the SMBF has probably had Quaternary seismogenic events. In effect, 46 epicenters were reported in the vicinity of the fault between 1994 and 2007, producing seismic activity with events of magnitude between 2.4 and 6.1, at depths up to 185 km. (Idárraga, 2008).

The SMBF, which borders the eastern limit of the study site, extends for a distance of 550 km from the Caribbean coast to the *Cordillera Oriental* (Eastern Range) (Campbell, 1967; Paris et al., 2000). SMBF constitutes a major wrench fault, with about 110 km of left-lateral

displacement (Campbell, 1967) marking a contrasting relief change between the Sierra Nevada de Santa Marta (SNSM) range east of the structure, and the low relief of the floodplain of the Magdalena Lower Valley west of the structure (Idárraga and Romero, 2010). Based on seismic profiles taken in the Colombian Caribbean margin, the structure was traced over the sea bottom north of the town of Ciénaga as a fault with a reverse component, with the western block downthrown (Figure 10). The fault has an average strike ranging from N-S to N15W (Sheppard, 1973). A thermal spring, located close to the river Córdoba, east of the study site, with X/Y coordinates 984261/1711038 (Magna-Sirgas projection, values are given in metres), has been related to this fault system (Wiedemann, 1973).

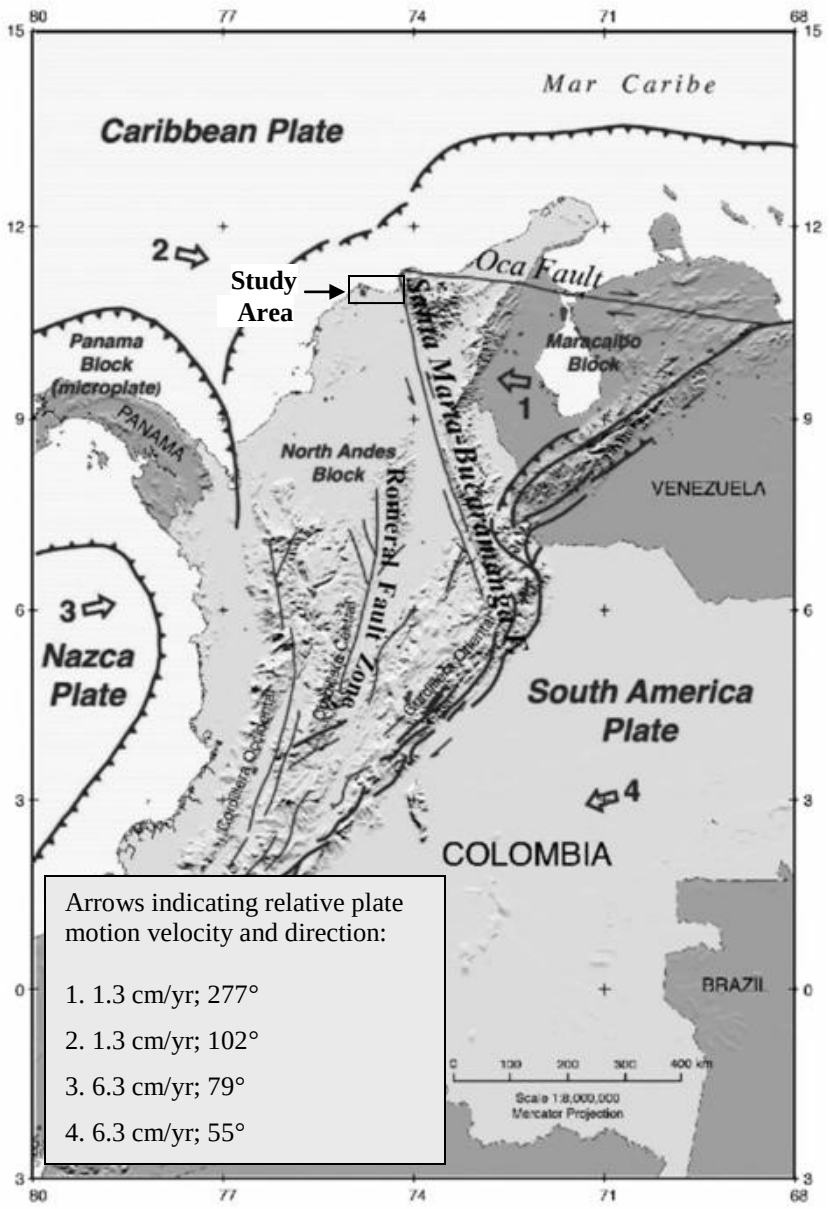

Figure 9. The tectonic setting of Colombia (Modified from USGS and Paris, 2000).

Another major structure likely influencing the study area is the Romeral Fault System (RFS). This is one of the most active and continuous fault systems in Colombia, crossing the length of the country from south to north, and defining the transition zone between two distinct geologic provinces: continental east of the fault and oceanic west of the fault system (Duque-Caro, 1979; Paris et al., 2000). Even though most research traces its northernmost extension far

south from the Caribbean coast at about latitude 8°N (e.g., Kellogg et al., Paris et al., 2000), some studies extend its northernmost extreme, as a tectonic province limit, east from the Magdalena River mouth, so that it lies inside the limits of this project study site (e.g., Duque-Caro, 1979; Duque-Caro, 1980; Etayo, 1983; Vinnels et al., 2010). For instance, in agreement with Duque-Caro (1979), along the flat lands surrounding the Magdalena River mouth, the RFS is concealed at depth by the Tertiary and Quaternary deposits of the San Jorge basin (Figure 10). Nonetheless, fault traces associated with the RFS are less visible between latitudes 8°N and 11°N than south from latitude 8°N, and neotectonic activity is very low (Taboada et al., 2010).

East from the RFS is the Plato-San Jorge Basin (Figure 10), a back-arc basin filled with Oligocene to Pliocene sediments from the proto-Magdalena River, with an underlying Paleozoic metamorphosed crust (Duque-Caro, 1980; Flinch, 2003). The CGSM lies under the northernmost limit of the Plato Basin. On the other hand, the Quaternary sediments located seaward of that body of water, along the shoreline, are medium to fine sands composed of quartz, feldspar, shell fragments, and heavy minerals (Wiedemann, 1973) (Figure 10).

Unfortunately, the lack of seismographic instrumentation and tidal stations near to the study area do not permit a precise assessment of the effect of the SMBF and RFS in the coastal evolution. Nevertheless, the expected installation by the Colombian Geological Survey of a GPS field station based on Global Navigation Satellite System (GNSS) instrumentation, may help assessing the effect of these structures, as well as crustal deformation on the changing coastline.

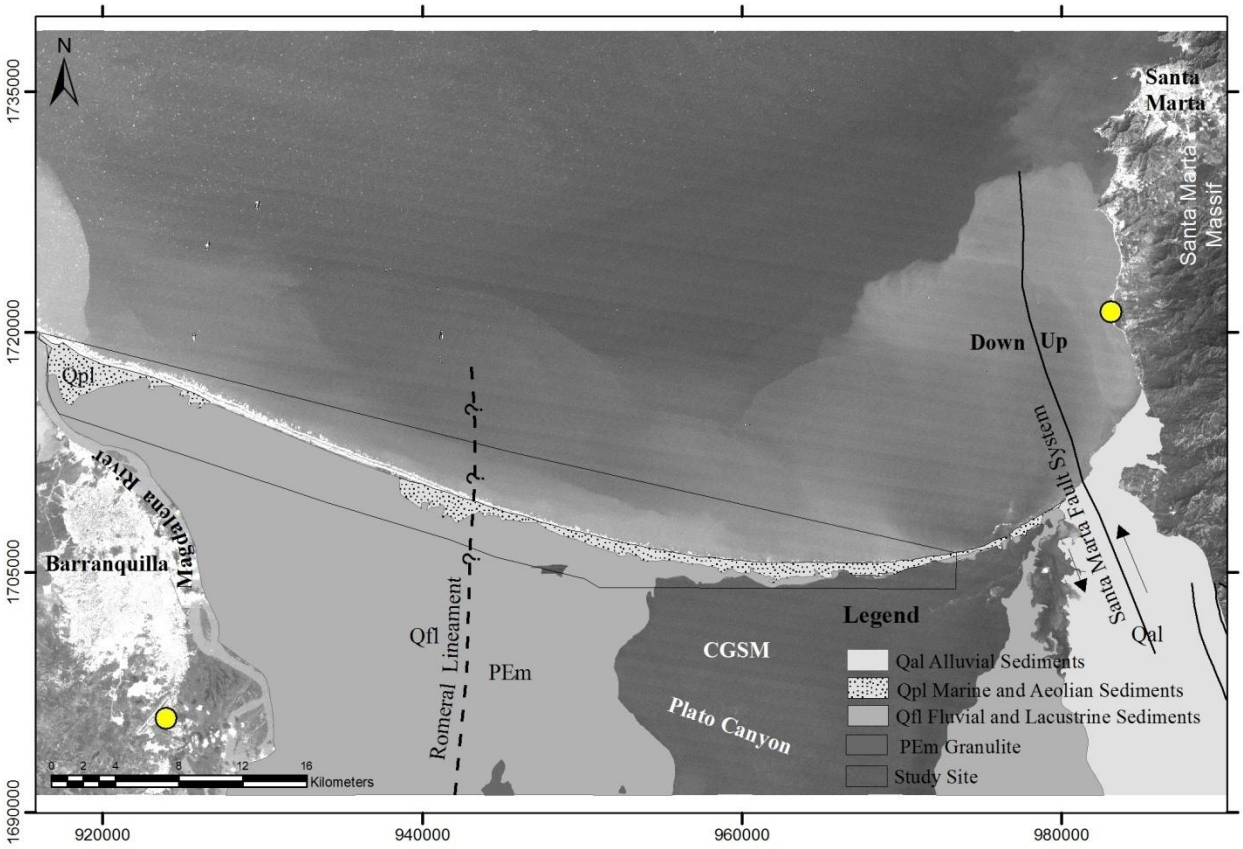

Figure 10. Geological units in the surrounding area of the study site (yellow points are showing the location of the airports in Santa Marta and Barranquilla) (Modified from Duque-Caro, 1979; Shepard, 1973; Colmenares et al., 2007; Idárraga, 2008).

1.2.4 Vegetation

Whether or not a shore zone and particularly a dune surface is covered by vegetation has implications for sediment transport rates and sediment transport mechanisms. Plants trap sand transported from the beach in two ways: (1) by reducing the wind speed within and in the lee of individual plants, leading to sand deposition and the formation of small discrete shadow dunes that extend downwind from the plants (Hesp, 1981); and (2) by their leaves and stems providing a physical obstacle to saltating grains (Davidson-Arnott, 2010). At some point, a dual interaction may occur, when colonizing species both create and affect topography, and in turn, topography

determines vegetation association and succession patterns (Hesp et al., 2010). In short, a reciprocal feedback process may take place between dune morphology (e.g., height, slope) and vegetation associations. As a result, plants−sometimes aided by fertilizers−have been used to stabilize dunes as a way to strengthen sea-defences, to prevent mobile sand blowing affecting roads or other infrastructure (Boorman, 1977), and to halt natural geomorphic processes of erosion. Contrastingly, some restoration projects are currently seeking to reactivate aeolian activity and dune mobility via vegetation removal (Walker et al., 2013).

Medina et al. (1989), while studying isolated patches of vegetation growing in salt plains −also termed vegetation islands−particularly in a coastal alluvial plain in northern Venezuela, suggested that vegetation free areas may initially be colonized by salt-tolerant species such as *Sporobulus virginicus*, *Batis maritima*, and *Conocarpus erectus*. These species produce soil accumulation in their surroundings, elevating the soil level above the salt flat and therefore facilitating the leaching of salts during the rainy season. As a result, salt-intolerant species become established (Medina et al., 1989).

Likewise on other coastal alluvial plains on the continental Caribbean under dry climate conditions, vegetation patterns in Isla Salamanca are somewhat controlled by the interplay between soil salinity and microtopography. Mangrove species (e.g., *Rizhophora mangle*, *Languncularia racemosa*) are common around lowlands surrounding the lagoons in ISNP, whereas sand-tolerant species−that is, psammophyte plants−such as *Sessuvium portulacastrum*, *Sporobulos virginicus*, and *Batis maritima* are found seaward from the brackish lagoons. The middle zone between these extremes is occupied by mixed-growth thickets where xerophytic species such as *Pereskia guamacho* (also called *Pereskia colombiana*), *Prosopis juliflora*, and

Stenocereus griceous are common. A well-adapted non-native species widely distributed over the dunes along Isla Salamanca is *Calatropis prosera*.

Before the road construction, when mangroves trees were abundant on the boundary between the lagoons and dune fields, sediments dredged from the sea may have been buffered by the vegetation fringe, preventing most of these sediments from being transported to the bottom of the lagoons. After the road was built, increasing salinity levels have halted mangroves distribution and population on wetlands located in backshore areas of the Ciénaga Grande de Santa Marta (Elster et al., 1999). The high salinities there, partially resulting from the blocking effect that the road has on the water interchange between the sea and the lagoons, has been especially detrimental to mangrove seedlings (Elster et al., 1999). In an effort to regenerate the ecosystem, three canals were reopened between 1996 and 1998 in order to reestablish the water exchange between the Magdalena River and the lagoon system and to lower the salt levels through periodic flooding (Blanco et al., 2006; Ensminger, 1997). Furthermore, box-culverts were built under the road to favour water interchange.

Chapter 2 Methods

Analyzing dune and coastal evolution requires understanding and deciphering the interplay between numerous variables. This project focuses its analysis on the following: studying recent climate trends of precipitation and wind, geomorphology evolution, coastal and bathymetry changes, and vegetation associated with dunes (Figure 11).

Georeferencing and mapping of landforms and shorelines in this work were done with the support of ESRI ArcGIS software. All data were set to the standard Colombian projection system, which is Magna Sirgas, datum Bogotá. Statistics and graphs were developed with the open source software R. On the other hand, field observations of landforms and vegetation were made during two field trips carried out in December 2013 and May 2014.

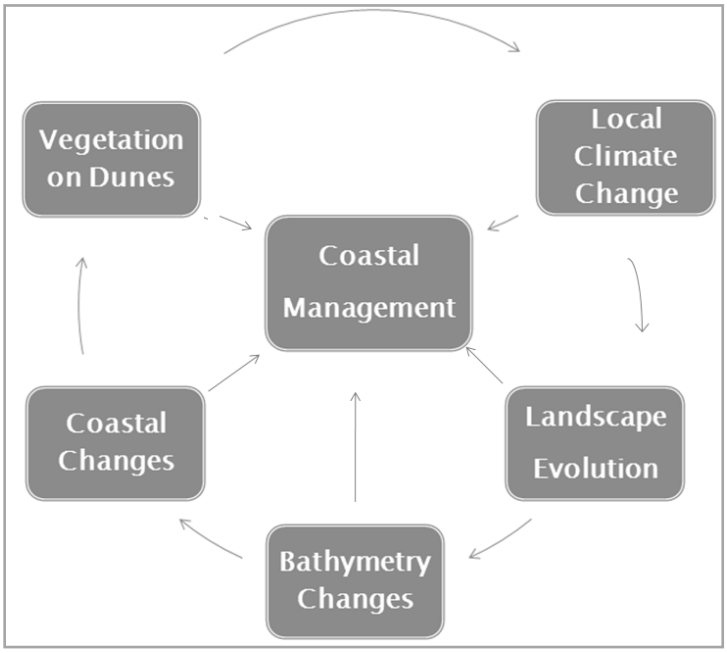

Figure 11. Interlinked variables analyzed for the study site.

2.1 CLIMATE

Rain (Santa Marta and Barranquilla) and wind data (Santa Marta) from the stations located inside and nearby ISNP were obtained from IDEAM; the trend of these variables through time was assessed in order to determine their influence, if any, over the coastal dune dynamics. The analysis for the existing longest precipitation time series (Barranquilla and Santa Marta weather stations began collecting data in 1942 and 1954, respectively), included: (1) fit the data to linear regression models, (2) verify that the samples are normally distributed, and (3) check for autocorrelation between the data. All the above tests were done considering a level of significance of α=0.05; for instance, if the calculated *p* values are smaller than the threshold chosen for a particular statistical significance level (0.05 for this research), then the null hypothesis, ($H_1 = H_0$), that the outcome was found by chance is rejected in favor of the alternative hypothesis ($H_1 \neq H_0$), meaning that the result (e.g., a significant trend exists) is not the product of chance (Crawley, 2007). The next paragraphs present a detailed explanation of these procedures.

The first approach consisted of adjusting linear regression equations to the data to establish statistically whether significant trends of annual rainfall and wind exist. A trend is a significant change over time exhibited by a random variable, detectable by statistical parametric and non-parametric procedures (Longobardi and Villani, 2009). To assess the significance of the values obtained for both the slope and intersect of the line equation, *t* test and *p* values were obtained. These values assisted in accepting or rejecting the validity of the line equation.

In order to verify whether or not the data have a normal distribution, the Shapiro-Wilk and Anderson-Darling tests were used. Using R (the software package), the null hypothesis for

the aforementioned tests is that the data are drawn from a normal distribution. In this case, *p* values larger than 0.05 imply that the samples are normally distributed (Harris and Jarvis, 2011).

Moreover, for the time series analysis, it is essential to consider autocorrelation, also called serial correlation, defined as the correlation of a variable with itself over successive time intervals. Autocorrelation increases the chances of detecting significant trends even if they are absent and vice versa. To avoid the effect of trends resulting from data autocorrelation, Hamed and Rao (1998) suggest a modified Mann-Kendall test, which considers the autocorrelation between the rank order of the observed values and their order in time (Hamed and Rao, 1998). According to this test, the null hypothesis, $H_{0,}$ assumes that the data are independent and randomly ordered (no trend is observed). This assumption is tested against the alternative hypothesis, H_1, that there is indeed a trend (i.e., there is a monotonic upward or downward trend of the variable of interest over time). Hence, if the *p* value obtained is less than the significant value, α (0.05), H_0 is rejected.

Regarding the wind record, hourly data are available for the period 1981-2012 taken at a height of 10 m with a mechanical fuess device located at the station in Santa Marta's airport. These data were analyzed to identify and extract every record of wind events of over 6.0 m/s. As a result, the yearly sum of all the events over this threshold (6 m/s) was accounted and graphed.

It is worth mentioning that the linear regression models resulting from this section are not suggesting that the correlation between the independent (time) and dependent (rain/wind) variables is linear; the regressions used are simply defining whether or not a trend exists for the time span studied. Other approaches, such as non-stationary models, are more feasible to forecast time series presenting trends or seasonal effects.

2.2 COASTLINE CHANGES

Coastline changes were quantified using historical air photos and satellite imagery prior to carrying out field work in order to select sites presenting contrasting coastline morphodynamic for the detailed study of dune characteristics, specifically dune vegetation.

In order to quantify coastal changes through time, previous work (e.g., BaMasoud and Byrne, 2013; Allen et al., 2002; Correa et al., 2005) has examined historical imagery and field data taken either with GPS or conventional topographic equipment. Regardless of the methodology chosen to trace landforms along the coastline, given the highly dynamic nature of the shore zone, obtaining coastline or dune trends from unevenly time-distributed data entails a margin of error that depends on whether the feature is extracted from historical maps, aerial photographs, satellite images or collected during fieldwork. Additionally, seasonal or daily events such as storms, tides and waves, constantly affect the position of the dune or coastline. Cutting edge technologies like the light detection and ranging (LiDAR) system and high resolution satellite images have improved the accuracy of coastline measurements; however, for comparing current tendencies with those of previous years, historical aerial photographs are commonly the only resource available. Therefore, despite their shortcomings (e.g., distortions associated with aircraft tilts, terrain relief or camera lens), airphoto sets remain one of the most cost-effective ways to depict shoreline positions over time (BaMasoud and Byrne, 2013).

To assess the coastal changes along Isla Salamanca over time, historic aerial photographs, taken by the Colombian Survey Institute (IGAC for its acronym in Spanish) in 1947, 1953/1954, 1968 and 1985, were used. The scales for these sets of photos are 1:20.000, 1:60.000, 1:20.000, and 1:28.820, respectively. Unfortunately, all the pictures but those from 1985 were taken

perpendicular to the coastline, covering just small sections within the study site. Therefore, the shoreline length for a particular year depends on the flight coverage. In addition to aerial photographs, coastlines from 2010 to 2013 were obtained from Ikonos and Geoeye satellite images as well as from transects made with a GPS Garmin Legend HCX. After scanning the photos at a resolution of 1,200 dots per inch, they were georeferenced, using ESRI ArcMap software, with respect to the satellite images in the Magna coordinate system, Sirgas projection; this step was a challenging task because of the lack of buildings and recognizable landmarks in Isla Salamanca. Hence, the road, small mangrove islands inside the lagoons, and recognizable features around the lagoons and along creeks, were used as reference points for georeferencing.

Once each of the aerial photographs was georeferenced, a linear shapefile was generated to delineate the coastline on the image, on which was traced the limit between the wetted and the dry beach, herein High Water Line (HWL) (McCurdy, 1947). Even though this limit is not a geomorphic feature, it is assumed to represent the mean high water line (MHWL) (Dolan et al., 1980; Moore, 2000; Dean and Dalrymple, 2002). Given the small tidal range in the Colombian Caribbean, the wet/dry line provides a consistent measure between different years. An initial attempt to trace the vegetation line was discarded because in addition to the discontinuity of this feature, it was hardly discernible in the black and white aerial photographs.

To quantify coastline changes through time the tool Digital Shoreline Analysis System (DSAS; Thieler et al, 2003), was used. DSAS is a script released by the United States Geological Survey (USGS), which runs as an ArcGIS extension, calculating the accretion/erosion rates in metres per year (m/yr) through different equations, where a positive value of shoreline displacement indicates a shoreline advance in relation to the older shoreline

and vice versa. Between the parameters obtained by running DSAS, only the values obtained for End Point Rates (EPR) and Average of Rates (AOR) are graphed. The EPR equation is calculated by dividing the distance of shoreline movement by the time elapsed between the earliest and the latest measurements (i.e., the oldest and the most recent shorelines). The AOR, on the other hand, is the result of the average of calculating separate end-point rates for all combinations of shorelines when more than two are available (Thieler et al., 2001). This research emphasizes its analysis on the AOR outcomes, defining rates on shoreline perpendicular transects spaced at 25 m intervals. Before running DSAS and in order to provide a starting point for each one of the transects, a baseline located landward from the shoreline was traced approximately parallel to the highway. As a whole, starting from transect number 1 in the easternmost sector (i.e., Tasajera), 2380 transects oriented perpendicular to the shoreline were obtained after running DSAS (Appendix A).

When delineating the coastline, there is a range of uncertainty associated not only with the scale of the photograph, but also with the skills of the interpreter (Smith, 2011) to identify the coastline properly. However, given the variability of the error itself, estimating the margin of error is not a straightforward process. Based on the methodology proposed by Del Río and Gracía (2013), an error worst-case value or maximum error was assessed to estimate the uncertainty associated with the traced coastlines. Accordingly, three specific factors were taken into account to quantify the error: (1) scanning error (R), which depends on the image resolution; (2) georeferencing error (G), which is equal to the Root Mean Square Error (RMSE) value obtained from ArcGIS; and, (3) a physical component of the error (D) related to the inherent characteristics of each shoreline (e.g, slope).

Specifically, this last uncertainty is related to the tidal changes and the slope of the beach. Thus, the difference between the highest and lowest tide values for the specific date when the photograph was taken is divided by the tangent of the slope. Although there are other potential variables (e.g., wave setup after storms), Del Río and Gracía (2013) include only errors associated with tide and beach slope changes. These parameters are expressed in the following equation, where the total uncertainty in shoreline position on a certain photograph (E_P) is:

$$E_P = \pm\sqrt{R^2 + G^2 + D^2} \quad \text{(Eq. 1)}$$

where R is the scanning error, G is the georeferencing error and D is an error related to the specific characteristics of the shoreline.

Consequently, the total uncertainty for a given rate of shoreline change calculated between two shoreline positions should be computed by considering individual errors for each photograph (i.e., Ep_1^2 and Ep_2^2):

$$\text{Erate} = \frac{\pm\sqrt{Ep\,1^2 + Ep\,2^2}}{T} \quad \text{(Eq. 2)}$$

where T is the time span (in years) between the two photographs used to extract the shorelines (Del Río and Gracía, 2013).

2.3 BATHYMETRY

In contrast to coastline change assessment described above, analysis of bathymetric changes over time was based on overlaying two bathymetry maps from different years. These maps were published by the Hydrographic Office of the United Kingdom's Royal Navy with a scale of 1:200.000 in 1944 (Figure 2) and 2012. For doing so, the known depth values were

interpolated using Spatial Analyst Tools within Arctoolbox, an application of ArcMap that enables users to obtain Digital Elevation Models (DEM) representing contours such as those of the sea-bottom surface.

Many attempts were made in a trial and error process in order to find the model that would best represent the data, Inverse Distance Weight (IDW), spline, and Kriging interpolation techniques were attempted on the original bathymetric charts, the former resulting in multiple "bulls eye" patterns around single depth values. Since having multiple isolated rounded seamounts for a relatively small area is somewhat unrealistic for bed surfaces, the outcomes obtained with the IDW were not used for the bathymetry analysis. On the other hand, few differences were found between the interpolation models resulting from Kriging and spline. Spline involves fitting a polynomial regression equation to discrete groups of the data points along sections of the surface. These splines are then 'tied' together to produce a smooth curve following the overall surface (Walford, 2011). Reasonably, while comparing Kriging and spline, Laslett (1994) stated referring to the latter: "why should the trend be smooth?." Moreover, given that there are some clusters in the bathymetry data, especially for the data published in 2012, Kriging was chosen over spline because of its capacity to assess those clusters by reducing the weighting applied to samples in close proximity with similar values. In other words, when running Kriging, clustered samples do not necessarily carry more weight than a single sample (Swales, 2002).

Finally, based on their depth values, two Digital Elevation Models (DEM) were generated using the Kriging interpolation model. To choose the nugget, range, and sill values for the Kriging model, an empirical semivariogram was done using the software R. This

semivariogram, in addition to indicating the distance over which depths are correlated, provided the values for the parameters to properly run the Kriging interpolation model within ArcMap (Figure 12). From these values, the range is the distance over which a reliable prediction can be made, whereas the nugget quantifies the uncertainty of the deep values (Walford, 2011). Yet, within Kriging, spherical and Gaussian surfaces were used to fit the experimental data (Table 10). Some 'known' values were deleted purposely from the 2012 bathymetric chart (i.e., depths obtained during the field campaign), so that a comparison of the outcomes between the Gaussian and the spherical surface could be performed (Table 11).

Once the DEMs were obtained, two bathymetry (contour) maps−one for 1938 and another for 2012−were generated with pixel sizes of 50 m. After trying different pixel sizes, this size was chosen because it is considered to properly represent the original resolution of the maps. Developing the DEM and the contours was done using the Spatial Analyst extension and the Surface tool within Arctoolbox of ArcMap, respectively. Finally, the raster calculator tool, another Arctoolbox application within Spatial Analyst, was used to subtract the 2012 from 1938 elevation models, resulting in the changes over time for these surfaces, where positive values resulting from this subtraction indicate gain of sediment through time and vice versa.

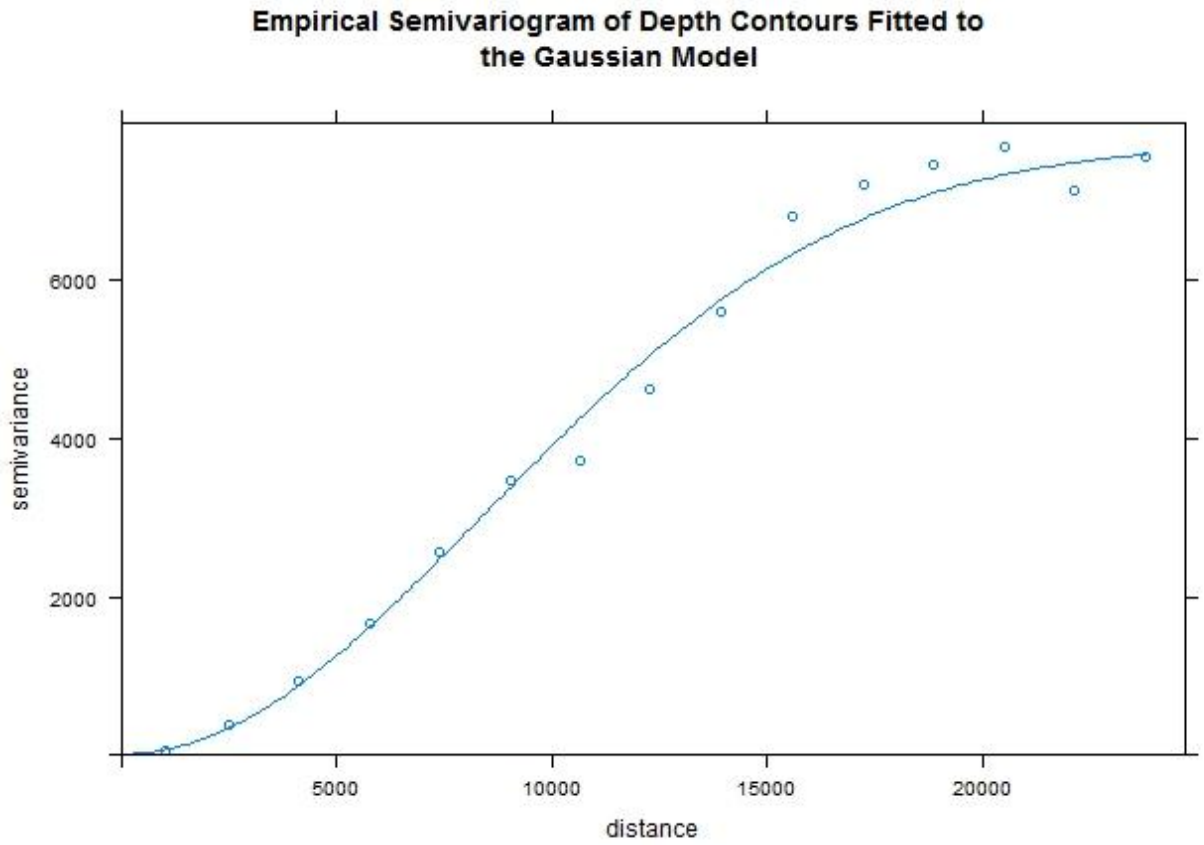

Figure 12. Empirical semivariogram resulting from the 1938 depth contours map.

In order to define a common area to make the contour subtraction between both maps, an arbitrary polygon (see labeled Bathymetry Area in Figure 1), was traced; in this polygon, the zero contour matches the 1938 coastline. However, due to the inherent dynamic nature of the shoreline, this zero contour no longer represented the shoreline in 2012 but was under sea level. As a result, a thin fringe of sea parallel to the 2012 shoreline was not taken into account in the bathymetry changes. Nonetheless, neither the 1938 nor the 2012 original maps contained bathymetry data along this fringe.

2.4 DUNE PROFILES AND VEGETATION SURVEYS

Vegetation surveys were conducted in the field in December 2013 and May 2014 on six cross-sectional shore-normal profiles over dunes previously identified in the satellite images

(Table 8 and Figure 22). Contrasting processes and coastline trends were some of the criteria taken into account to select the sites. Other criteria to choose these sites were location (ideally, at least one dune should be approximately in the middle of the study site and the other two on the extremes), size (since larger dunes are easier to identify and delineate from aerial views), permanency (although mobile, dunes should be trackable on the images over time), and accessibility. As a result of this activity, three sectors (east, central and west) characterized by contrasting morphodynamic processes within the park were selected to study vegetation on the dunes.

Together with the vegetation survey, topographic profiles were made using an AT G6 Topcon level, a stadia rod and an open reel measuring tape. These profiles measured relative elevation for each dune with respect to the sea-land limit at the time of the survey. Along the profiles, topographic changes from the sea-land limit to the lee face of the dune were measured about every 5 metres or at shorter distances when an abrupt topographic change occurred.

The vegetation surveys were conducted utilizing contiguous 1 m^2 quadrats, where plant species and vegetation percentage coverage were identified (Figure 13). The profiles were oriented perpendicular to the shoreline, extending onshore from the coastline to the lee face limit of the dune (i.e., landward edge of the dune). Occasionally, on the lee face of the dunes dense patches of xerophytes were found, so it was not possible to place the quadrat there. Instead, approximate species proportions were visually estimated for these sectors.

Vegetation distribution and abundance was assessed utilizing the Shannon diversity index (eq. 3), which accounts for both abundance and evenness of the species present.

$$H = -\sum_{i=1}^{s} Pi * LnPi \qquad \text{(Eq. 3)}$$

where S is the total number of species in the community, and P_i is the proportion of individuals that belong to the ith species. Accordingly, high values of H (i.e., diversity) are found in samples with a high number of species that are evenly distributed.

Last, the Sørensen similarity index was used for comparing the incidence of species against every other profile; this index assesses profile similarities, with values above 0.5 indicating stronger relationships (Eq. 4). As evident from Equation 4, no weight is given to coverage proportion in the formula.

$$QS = 2C/A+B \qquad \text{(Eq. 4)}$$

where A and B are the number of species in samples (communities) A and B, and C is the number of species shared by the two samples.

In addition to the above, wind speed measurements over the dunes were taken during wind gusts at two heights over the surface (1 cm and 45 cm) with a Kestrel 3500 device.

Figure 13. 1 m² quadrat to identify and quantify vegetation (left) and topographic profile along dunes, the latter using an AT G6 Topcon level (right).

2.5 GEOMORPHOLOGY

Land morphology reflects the interaction between Earth surface geomorphological processes and the rock, regolith, and soil at Earth's surface (Bishop, 2007). There are a few methodologies describing different approaches to depict surface morphology on maps, depending on focus of a project and scale of study. Extended reviews describing the proposed approaches for medium scale geomorphological mapping are found in Demek and Embleton (1978), whereas a methodology for detailed scales (1:25,000 and 1:100,000) mapping was compiled by Demek (1972). Nonetheless, a common pattern within these methodologies is that they are explicitly or inherently based on hierarchical systems, where each system is divided into subsystems, and these in turn into wholes of still lower order (Richling, 1999). In hierarchical systems, higher levels are characterized by slower and larger entities (or low-frequency events), whereas lower levels are characterized by faster and smaller entities (or high frequency events) (Wu, 1999). Likewise, the effects of exceeding certain stress limits or thresholds become more apparent as the size of the responding unit increases, or as the time scale at which the landscape is viewed is extended (Campbell and Honsaker, 1982) (Figure 14). In effect, after simulating extreme waves approaching the Magdalena River mouth, Urbano et al. (2013) found that the expected highest waves approaching the port were those coming from the north, obtaining significant wave heights of 5.75, 6.25, and 6.85 metres for recurrence intervals of 10, 20, and 50 years, respectively. As expected, the consequences of the highest and least frequent waves will have a greater effect in transforming the landscape.

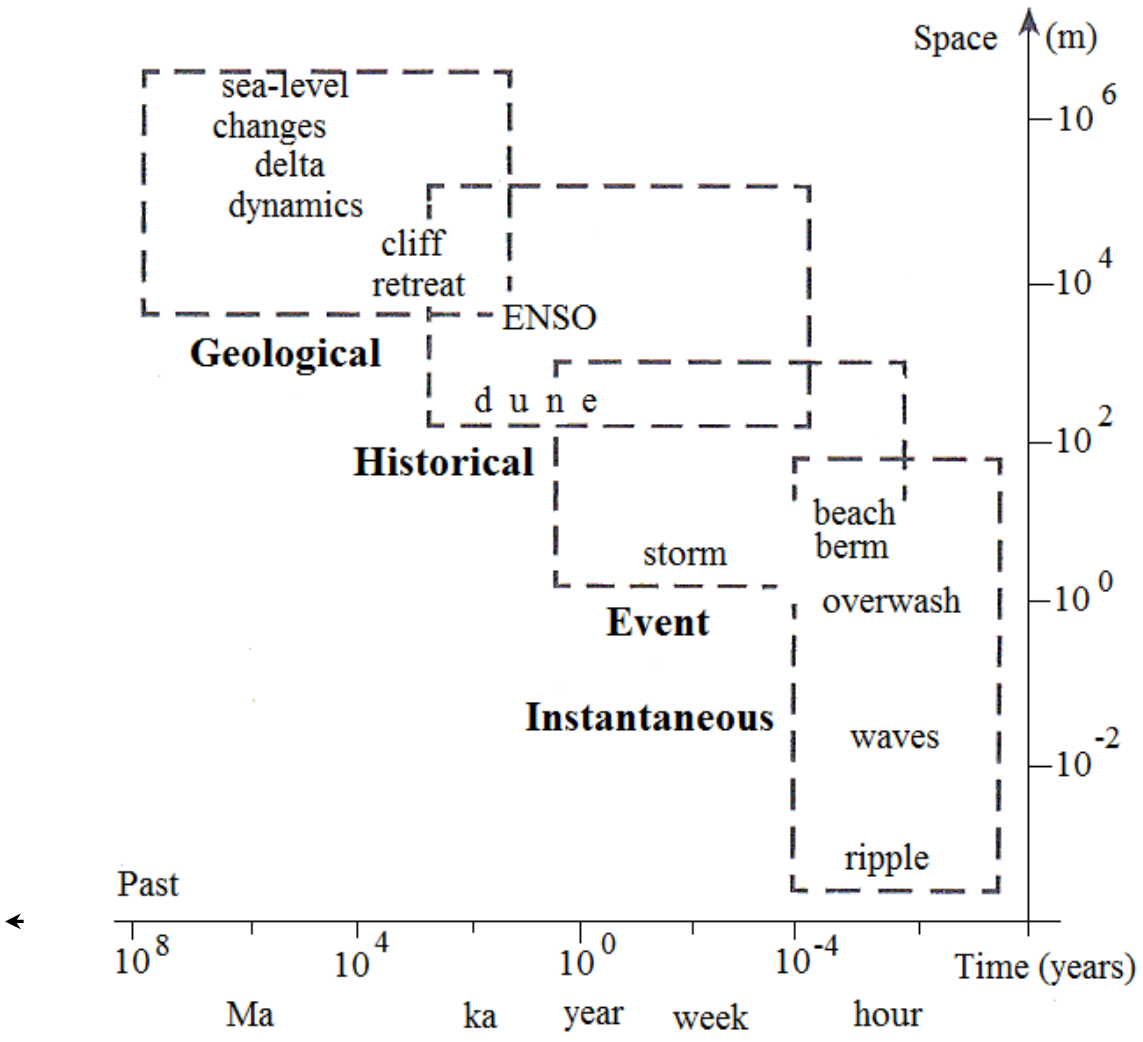

Figure 14. Representation of space and time scales phenomena in coastal systems. Examples of characteristic geomorphological features or landforms found nearby and within ISNP are shown (Modified from Woodroffe, 2003 and Murray-Wallace and Woodroffe, 2014).

Given the interplay of the factors described in this project (i.e., climate, coastal changes, bathymetry, vegetation) that contribute to shaping the landscape, a geomorphology map may be considered a synthesis of the aforementioned variables. Coastal, aeolian, and fluvial morphological units such as beaches, lagoons, dunes, and floodplains were delimited based on visual morphological interpretation of four panchromatic satellite images with 2 metre pixel resolution taken between 2010 and 2013. Different band combinations were applied using the

software ENVI to highlight specific features along the area. In that sense, the infrared band was particularly useful to identify flooded areas. Additionally, historical maps, previous geomorphology maps from the area (for example the works developed by Raasveldt and Tomic, 1958, and Bernal, 1996), and aerial photographs were compared with the satellite images in order to decipher landform evolution. The second fieldwork, undertaken in May 2014, was done after having a preliminary geomorphological map; therefore, when accessible, unidentified or uncertain features in the image were checked on the terrain.

This activity resulted in a geomorphology map linked to a database containing the geomorphological and coastlines files. As proposed by Gellert (1972), the main element of the content of detailed geomorphological maps is the genesis of the surface forms constituting Earth's relief. Accordingly, landscape units on this map were coloured differently in accordance with their origin, following mapping standards that suggest using green, blue and yellow tones to map units in which origin is related to marine, fluvial and aeolian environments, respectively. However, since it is not uncommon to have polygenetic landforms, whether a landform is classified as marine, fluvial or aeolian may be sometimes subjective. For instance, even though there is a definitive morphological imprint of aeolian process in coastal dunes, essentially they have a polygenic origin (marine and aeolian). Nevertheless, the geomorphology map colours point out the predominant processes most-recently shaping the landform.

Chapter 3 Results

The results related to recent climate trends of rainfall and wind, coastal and bathymetry changes overtime, as well as a description of dune vegetation and geomorphology, are presented in the this section.

3.1 CLIMATE

Linear regression models were used to identify the trends in rain and wind data taken at the weather stations of Santa Marta and Barranquilla airports. To verify whether or not the trends found were statistically significant, a *t* test, having as null hypothesis (H_0) that there is not a trend (e.g., no statistically significant changes are detected in the rain for the studied data series), and as alternative hypothesis (H_1) that there is in fact a trend, was run. Specifically, H_0 is rejected when the probability of obtaining a test result more extreme than the one observed is less that the chosen alpha value (Harris and Jarvis, 2011).

3.1.1 Annual Precipitation

To assess rainfall trends for the longest rainfall series from Santa Marta and Barranquilla airports, a linear regression model was fit to the data. The results of this analysis showed a statistically significant increasing rainfall trend over time for both stations (Tables 1 and 2 and Figure 15). Similar trends in the Colombian Central Caribbean for the period between 1960 and 2005 were reported by Pabón (2012).

Table 1. Summary statistics for a regression analysis of the relationship between mean annual precipitation and time for the weather station at Santa Marta for the period 1960-2012.

Parameter	**Estimate**	**Standard error**	***t***	***p***
β_o	-11737.13	3326.360	-3.529	0.000895
β_1	6.163	1.675	3.680	0.000563
R^2	0.2098			
R^2 Adjusted	0.1943			
$F_{(1,51)}$	13.54			0.0005634

Table 2. Summary statistics for a regression analysis of the relationship between annual precipitation and time for the weather station at Barranquilla for the period 1942-2012.

Parameter	**Estimate**	**Standard error**	***t***	***p***
β_o	-10533.15	3128.95	-3.366	0.001240
β_1	5.745	1.583	3.629	0.000537
R^2	0.1584			
R^2 Adjusted	0.1463			
$F_{(1,70)}$	13.17			0.0005365

Accordingly with Tables 1 and 2, the line equations resulting from the linear regression for Santa Marta and Barranquilla are, respectively:

$$y = -11737.13 + 6.16x \quad \text{(Eq.5)}$$

$$y = -10533.15 + 5.74x \quad \text{(Eq. 6)}$$

Dividing the estimate of the slope (β_1) by the standard error give *t* test values of 3.680 and 3.629 for Santa Marta and Barranquilla, respectively. The probability that these results arise

by chance is therefore less than $p = 0.005$ (see p values of 0.000563 and 0.000537 in Tables 1 and 2, respectively), so with a confidence larger than 95%, a statistically significant relationship is assured. According to equations 5 and 6, precipitation has increased 61.6 mm/decade and 57.4 mm/decade at the weather stations of Santa Marta and Barranquilla, respectively.

In order to verify whether the data are normally distributed, the Shapiro-Wilk (W) and Anderson-Darling (A) tests were used. The outcomes for these tests point out that for a significance value of $\alpha=0.05$, both stations have normal distribution (Table 3). In other words, given that the *p* values are larger than 0.05, there is no compelling evidence on which to reject the null hypothesis that the data are normally distributed. Therefore, the obtained outcomes, based on parametric tests (linear regression models), are valid for the precipitation data.

Table 3. Summary statistics to test for normality of annual precipitation for the weather stations at Santa Marta and Barranquilla.

Station/Test	**W**	**A**	***p-value***
Santa Marta/ Shapiro-Wilk	0.9417		0.1206
Santa Marta/ Anderson-Darling		0.7368	0.05155
Barranquilla/ Shapiro-Wilk	0.9746		0.1539
Barranquilla/ Anderson-Darling		0.4497	0.2691

To confirm that the observed upward trends in the rainfall are not the product of data autocorrelation−that is, the correlation between adjacent values in space or time (Clark and Hosking, 1986)−the nonparametric Mann-Kendall and Modified Mann-Kendall tests were used. Table 4 shows that for a confidence level of 95%, the *p* values found are smaller than 0.05−*Z*

values are larger than 1.96−; hence, the alternative hypothesis (i.e., a monotonic trend is present), is therefore accepted.

Table 4. Test results for the original and modified Mann-Kendall tests to assess trends in precipitation taking into consideration data autocorrelation.

Station	**Z**	**Modified Z**	***p* value**	**Corrected *p* value**	**Slope**	**Tau**
Santa Marta	3.199	7.145	0.00138	9.015e-13	6.066	0.303
Barranquilla	3.388	3.388	0.00703	0.00703	5.4	0.273

Rainfall variability in Colombia–and consequently river discharges–are controlled by the effects of both phases ENSO (Restrepo, 2005). Likewise, extreme events associated with either dry or wet seasons in the study site are generally related to El Niño and La Niña episodes, respectively. A visual comparison of yearly precipitation at each station with the Southern Oscillation Index (SOI) variations, reveals that the overall effect of decreasing (El Niño) and increasing (La Niña) interannual precipitation is observed for Santa Marta and Barranquilla weather stations. As a case in point, reportedly extreme El Niño and La Niña events occurred during 1992-1993 and 2011-2012, respectively (Figures 15 and 16).

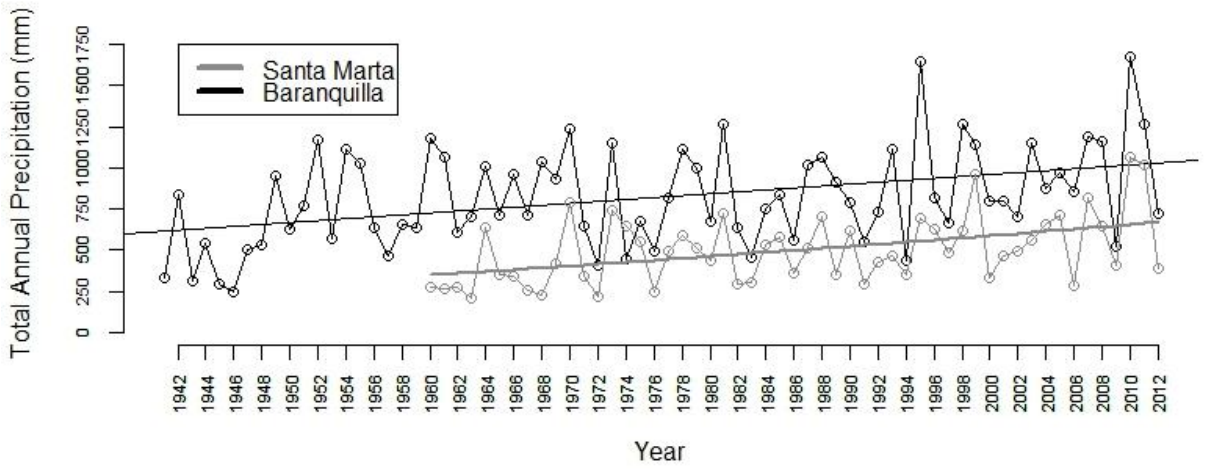

Figure 15. Yearly total rainfall positive trends at Santa Marta and Barranquilla weather stations (Source: modified by the author from data collected by IDEAM).

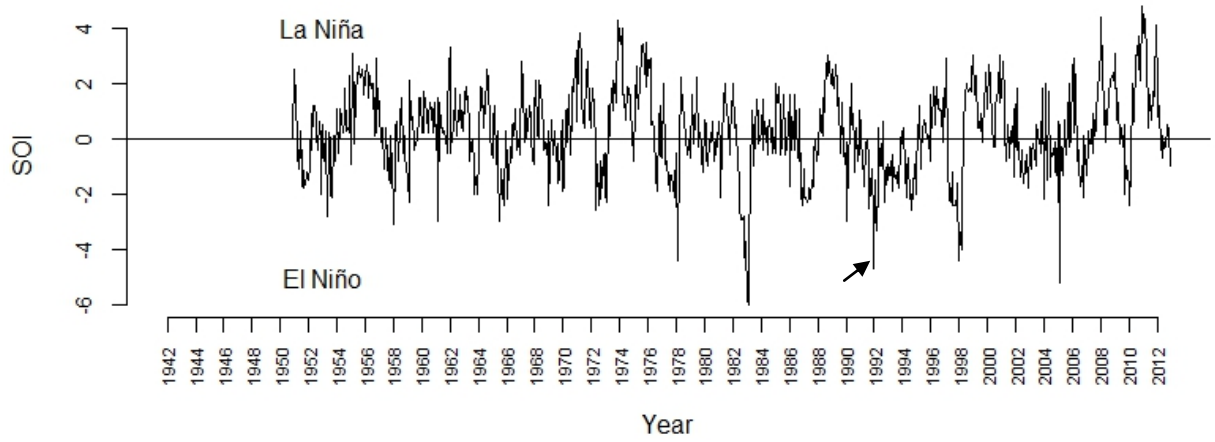

Figure 16. Variability of the yearly SOI index for the period 1951-2012. El Niño years are associated with negative values while La Niña years are positive values. The arrow emphasizes a strong Niño event in 1992 (Source: modified by the author from data provided by the NOAA web site, http://www.esrl.noaa.gov/psd/data/correlation/soi.data).

3.1.2 Wind

A decreasing trend in the total number of yearly wind events with speeds over 6 m/s was found from 1981 to 2012 at the Santa Marta weather station. Unfortunately, missing data during

1988-1989 result in an incomplete record for the analyzed period. Nonetheless, the outcomes for a linear regression model based on the available data are shown in Figure 17 and Table 5.

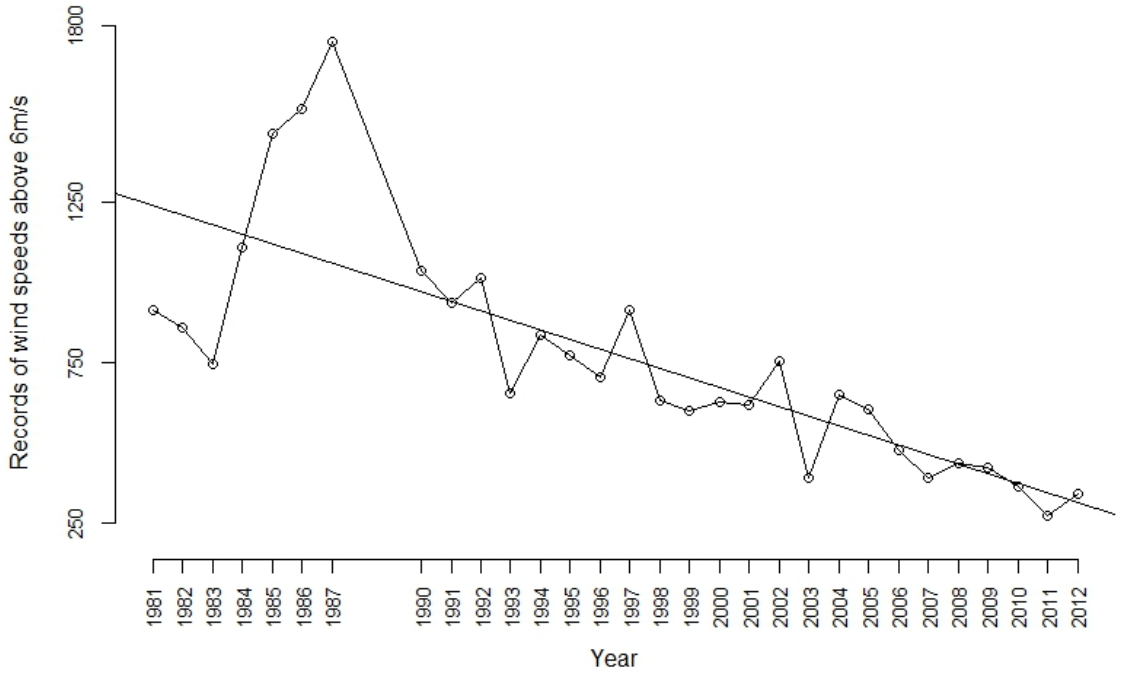

Figure 17. Wind events of over 6 m/s from 1981 to 2012 (Source: modified by the author from data yielded by IDEAM).

Table 5. Summary statistics for a regression analysis of the relationship between wind velocity and time for the weather station at Santa Marta.

Parameter	**Estimate**	**Standard error**	***t***	***p***
β_o	60330.498	8856.519	-6.812	2.12 e-07
β_1	-29.830	4.435	-6.726	2.66 e-07
R^2	0.6177			
R^2 Adjusted	0.6041			
$F_{(1,28)}$	45.24			2.655e-07

In accordance with the above table, the line equation resulting from the linear regression for the wind trend through time is:

$$y= 60330.5 - 29.8x \quad \text{(Eq. 7)}$$

Since *p* values in Table 5 are much less than 0.05, the probability that the resulting decreasing wind trend was found by chance is less than 5%. Remarkably, the maximum number of episodes of over 6 m/s was found in 1987, which coincides with an El Niño event. In contrast, the lowest number of wind episodes of over 6 m/s occurred in 2011, a year that presented La Niña phase (Figure 16). Overall, Equation 7 indicates that since 1981, a strong decreasing trend of wind events above 6 m/s is apparent.

Likewise with rainfall data, for wind data the Shapiro-Wilk (W) and Anderson-Darling (A) tests were used to check for normality, whereas the modified Mann-Kendall test was used to check data autocorrelation. The outcomes for these tests are shown in Table 6 and Table 7, respectively.

Table 6. Summary statistics to test for normality of wind data taken in Santa Marta.

Test	**W**	**A**	***p-value***
Shapiro-Wilk	0.9081		0.01334
Anderson-Darling		0.8175	0.03054

Table 7. Test results for the original and modified Mann-Kendall tests to assess trends in wind taking into consideration data autocorrelation.

Station	**Z**	**Modified Z**	***p* value**	**Corrected *p* value**	**Slope**	**Tau**
Santa Marta	-5.55	-7.07	0.00138	1.4755e-12	-30.32	-0.7180

The results shown in Table 6 reveal that wind data are not normally distributed. Since the probabilities (*p* values) shown in Table 6 are given for normally distributed populations, the validity of the results shown in Table 6 is somewhat uncertain. However, the outcomes of the Mann-Kendall test and modified Mann-Kendall test−nonparametric tests−shown in Table 7

indicate that indeed a monotonic decreasing trend is present in the wind data. The implications of these outcomes are explained in the Discussion chapter.

In addition to the described tests, the residuals of both precipitation and wind data were calculated for the mean to assess whether their distributions have homoscedasticity or heteroscedasticy; the latter through the Breusch-Pagan test. The outcomes indicate that the mean of the residuals is zero, and that the variance of the residuals is constant across all levels of predicted values (so-called homoskedasticity).

3.2 COASTLINE CHANGES

Based on the results obtained after running DSAS, it is noticeable that erosion trends increase from Tasajera to El Torno lagoon, locally reaching average erosion rates up to 15 m/year seaward from the lagoon known as *Cuatro Bocas* (Figure18). In contrast, close to the Magdalena River mouth, at the westernmost extreme of the study site, accretion processes are dominant. Nonetheless, average coastline changes of -4.8 m/yr for the period 1953-2013 reveal that erosion processes are predominant along the shoreline, currently reflected by the generalized beach retreat, scarped dunes, and by the frequent overwash events. As Dolan et al. (1980) noticed for a study carried out along the barrier island chain between New Jersey and North Carolina, it is worth keeping in mind that the calculation of mean rates of coastal changes for long stretches does not give an accurate picture of the local dynamics, as most of the barrier islands have irregular change patterns.

Within ISNP, when sorting out coastline changes between 1953/1954 to 1985, from those between 1985 and 2013, the latter shows larger erosion values for the same transects from

Tasajera to Cuatro Bocas (Figure 18). However, west from Cuatro Bocas, erosion has been decelerating since the 1980s. Conversely, at the westernmost area of ISNP, west of El Torno lagoon and the Magdalena River mouth, accretion processes are dominant for coastlines transects from 1953/1954 to 1985, as well as those from 1985 to 2013 (Figure 18). Unfortunately, aside from historical maps from the 19th century, no coastline data are available prior to the jetties and harbor construction. Therefore, assessing the impact of these structures in terms of coastal changes is not feasible.

The historical maps available (e.g., Figures 3 and 4), make evident the large scale changes that have taken place in ISNP since the 1800s, where a former active multichannel delta had been replaced by a sandy bar shaped by wave and wind action. For instance, in the westernmost sector of this project, a small delta-island (formerly known as Isla Los Gómez), that separated the river channel before flowing into the ocean disappeared during the early 20th century.

Overall, quantifying coastline changes during the last 60 years was the starting point to select sites with contrasting erosion and accretion rates for the surveys. During the fieldwork, the vegetation and topography of the dunes over these sites were surveyed and compared (Figure 22 and Table 8).

Table 8. Location of surveyed dunes.

Profile Number (From E to W)	Starting X/Y Position	Length (m)	1. Dune Direction*	2.Coastline Direction	Angle B/W 1 and 2
1	968273/1705497	88	S20W	N90W	70
2	967089/1705355	202	S16W	N90W	74
3	939800/1710253	115	S42W	N67W	74
4	939411/1710395	94	S36W	N67W	87
5	922869/1717045	105	S53W	N64W	63
6	918305/1718821	115	S62W	N56W	69

*Dune directions were taken with a compass pointing from the shoreline to the stoss face of the dune.

3.2.1 Coastlines Error Assessment

Following Del Río and Gracia (2013) equations indicated in the Methodology chapter, beach slope in the intertidal zone, aerial photographs resolution, and georeferencing accuracy have been considered to estimate the error when tracing coastlines. Based on specific aerial photographs taken in 1954 and 1985, where the highest errors after georeferencing were obtained (largest RMSE value), the parameters described in Table 9 were used.

Table 9. Parameters used in the determination of uncertainty for a HWL proxy.

Image	*G* (m)	*R* (m)	$M_{1\text{-}2}$ (m)	Tanβ	$D_{1\text{-}2}$ (m)	Interval (year)	*D* (m)
1954	14	1	0.40	0.17	2.35	31	0.0076
1985	22.5	0.5					

G: RMSE of the georeferencing; *R*: pixel size; M_{1-2}: height difference between the two high waters; tanβ: intertidal beach slope; D_{1-2}: tide-related horizontal variability in HWL position between the two photographs; *D*: annualized physical component of error.

According to equations 1 and 2, when adding the error for 1954 and 1985 aerial photographs, the following results were found for a worst-case scenario (i.e., RMS of 14 m and 22.5 m for the photographs taken in 1954 and 1985, respectively):

$$E_{1954} = \pm\sqrt{1^2 + 14^2 + (\frac{0.40}{0.17})^2}$$

$$= 14.03 \text{ metres}$$

$$E_{1985} = \pm\sqrt{0.5^2 + 22.5^2 + (\frac{0.40}{0.17})^2}$$

$$= 22.63 \text{ metres}$$

$$E_{rate} = \pm\sqrt{14.03^2 + 22.63^2}/T \qquad = 26.62/31 \quad = \pm 0.86 \text{ m/yr}$$

Otherwise stated, coastline change rates would only be significant if they are above ± 0.86 m/yr. After checking the coastal changes AOR values, it was found that most of the values where coastline changes range between $\pm$0.86 m/yr are located on easternmost extreme of the study site, close to Tasajera. These outcomes within the margin of error do not necessarily mean that the coastal changes there do not exist. On the contrary, because this area is close to sediment sources such as the Córdoba (Figure 32) and Toribio rivers, and somewhat sheltered from the direct impact of wave action, these smaller changes in comparison to areas west from Kangarú are not surprising (Figure 18).

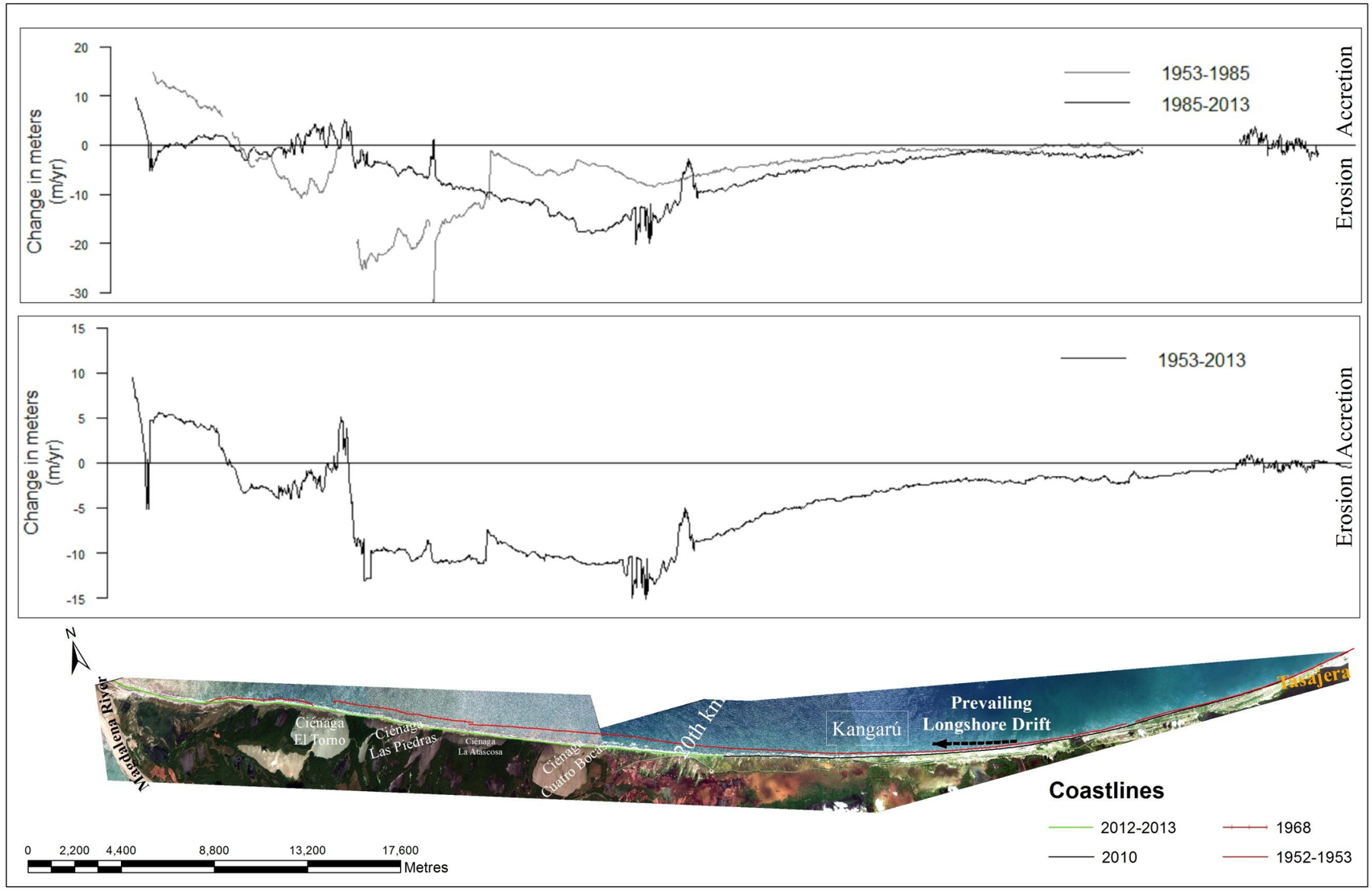

Figure 18. Coastline position changes along Isla Salamanca since the early 1950s.

3.3 BATHYMETRY CHANGES

As described in the methods section, three different interpolation models were applied to the bathymetry charts. In so doing, a comparison of the resulting surfaces was performed to see whether IDW, spline or the Kriging interpolation method was more reliable for modeling the bathymetry. Within Kriging, two different approaches were attempted, that is, the spherical and Gaussian models. As detailed below, the Gaussian model was the chosen method to assess the changes on bathymetry over time.

A comparison of the Gaussian semivariogram model outcomes with the spherical semivariogram, resulted that on average, the former model obtained values closer to the "true" depth–those values that were deleted purposely from the original chart–than the spherical semivariogram. In so doing, the parameters shown in Table 10 and the semivariogram graph are taken into account (Figure 12). After all, it was found that the Gaussian polynomial regression fits the bathymetry surface better than the spherical polynomial regression (Table 11). Swales (2002), while developing geostatistical estimators of short-term changes for a beach in New Zealand, also found that the best model to capture beach changes was obtained with Kriging, specifically with the Gaussian polynomial regression.

Table 10. Parameters for spherical and Gaussian models.

Kriging Model	Bathymetry Year	Range	Psill	Nugget
Spherical	1938	32991	16782	1
Gaussian		15527	12563	1
Spherical	2012	32991	16782	1
Gaussian		9457	12270	1

Table 11. Comparison of the outcomes for the spherical and Gaussian semivariograms interpolation models after deleting known deep values from the 2012 survey.

PARAMETERS					
FID	**X**	**Y**	**2012 Survey/ Deleted depth (metres)**	**Spherical Semivariogram/ Depth (m)**	**Gaussian Semivariogram/ Depth (m)**
03	919708	1723509	109	128	121
207	942708	1715749	126	109	121.9
267	976555	1721804	48	43.15	42.5
288	974488	1707261	3.5	1.88	3.3
540	968910	1726431	291	288.27	284.22
			∑DIFFERENCE	**45.22**	**15.22**

3.3.1 Error Assessment

Accurately quantifying error from output data obtained by aggregating or disaggregating given input data from different sources and scales is challenging. For bathymetry surveys, the International Hydrographic Organization (IHO) is in charge of establishing the standards for hydrographic surveys. Recognizing that there are both depth independent and depth dependent errors that affect the uncertainty of the depths, the IHO provides the formula below to compute, at the 95% confidence level, the maximum allowable Total Vertical Uncertainty (TVU) for specific depths:

$$\text{TVU} = \pm\sqrt{a^2 + (\text{b x d})^2} \qquad \text{(Eq. 8)}$$

where **a**, represents that portion of the uncertainty that does not vary with depth (i.e., precision of the device), **b** represents the portion of the uncertainty that varies with depth (it is known that deeper depths are related to larger errors), and **d** is depth.

For instance, for depths ≤ 20 metres, based on values given on tables by the IHO (2008) for a and b, the uncertainty obtained is:

$$TVU = \pm\sqrt{0.5^2 + (0.013 \text{ x } 20)^2}$$

$$TVU = +/- \ 0.56$$

Hence, bathymetry changes with values less than or equal to +/- 0.5 metres are considered within the margin of error of this project.

3.3.2 Bathymetry Changes Assessment

Contrasting changes were found between the 1938 and 2012 sea bottom surfaces. With few exceptions, a general trend of surface decrease over time for those contours close to the coastline was discovered. This pattern of loss of sediment from the sea bed matches well with the coastline trends for a period beginning in the early 1950s and lasting until 2012, with retreating coastlines being the predominant process along the study site. In contrast, most of the areas that have experienced an increase in the elevation of the surface of the sea bottom over time, except for a single location in the westernmost sector of the study site, are located beyond the 10 m depth contour.

Another result that is worth noting is that at the sites with the highest coastline erosion rates (20th km-Cuatro Bocas lagoon), the 10 m bathymetry contour for 2012 appear consistently closer to the shoreline than the 1938 10 m contour (Figure 20). In other words, close to the shoreline, the bathymetry for these sites with the highest erosion is now considerably deeper than was the case in the past. It is known that deeper nearshore bathymetry reduces wave refraction and wave energy loss due to friction at the seabed (Aagaard and Sørensen, 2013).

Regardless of the clear trends in erosion and accretion, some of the sea bottom change values found are within the margin of error (± 0.56 m). Akin to coastal changes, these minimal changes may be related to either instrumental or human errors, or they may also be revealing minimal changes in areas where the wave energy is buffered by the bathymetry configuration. This seems to be the case at the extreme east end of the study site (gray polygons in Figure 19), an area where the sea bed contours are widely separated, forming a shallow platform (Figure 2). Contrastingly, at the top center of Figure 19, positive change values of over 20 m were found (see dark green polygon in Figure 19). These high volume changes at depths larger than 280 m are hardly explainable by oceanic processes. When comparing data taken in shallow and deep waters, it is expected that the data closer to the shore, with higher density data spacing, have less uncertainty in both vertical and horizontal values; thus, the aforementioned large changes, occurring at depths of over 300 m, could be attributable to either error propagation or large scale submarine movements, such as the slope processes described by Nummedal (1982) on the Mississippi River delta front.

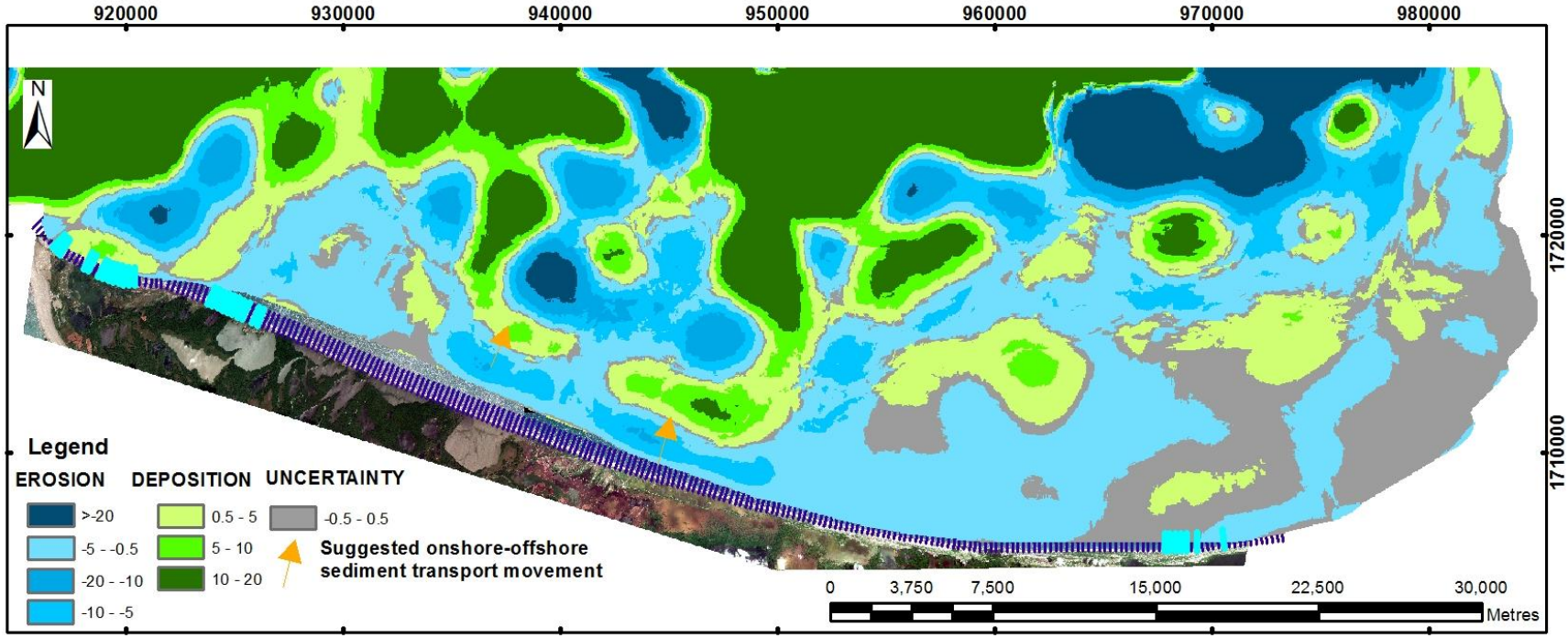

Figure 19. Assessment of bathymetric changes between 1938 and 2012 (the highlighted transects point out locations of accretive shoreline trends over time, whereas blue transects are indicating erosive shoreline trends). In the legend, eight main areas of change are indicated from dark blue to dark green as follows:

1. More than 20 m of seabed deepening
2. Between 20 and 10 m of seabed deepening
3. Between 10 and 5 m of seabed deepening
4. Between 5 and 0.5 m of seabed deepening
5. Up to 5 m of seabed shallowing
6. Between 5 and 10 m of seabed shallowing
7. Between 10 and 20 m of seabed shallowing
8. More than 20 m of seabed shallowing

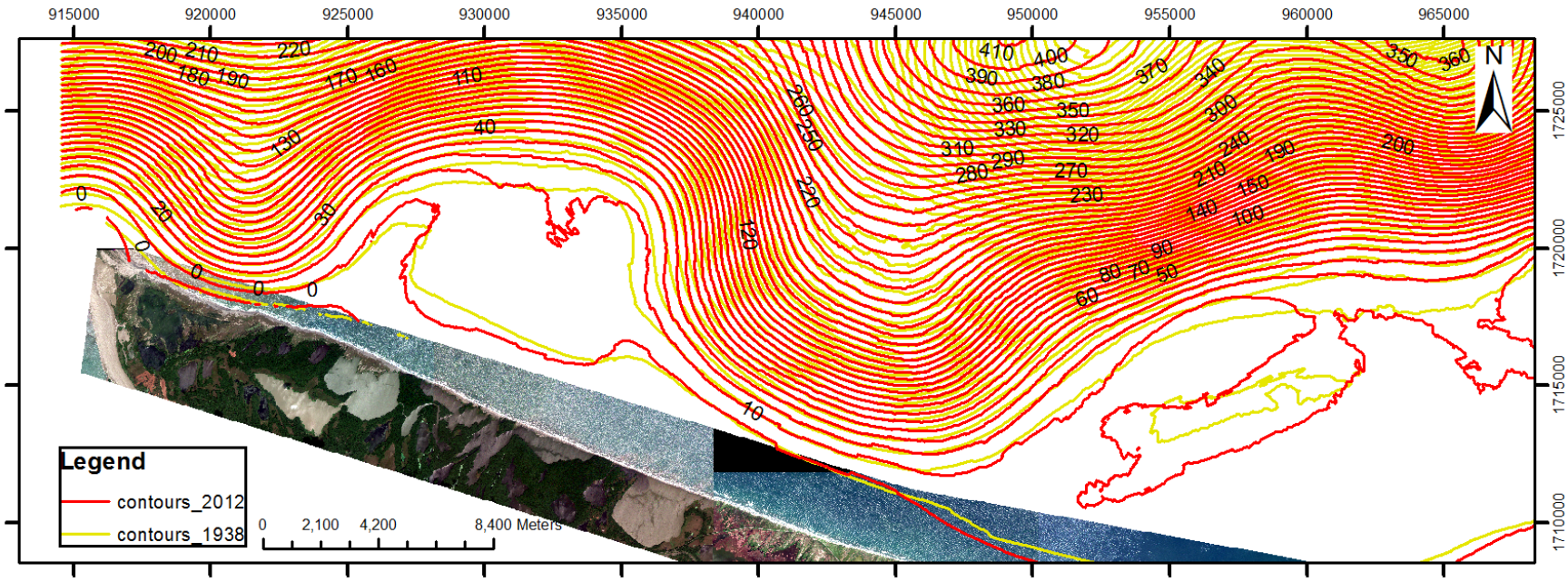

Figure 20. Bathymetric contours for 1938 and 2012 from the 20th km to the Magdalena River mouth.

3.4 DUNE EVOLUTION

Two different dune types can be recognized along the study site: parabolic dunes and embryo dunes. Within the parabolic dunes, vegetated scarped dunes, and backshore vegetated (or inactive dunes) were identified. Vegetated scarped dunes are so characterized because they are repeatedly affected by wave action and hence are scarped; another common feature is that they are interdigitated with either washover fans or overwash channels. Embryo dunes, on the hand, are located on the western sector, where the copious supply of sediment provided by the littoral drift and Magdalena River, added to the coastline direction, provide favorable conditions for the continuous formation and evolution of these small dunes. Inactive dunes, on the other side of the spectrum, are usually deflated and located landward from the road, away from the direct influence of wave action.

Based on the size and landward location of parabolic dunes, it is plausible that the stretch of coast within ISNP once had the conditions that have contributed to dune formation, that is to say, ample fine to medium sand supply, winds blowing directly onshore due to the east-west oriented coastline, and presumably dissipative beaches. Yet, after analyzing the dunes on historical aerial photographs and during fieldwork, it was observed that with the exception of the westernmost sector, dunes are no longer forming; instead, they are retreating as a result of coastal erosion.

In accordance with fieldwork visits and remote sensing images, it was found that dunes are less affected by erosion in the easternmost area, an area where coastline changes are within the margin of error, than the dunes located west of Kangarú to Cuatro Bocas (Figure 1). In

contrast, the westernmost area is characterized by abundant low embryo dunes, also termed shadow dunes (Hesp, 1981)

The maximum wind speeds measured in the field, taken at dune brinks at a height of approximately 2 cm, and at 45 cm above the surface, were 5.6 m/s and 8.6 m/s, respectively. These values were obtained in dune number 5 (Figure 22 and Table 8), a dune reaching a brink height of 3.80 metres APSL. Nonetheless, these data were taken on December 21st, 2013, but the strongest winds usually occur from January through February.

Dune direction analysis over the satellite images reveals that parabolic dunes in the study site are neither parallel between themselves, nor completely perpendicular to the coastline; instead, when moving westward from Tasajera along the coastline, dunes increasingly shift from north-south to southwest orientations (Table 8), in what seems to be a tandem arrangement between wind and coastline direction. Specifically, from east to west dunes "rotate" clockwise from directions around N-S near Tasajera to S60W close the mouth of the river (Table 8). In that sense, the most extensive dune fields were observed landward of the 20th km (Figure 21) and west of El Torno (Figure 1).

Figure 21. Image taken on January 22nd, 2013 showing 1. stabilized dunes at the 20th km with dunes length up to 1.3 km. 2. Overwash channels approximately parallel to the direction of the dunes. 3 and 4. Location of overwashes detailed in figure 30.

3.4.1 Vegetation on Surveyed Dunes

Six dunes associated with different erosive and accretive coastline changes were chosen to characterize their vegetation after analyzing coastal changes recorded in aerial photographs and while developing fieldwork (Figure 22 and Table 8). The dunes' topographic profiles of the dunes along with a scheme showing their associated vegetation (not to scale) are shown in Figures 23 to 28. In those schemes, because species in a single quadrat can overlap, a greater than 100% total cover was found for dunes 2, 3 and 4.

Figure 22. Dunes where topographic profiles and vegetation transects were made (photos 1-5 were taking looking to the southwest; photo 6 was taken to the northeast).

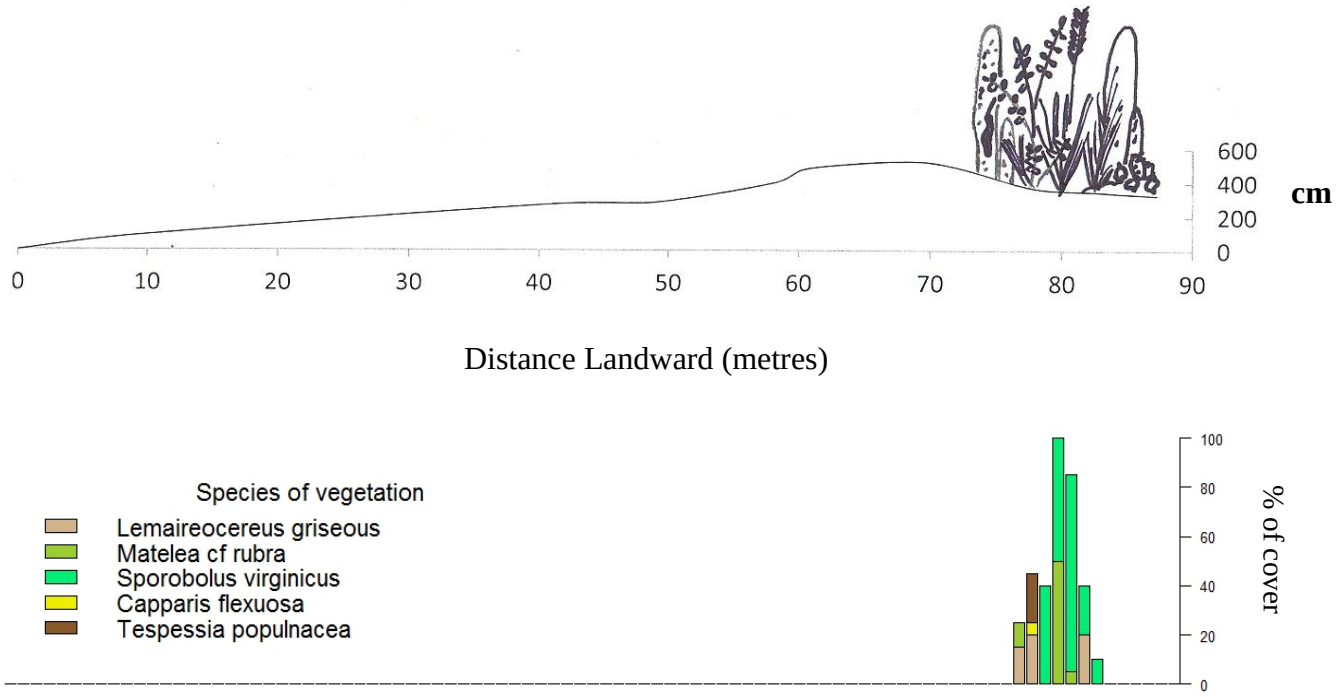

Figure 23. Vegetation cover per m^2 (%) along Dune 1 (X=968273/Y=1705497).

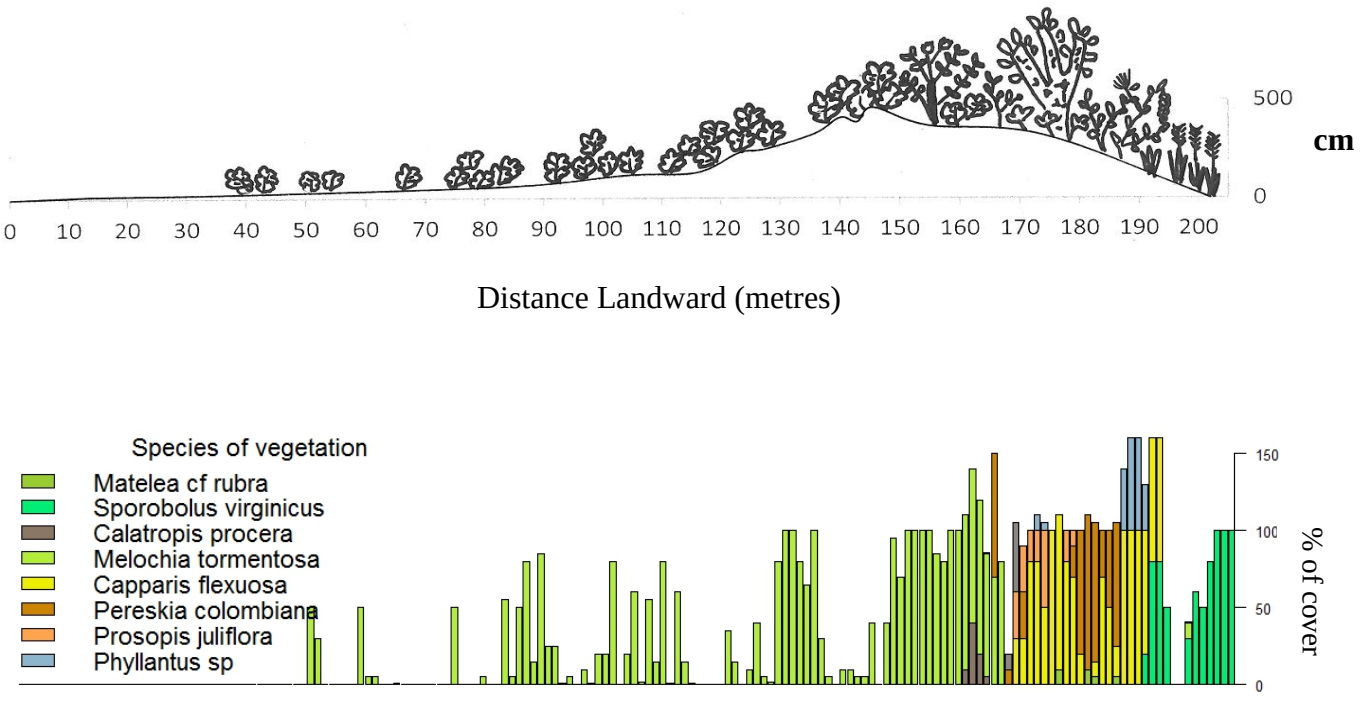

Figure 24. Vegetation cover per m^2 (%) along Dune 2 (X=967089/Y=1705355).

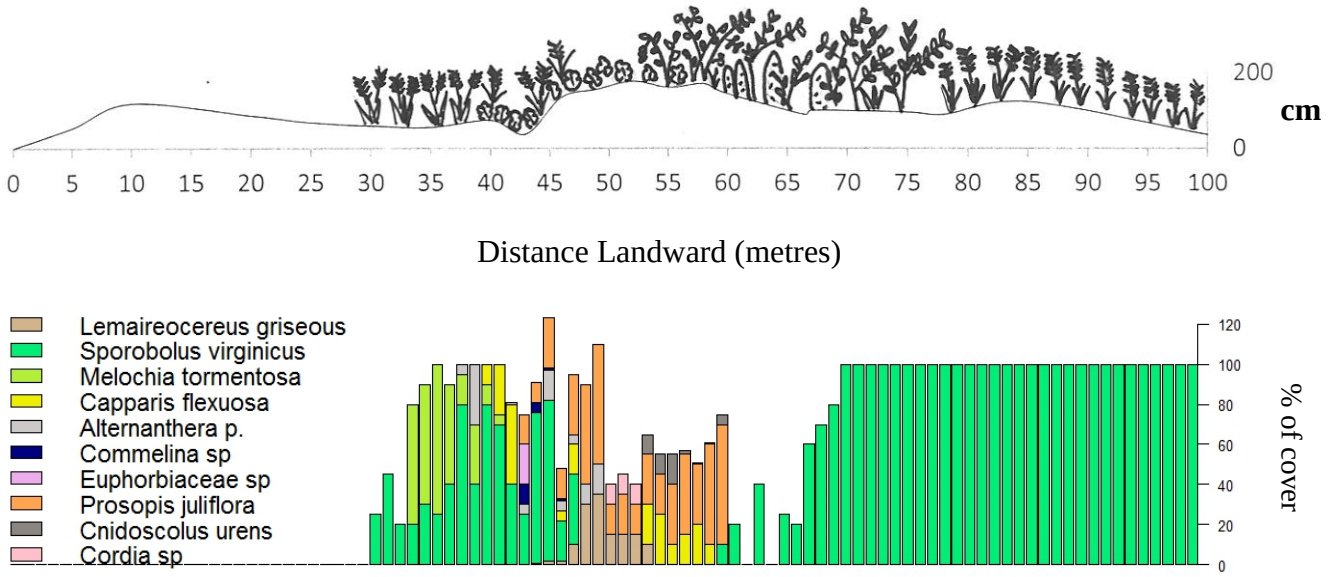

Figure 25. Vegetation cover per m^2 (%) along Dune 3 (X=939800/Y=1710253).

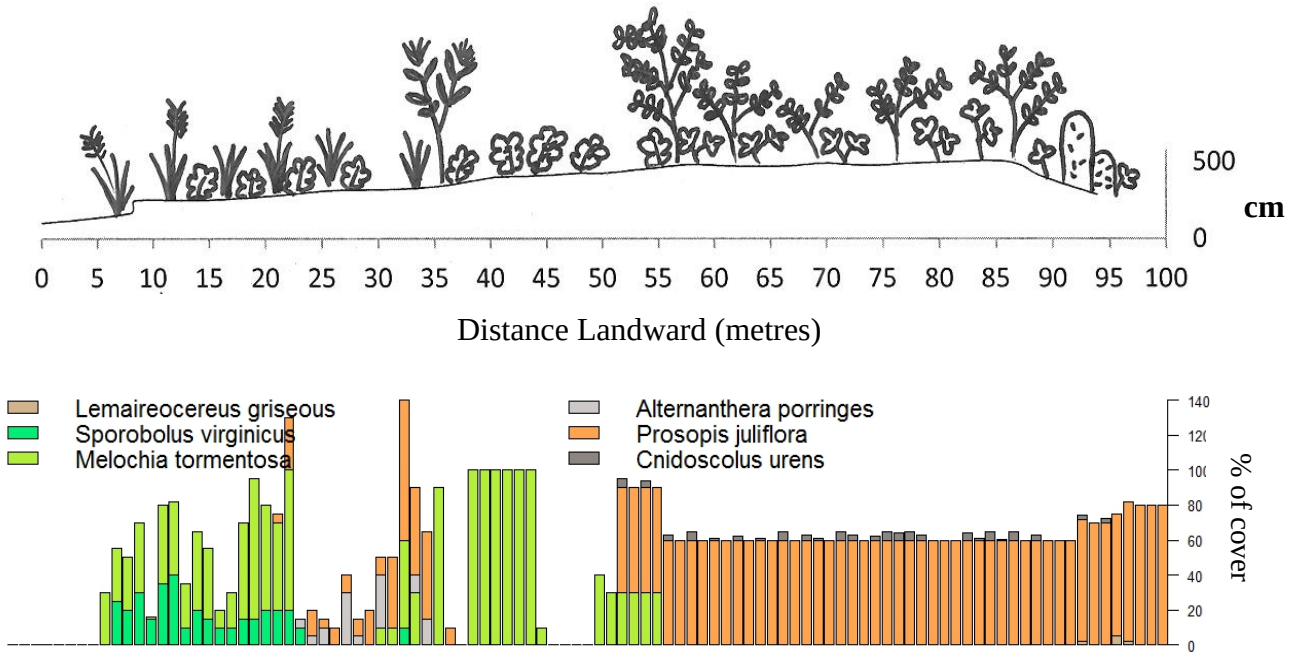

Figure 26. Vegetation cover per m^2 (%) along Dune 4 (X=939411/Y=1710395).

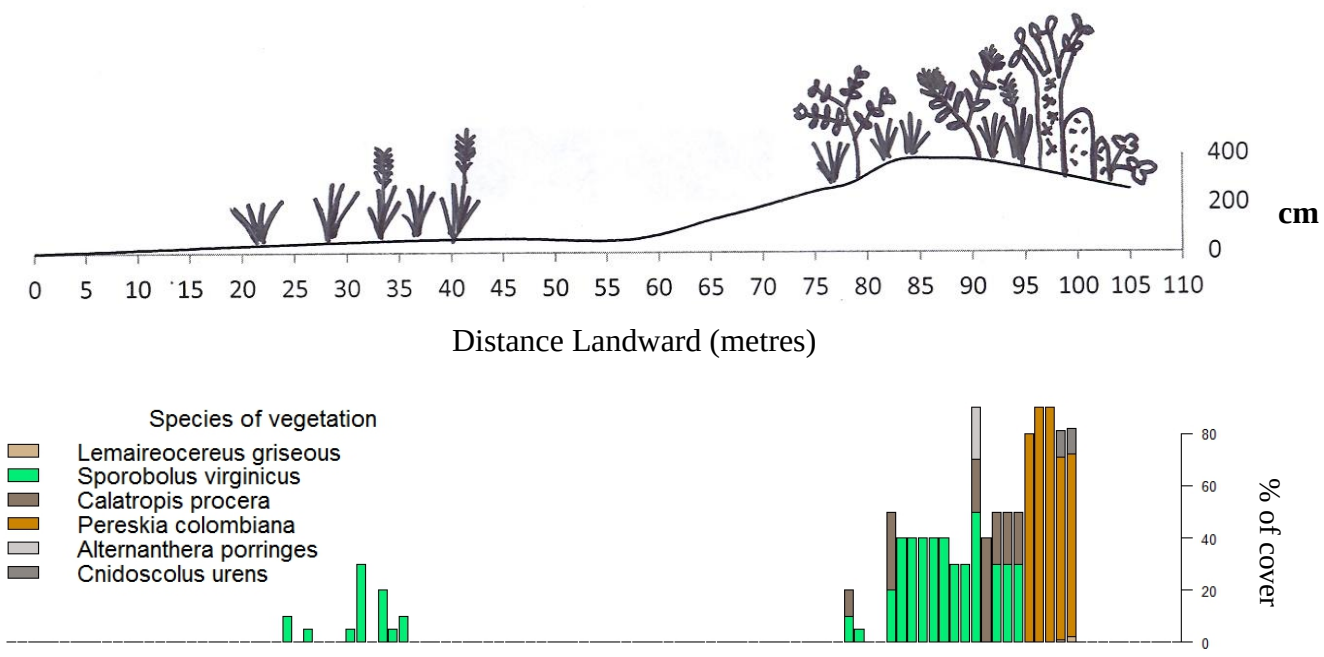

Figure 27. Vegetation cover (%) per m^2 along Dune 5 (X=922869/Y=1717045).

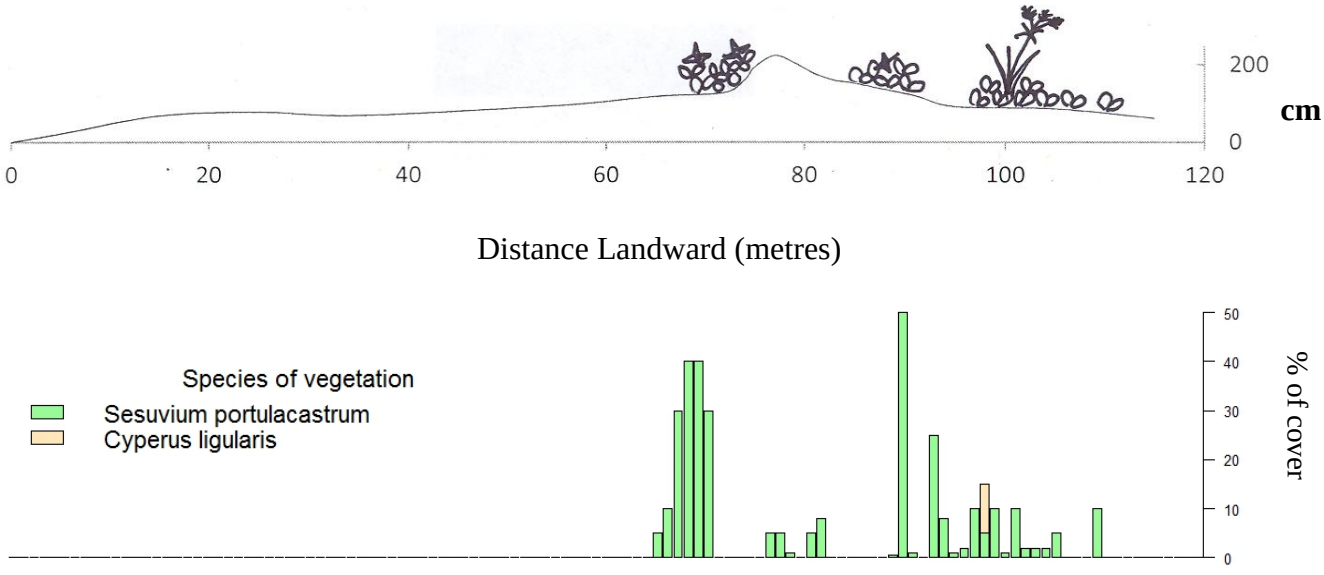

Figure 28. Vegetation cover (%) per m^2 along Dune 6 (X=918305/Y=1718821).

Akin to coastline changes and dune direction, vegetation over the dunes changes from east to west along ISNP. For instance, when comparing dune vegetation under erosional or accretional conditions, the former not only have higher species diversity, but are also more populated. Under the assumption that high, vegetated, and scarped dunes are older than low unvegetated embryo dunes, it is somehow expected that old dunes have more plant diversity and abundance since they have had a longer time to establish larger diverse plant assemblages than embryo dunes. Analogous outcomes were reported by Bitton (2013) while studying vegetation over scarped dunes in the Florida Panhandle.

Common species found on scarped dunes in the park are *Calatropis procera*, *Stenocereus griceous*, *Cnidoscolus urens*, *Capparis flexuosa*, *Pereskia colombiana*, and *Prosopis juliflora* (Figures 23, 24, 25, 26). These species were not found on young dunes, but rather only on old dunes affected by coastal/dune retreat. Conversely, accretive sectors located close to the Magdalena River mouth are characterized by unvegetated embryo dunes or embryo dunes with a few isolated patches of *Sesuvium portulacastrum* and *Cyperus ligularis* (Figure 28). Field observations indicate that some sediment and detritus coming from the Magdalena River supply this area, providing sediment for both beach and dune development.

The Sørensen index, a parameter to assess the similarity between the dunes in terms of vegetation, indicated that Dune number 6 is quite different from the other dunes. Conversely, Dunes 2, 3, and 4 have many species in common and are therefore similar (Table 12). Sørensen index values smaller than 0.5 may offer comparisons between dunes formed at different times, thus presenting different stages of evolution.

The diversity index value indicates that the dune with the highest diversity index (i.e., the largest number of species) is Dune 3, located in the area with the highest erosion rates since the 1950s. By contrast, Dune 6, where accretive processes are dominant, has the lowest diversity index (Table 12). To sum up, when comparing erosive dunes and dunes located in areas under accretion, the former group have not only higher species diversity and density, but also have a more advanced successional stage.

Table 12. Matrix of Sørensen similarity index and Diversity Index (Italic)

SORENSEN INDEX/*DIVERSITY INDEX (H)*						
	Dune1	Dune2	Dune3	Dune4	Dune5	Dune6
Dune 1	*1.33*					
Dune 2	0.47	*1.44*				
Dune 3	0.47	0.73	*1.55*			
Dune 4	0.31	0.56	0.55	*1.12*		
Dune 5	0.4	0.4	0.27	0.54	*1.05*	
Dune 6	0	0	0	0	0	*0.13*

3.5 GEOMORPHOLOGY

A thoughtful interpretation of present day geomorphology requires understanding the imprints left by past processes. In that sense, historic maps published in the early nineteenth-century indicate that during that time the Magdalena River and the lagoons at Isla Salamanca were directly connected through channels. According to Figure 3, the oldest map obtained, the area at that time was an active delta. From later maps it may be deduced that as time passed, sediment filled the river-lagoons connections, resulting in a gradual decrease in fluvial-dominated processes in favour of increasing wave-dominated processes shaping the landscape.

3.5.1 Mapping Landscapes/Geomorphology Map

Notwithstanding the numerous methodologies of landscape synthesis, most of them are grounded in hierarchical schemes, where smaller units are contained by larger units. Consequently, moving upwards towards smaller scales, landform units represented by polygons on a map may change to lines or symbols, whereas moving downward, landforms (polygons) may be decomposed into smaller features. In cartography this is termed a scale-dependent rendering (Dramis et al., 2011). From the existing hierarchic mapping systems' proposals (e.g., Demek, 1972; van Zuidam, 1986), the Salerno University Hierarchical Multiscale Taxonomy approach was selected for this project because, while taking advantage of GIS tools such as database building, it embraces many of the previous methodologies. From the nine hierarchical levels of the Salerno system, this work focuses on mapping level 7 or landform complexes (Figure 29). In the Salerno methodology, level 1 (not shown in Figure 29) contains the largest physiographic entities. Landform complexes include mid-size landforms produced by multiple geomorphic processes, like large river channels, coastal arcs, and large deflated dunes.

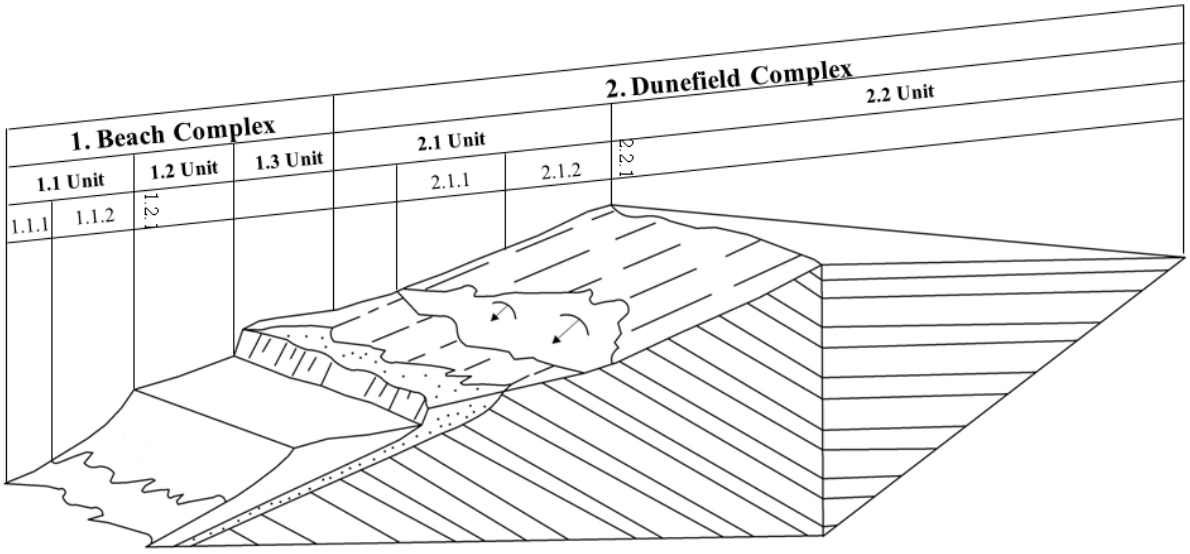

Legend

1.1 Shoreface unit	2.1 Stoss face unit
1.1.1 Intertidal zone component	2.1.1 Scarp component
1.1.2 Beach face component	2.1.2 Ramp component
1.2. Berm unit	2.2 Lee face unit
1.2.1 Berm scarp component	2.2.1 Brink component

Figure 29. Nested hierarchic sequence of landforms with subdivisions indicated on legend (Modified from Dramis et al., 2011).

On a regional landscape scale (<1:100,000), at present the shore in the park is a barrier coast with one free end. That is, attached to the continent by one of its limits (western end), and a free end at the Ciénaga Grande de Santa Marta mouth (eastern end). A similar barrier system to the current Isla Salamanca regional landscape, described by Benavente et al. (2013) for the Sancti Petri spit, is located on the southwestern Spanish Atlantic coast. They classified the landform as mixed formation between spit and sand barrier. Within the park, the areal extent of the following complexes were mapped: beaches, dunes, salt flats, floodplains, lagoons, channels

and road. A description of the most common features for each of these landforms is given in the following pages.

3.5.1.1 Beaches

Mapped beaches are limited to the subaerial fringe between mean high water level and mangroves, lagoons or dunes located landward (see Picture 2 on Figure 33). By far, eroding beaches are more common than accretive beaches along the shoreline of the study area. Normally, beach width, only taking into account dry areas, ranges from 5 to less than 0.5 metres during the months characterized by the most extreme wave conditions (i.e., December to March).

On the other hand, as mentioned in the Coastline Changes section, the westernmost sector is characterized by having accretive processes during the last decades; taking into consideration the constantly changing dynamic between embryo dunes and beaches in that sector, the limit between these units is unclear. Nonetheless, adding beaches to active dunes, they reach widths of over 60 metres in the area between Las Piedras lagoon to the Magdalena River mouth (see Picture 6 on Figure 22 and Figure 31d)

Another unit closely related to beaches and dunes is washover fans; this landform unit is normally produced during storms by overwash processes flowing over beaches and dunes, and into lagoons (Figure 30). In spite of their key role in terms of the barrier evolution, the scale of this work (1:10,000) is not detailed enough to map washovers; so, they were joined to beach polygons. Yet, washovers were identified on the terrain and taken into account to properly understand shore evolution.

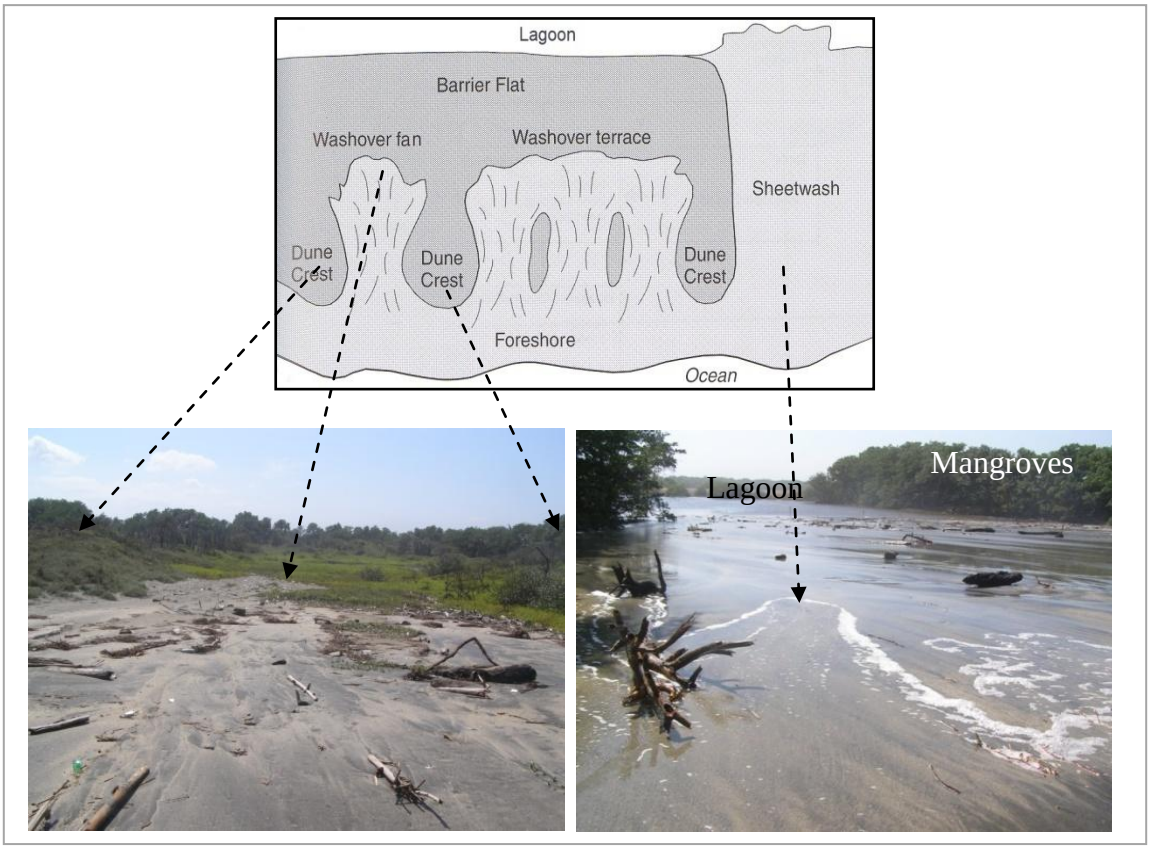

Figure 30. Washover fans as observed west of Dune 4. Photos taken looking to the southwest from X=938699/Y=1710743 (left) and X=938533/Y=1710800 (right). Numbers 3 and 4 in Figure 21 indicate the regional location of the above photographs (diagram after Sallenger, 2000).

Random samples of sand taken from the beaches during the fieldwork and observed under a 10X magnifier, show that the sand mineralogy includes quartz, minerals from the mica group, amphiboles (e.g., hornblende), calcareous fragments and heavy minerals. As noticed in previous studies (Frihy et al, 1995; Hatfield et al., 2010), because lower density and larger size grains are selectively entrained and transported by strong waves leaving behind the minerals with higher densities and smaller grains sizes, the latter group (heavy minerals) is commonly associated with erosion hot spots. Accordingly, black sand spots were found at sites where high

erosion was evident. Likewise, heavy minerals or black sands spots are characterized by having beach faces angles up to 15° (Picture 2 on Figure 33). Because the small scale of the map printed in Figure 31 added to the small areal extent of the beach complex in the park, beaches are hardly discernible in that Illustration.

3.5.1.2 Lagoons

Coastal lagoons are shallow water bodies found along coastlines subject to low to moderate tides; typically aligned parallel to the coast, they are separated from the ocean by barrier islands or dune formations (Jewell et al., 2012). ISNP is characterized by a large complex of interconnected lagoons. Water bodies of any type were included in this landform regardless of their salt content and distance from the sea. Furthermore, elongated water bodies initially formed from overwash channels are included under this landform (Number 2 in Figure 21 is placed over one of these channels).

In the park, because of the landward movement of coastlines, the area of these lagoons located next to the shore has decreased during the last 60 years. As an example, since 1968 La Atascosa and Las Piedras lagoons have lost an area of at least 1.6 km^2 and 1.1 km^2, respectively. By visual inspections in the field, it was possible to recognize the frequently infilling process, with sand-size sediment, taking place on the seaward side of the lagoons.

Even though no historic records exist of inlets opening between the lagoons and the sea over time, the role of these breachings in changing wave refraction and bathymetry configuration is not minor. In fact, during these breaching periods, lagoons are a sink for the sediment travelling alongshore and sediment transport reversal seaward from the lagoon may occur.

Based on the set of aerial photographs, as well as on oblique pictures taken from an airplane in 1970 for a PhD thesis (von Erffa, 1972), it was observed that El Torno lagoon was breached in the 1960s, enabling the formation of a flood tidal delta (Figure 31a). Accordingly, von Erffa (1972) noted that the inlet formation took place in 1967. Notwithstanding that a spit was growing eastward from the west side of the El Torno since the early 1970s (Figure 31a and 31b), a small inlet was still observed in aerial photographs taken in 1981 (Figure 31b). Nonetheless, by 1985 the breach had been healed by a sand bar separating the lagoon from the sea. During the field trip undertaken in December 2013, this bar was covered with copious low rolling sand mounds forming embryo dunes (Figure 31d), conditions comparable to those found for Dune 6.

Spit shapes growing from the lagoons extremes, akin to lagoons elsewhere (e.g., Islands in South Carolina as reported by Pilkey, 2003), indicate that sediment accumulation in front of lagoon inlets (ebb tidal deltas), may lead to a reversal of the predominant littoral drift, forming a bulbous end at the updrift extremity with a drumstick shape, whereas the downdrift is usually narrow. In order for a drumstick to form, a sizable ebb tidal delta is necessary (Pilkey, 2003). Accordingly with the spit landforms in front of El Torno lagoon and West from the former inlet of the Ciénaga Grande de Santa Marta (Figures 30 and 31), it is likely that similar process of local reversal of the prevailing longshore drift occurs seaward from these lagoons.

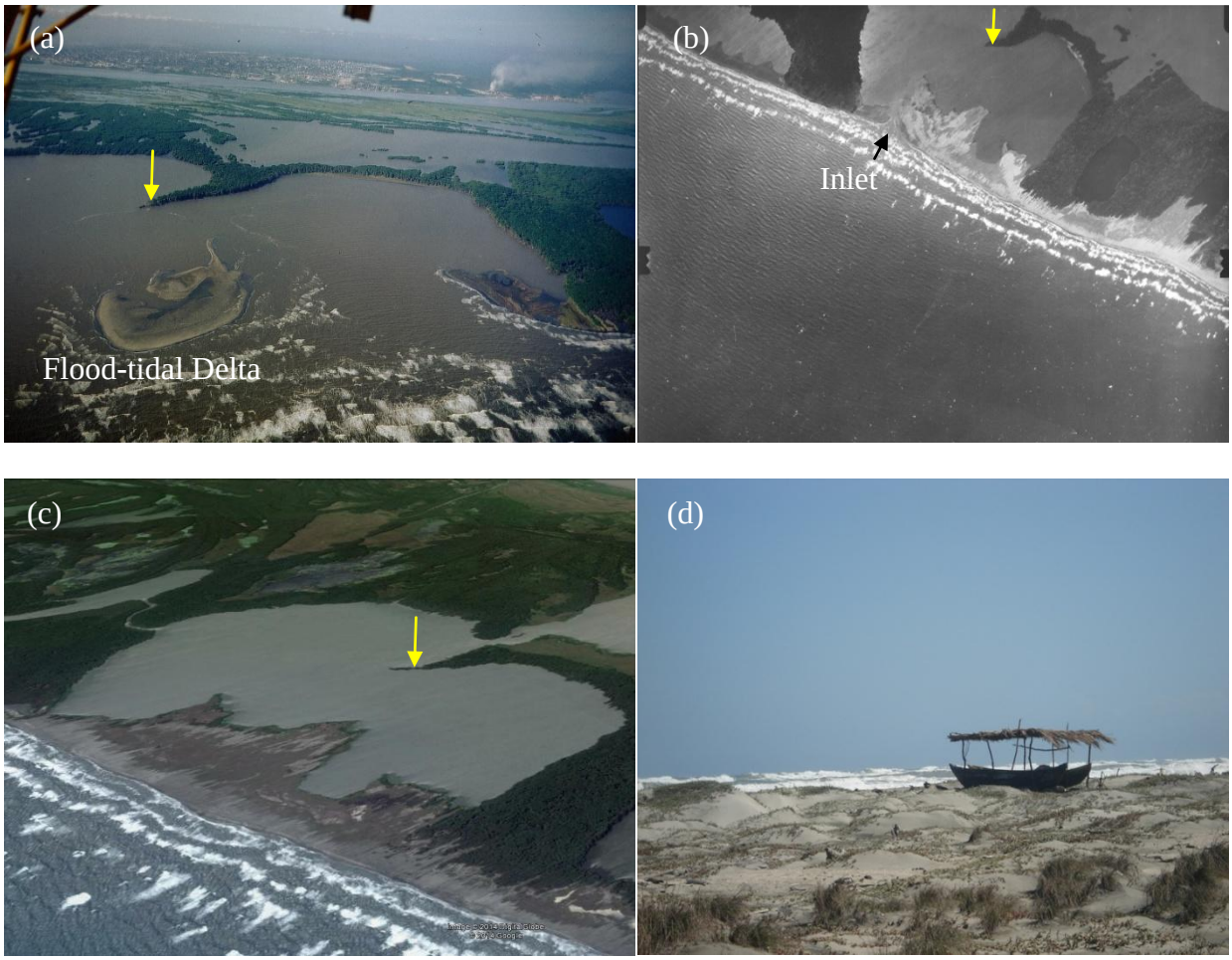

Figure 31. (a) Oblique aerial view of El Torno showing breaching of the lagoon as pictured in 1970 by Alex F. von Erfa. (b) Eastward growing spit as pictured in 1981. (c) Image from Google Earth taken in 2008 showing the spit evolution. (d) Incipient dunes in front of El Torno (photo taken on December 21st, 2013). Arrows point to the same location in each image.

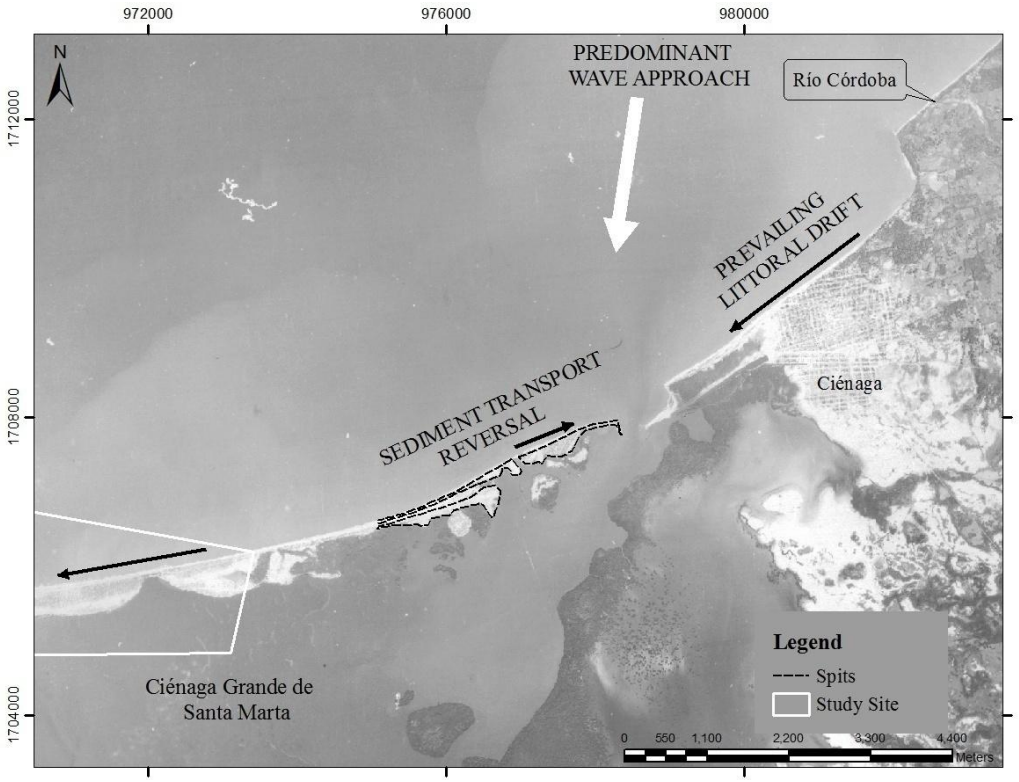

Figure 32. Spit on the west side of the former inlet of the Ciénaga Grande de Santa Marta as pictured on aerial photograph taken in1953. The white polygon is showing the easternmost extreme of the site of study.

3.5.1.3 Floodplains

Floodplains identified in this work included low areas associated with lagoons and abandoned channels (ox bows) that remain from the former and current Magdalena River drainage system. Inundation of these flat areas is commonly due to the combined effect of large or prolonged rainfall and high water table levels, as well as overflows coming from the lagoons and from the river channels (see Picture 4 on Figure 33). This is the most extensive complex unit in the study site.

Previous work developed in the park has also named and mapped within the floodplain a unit previously called mangrove forests (*see* Raasveldt and Tomic, 1958; von Erffa, 1972,

Bernal, 1996). By considering that the term mangrove forests has a land cover connotation, the term floodplain, which includes terrains currently occupied by mangroves in addition to low lands, is preferred in this work.

3.5.1.4 Salt flats

Upon prolonged dry conditions, floodplains may evolve into salt flats. Therefore, this complex unit may be considered transitional, extending its area after long periods without precipitation, such as those years under the influence of El Niño. Moreover, salt flats are present in enclosed areas without any fresh water irrigating the area, generating adverse conditions for vegetation growth (see Picture 1 on Figure 33). From aerial photographs and satellite images, salt flats can be recognized due to their high reflectance, with tones ranging from white to pink. Given the increasing precipitation gradient from east to west in the park, salt flats are mainly located east of the 20^{th} km.

3.5.1.5 Beach Ridge Plains

In the field, beach ridge plains are associated with flat areas of sandy soils covered by grasses. They are located landward from vegetated dunes and seaward from the road, southwest from Tasajera (see Picture 3 on Figure 33). According to inhabitants living on the outskirts of the study site for this research, before the park was officially established in 1965, this sector was used for livestock pasturing. Furthermore, remnants from an old road located seaward from the current road are still visible from aerial images. Even today, when heading toward the seashore, inhabitants, mainly fishermen, cross this flat area constantly, which is known as *La Cerca* (the fence), creating a web of paths. Given this fact, differentiating deflated dunes from beach ridges

in a highly disturbed terrain is somewhat imprecise. However, the flat topography, added to the medium sand soil texture, indicates a different origin from that of dunes. In that sense, Hesp (2005) stated that sand beach ridges are formed during storm wave events. Thus, it is considered that the flat terrain existing behind the scarped dunes is either an area of beach ridges or a former backshore.

3.5.1.6 Dunes

Two different dune types were mapped: firstly, in the westernmost extreme of this project, low rolling dunefields of embryo dunes (named embryo dunes in the map below); secondly, west of El Torno lagoon, vegetated parabolic dunes that appear either on or landward from the shoreline, were identified on Figure 33. Parabolic dunes located on erosive fringes usually develop scarp heights of up to 5 metres in front of the beach, being highly vulnerable to destabilization as a result of wave attack. Conversely, embryo dunes are usually located landward of extensive beaches that contribute to sheltering the dunes from the direct wave impact.

From a fine sand sample taken in a scarped dune west of Kangarú (see Kangarú location on Figure 1), the following minerals were observed: quartz (80%), hornblende (5%), tourmaline (5%), micas (5%), garnet? (<1%). The decomposition of minerals, presumably ferromagnesian minerals, has resulted in colouring the scarped dunes pale brown.

3.1.5.7 Road

Given the effect that the road has on the ecosystems of ISNP and particularly in the sea-lagoon water interchange, this development was mapped as a human-made unit (Picture 5 on

Figure 33). As observed in the field and from aerial photographs, at some sites such as at the 20th km, the road separated the dunes from the shore, somewhat halting the sediment that otherwise would supply the dune system. As a result, sand ramps are occasionally formed seaward from the road margin. The interplay of the road with the other mapped complexes is described further in the Discussion chapter.

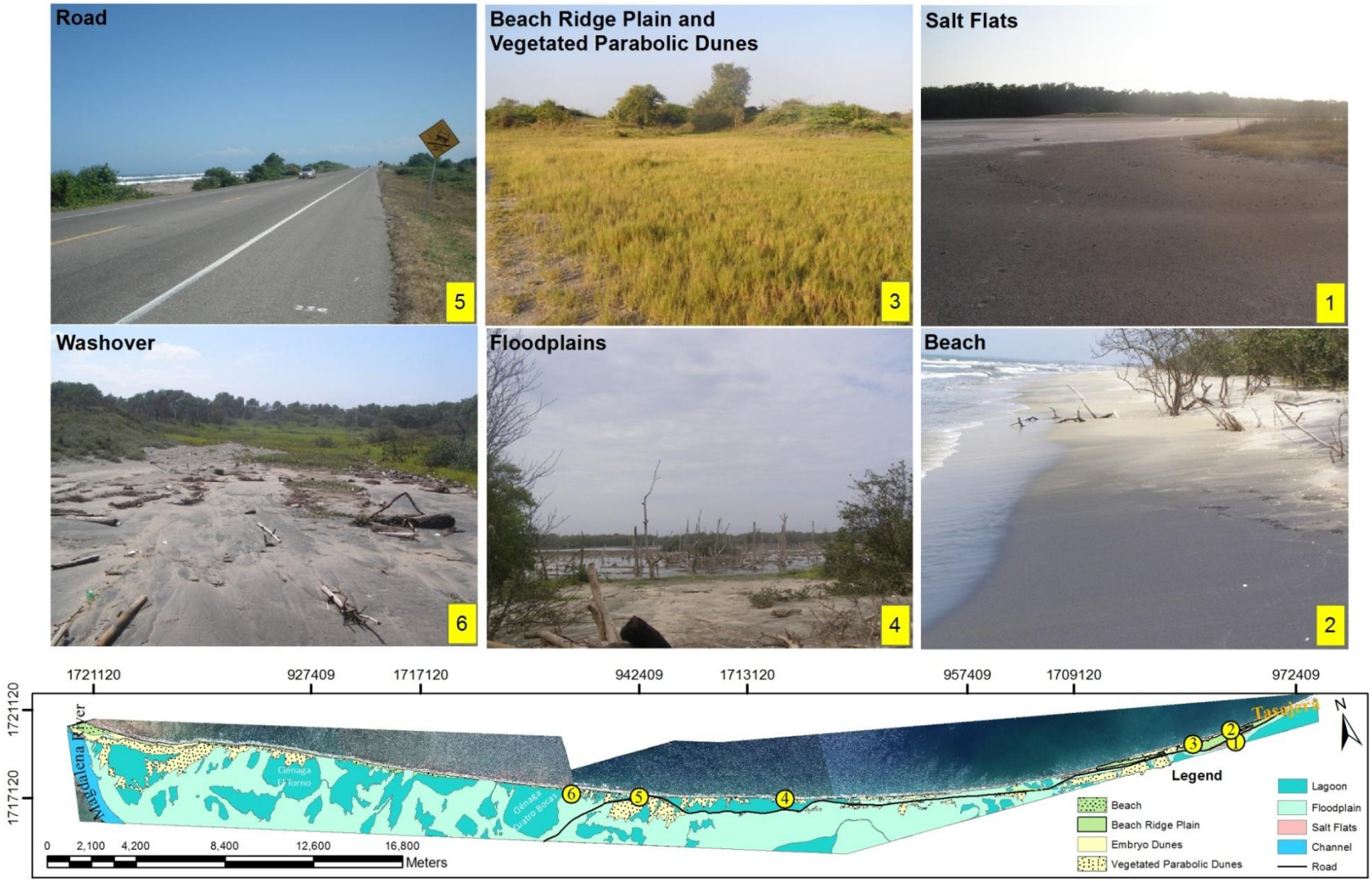

Figure 33. Geomorphology Map (yellow circles showing location of photographs).

Chapter 4 Discussion

From historical maps and reports made for the Magdalena River port construction, it is noticeable that prior to the 1930s fluvial-dominated processes had a larger impact on the landscape in the study site. Since this time, marine-dominated processes seem to be predominant. Maps from the seventeenth century portray Isla Salamanca as a delta barrier island, with multiple inlets along the coastline, likely produced by episodic high discharge flows of the Magdalena River associated with periods of high precipitation. In contrast, breachings in the present day lagoons result from the accumulative effect of both, washovers over the barrier and high lagoon levels after prolonged rainy seasons. As suggested by Inman and Dolan (1989) under erosional regimes, like those found in ISNP, dismantlement of the primary dune is a precursor to barrier denudation, frequent washovers, and the initiation of an overall barrier rollover process.

Considering the spatial and temporal variability of each of the many variables (e.g., climate, river discharges, human-made structures) affecting the coastal dynamic, it is challenging to gauge the weight of each factor in the evolution of the coast. Nonetheless, looking at discerning the reasons behind the changes that have taken place in the park and their relation with coastal and dune changes, the following sections discuss the coastal and bathymetry changes, vegetation coverage over dunes, and geomorphology separately. Each is then interlinked to help explain current landscape.

4.1 COASTLINE AND BATHYMETRY CHANGES

There are at least five potential sources of sediment for Isla Salamanca: (1) the detrital sediments coming from rivers; (2) the biogeneous remains of marine organism and reefs; (3) the fine sand coming from erosive dunes in the park; (4) the isolated cliffs of metamorphic and igneous rocks outcropping around the city of Santa Marta; and finally, (5) the relict sediments remnant from a paleodelta located on the continental shelf were likely a source of sediment in the past, but at the present moment it is not clear whether the shelf is a sink or a source of sediment.

In any event, human activities have altered at some degree these sources of sediment. Indeed, the construction of the dual jetty system at the Magdalena River mouth, which started in 1927 and was progressively extended until 1955 (Heezen, 1956), altered the sediment transport patterns in ISNP. On one side, the east jetty contributes to trapping the sediment transported by the westward predominant prevailing longshore drift. On the other, however, the jetties help in funneling the sediment from the Magdalena River through submarine canyons to ocean depths where they are hardly returned to the shorezone by wave action.

The erosion trend that was found since the early 1950s from Tasajera to El Torno, reaching a maximum east from Cuatro Bocas (Figure 18), is presumably due to the reduction of sediment added to changes in the interplay between bathymetry, waves, and littoral drift. The fact that this erosion spot is located approximately in the middle of the study site, far apart from terrigenous sources of sediment coming from the northeast, helps in understanding the accelerated retreat taking place there. Thus, the lack of sediment around the 20th km explains

why the engineering structures that have been installed there since 2011 have not been successful in accumulating sand.

Adding to that, the sector between the 20th km and Cuatro Bocas has a N70W direction; in other words, the predominant wave approach direction is almost perpendicular to the coastline. In fact, Ortiz et al. (2014), while investigating the conditions that caused the collapse of the Puerto Colombia pier (located 18 km southwest from the Magdalena River mouth) during a cold front that occurred on March 7 2009, reported that offshore-onshore waves direction during the cold front ranged between S50W and S59W (i.e., 230°-239°). Thus, the combined effect of the steep seabed slope in this sector (as described in the Results) added to the approach angle of the waves, resulted in high energy waves approaching the coastline. In the past, without the road decoupling the beach from the dunes, and presumably having larger accommodation space and sediment supply from the beach, the same conditions helped to create the large parabolic dunes aligned S35W that are still recognizable in that sector (Figure 21).

In contrast to the accelerated erosion rates existing around the 20th km, the westernmost area, located in the stretch west of El Torno lagoon and the mouth of the Magdalena River, presents accretive processes. There, longshore currents are accumulating sediment against the eastern jetty of the Magdalena River and the shore. Hence, it is likely that the westernmost sector of the study site constitutes the sediment sink for the westerly longshore sediment transport eroded either eastward or along the study site, where a pattern of updrift erosion and downdrift accretion is taking place.

When comparing coastline changes with bathymetry changes, it was discovered that the erosive and accretive trends found on the coastline continue offshore beyond the zero metre contour to depths equal to or larger than the 10 m depth contour. Even a couple of isolated locations where accretion occurred over the east and west extremes of the coastline, as opposed to erosion, by far the dominant processes along the coastline, are matched by increasing bed surface levels on the sea bottom close to the shoreline (Figure 19).

Albeit of the coupled matching between coastline and bathymetry changes, it is worth bearing in mind that results from any interpolation model like the one applied to obtain the bathymetry surface depend on data density and data quality. Thus, surface models are unlikely to produce a 100 per cent accurate prediction of the dependent variable (i.e., depth). To add to this issue, physical variables such as wave and tide conditions may affect the accuracy of bathymetry surveys, increasing the measurement's uncertainty. This is especially the case for deep sectors like the northern border bathymetry area (Figure 1 and Figure19), where there is a dearth of control points, resulting in a trend surface product of very few data points. Nonetheless, having obtained similar outcomes for sites on the coastline (subaerial) and in front of the coastline (submarine), lends confidence to the obtained results.

The bathymetry changes comparison between 1938 and 2012 turns out a general trend of bed surface decrease over time for those contours close to the coastline. This is particularly the case for the stretches with the highest erosion rates, where bathymetry is now deeper that was the case in 1938. It has been reported that the slope of the shoreface determines how much wave energy is dissipated as deep-water waves approach a coastal segment (Backstrom et al., 2007). Because deeper nearshore bathymetry reduces both wave refraction and wave energy loss via

friction with the seabed (Aagaard and Sørensen, 2013), it is expected that wave energy acting over the shore would be greater on steep platforms than on shallow platforms.

Even though towns located northeast of Tasajera such as Isla Rosario and the northern areas of Ciénaga have also been affected by coastal erosion, field observations showed that the changes there are not as dramatic as those occurring within the park. So, as mentioned before, coastal erosion hot spots, as the one found between Cuatro Bocas and the 20th km, are likely the result of the low incidence angle of the wave crests with respect to the coastline, their location away from sediment sources, and the possibility of presenting subsidence nearby the affected area.

It has been established that sediment loading (Bott, 1979) and sediment compaction may result in shelf subsidence, the latter processes taking place especially in deltas and wetlands where sediments can contain up to 50 per cent water (Masselink et al., 2011). Reportedly, the response of the Mississippi, Nile, and Niger river deltas to reduced sediment supply includes accelerated subsidence, rapid ocean front erosion (Nile and Niger deltas), or island migration and break up (Mississippi Delta) (Pilkey et al., 1998). Channeling or diverting a river, both practices present in the lower Magdalena river basin, can prevent fluvial sediment from reaching the delta, and thus, subsidence may not be compensated by new sediment accumulation (Timmons et al., 2010).

Even though local erosion rates as the ones revealed by the coastal changes analysis (Figure 18) are uncommon both in the Colombian Caribbean and overseas, similar coastal change values have been reported along some barrier islands. For instance, Martínez et al. (2000)

reported erosion values up to 8.3 m/yr since the early 1960s onwards in Isla Santa Barbara, a 8.4 km long island barrier located on the Colombian Pacific Coast. Allen et al. (2002), on the other hand, found average erosion values of 14.1 m/yr in Fire Island, New York, between 1933 and 1979. In addition, in a similar case to the section with the highest erosion rates of this work (i.e., 20th km to Cuatro Bocas lagoon), Penland and Boyd (1982), while deciphering the Mississippi delta barrier evolution, explained the pattern of erosion from around 15 m/yr in the central portion of the Isles Dernieres (an abandoned delta) to approximately 5 m/yr on the east and west adjacent areas of the island, as a result of the influence of the barrier orientation relative to the dominant wave approach.

It is likely that in addition to the interplay between sediment depletion and shoreline orientation relative to the dominant wave approach, there exist other factors affecting the studied stretch of coast, particularly in the span of coast between Cuatro Bocas and the 20th km (Figure 1). In an analogous case to this project, where dune accretion came to an end around 1970-1980, Aagaard et al. (2004) and Aagaard and Sørensen (2013), related the switch from accretion to erosion conditions along the Skallingen Barrier, in Denmark, to an increased rate of longshore sediment transport.

In any case, it is clear that without assessing the sediment budget and the spatial and temporal variability of the littoral currents, the importance that each specific factor has on the accelerated coastal retreat along ISNP remains somewhat speculative.

4.2 VEGETATION ON DUNES

Besides the dunes located west of El Torno Lagoon, the vast majority of present day coastal dunes in ISNP are located close to the high tide line forming scarped dunes regularly affected by storm wave-action. In that sense, the surveyed dunes 1 to 4, although not identical, are grouped as scarped dunes; whereas dunes 5 and 6 are named active dunes (Figure 22).

On the scarped dunes, erosive processes are faster than any sand accumulation carried out by wind; hence, making these dunes *inactive* from an aeolian standpoint. The term inactive does not imply that these dunes are not changing; rather, since runup frequently collides with their base forcing erosion, the retreat of these dunes is somewhat coupled with the accelerated coastal retreat. Sallenger (2000) defined this process of dune erosion as the collision regime, in which the eroded sand is transported offshore (or longshore) and does not typically return to re-establish the dune. The active dunes, on the other side, are located in the western area in front of wide beaches that have a twofold function: preventing runup from reaching the dune base during high sea levels, and supplying the dunes with sand during the windy season.

Parabolic dunes, such as dunes 1 to 5 (Figure 22), are characterized by high, U-shaped, migrating trailing ridges with an active slip face at the landward margin. Eventually, sand supply to the slip face and forward migration of the dune cease as a result of the spread of vegetation (Davidson-Arnott, 2010). For instance, when it was attempted to track dune movement on aerial photographs and satellite imagery from the early 1950s onwards, movement was not evident over dunes 1 to 5. On the contrary, the dunes appear to be impeded, fixed in position by vegetation. Regarding the effect that vegetation has on dunes mobility, Ojeda et al.

(2005) associated a decreasing rate of dune movement from 5 m/yr to 1.2 m/yr in Doñana Natural Park, Spain, with increasing vegetation coverage over time.

A different case is Dune 6, a small (less than a meter in height) rolling mound not visible from a Geoeye image taken on November 13, 2012. This embryo dune presents lower vegetation cover than Dunes 1 to 5, as well as a copious supply of sediment coming from updrift erosion. The lack of vegetation, abundant availability of sediment, and increasing distance from the shoreline to the lagoon over the last 70 years, favour embryo dune formation and dune mobility in the sector nearby Dune 6, the westernmost extreme of ISNP.

In addition to the stabilization effect produced by vegetation coverage, the lagoons located landward from dunes 3 to 5 have further prevented inland dune displacement by hindering the offshore-onshore travel of sediment. In that sense, Dune 5 may be considered a transitional environment between scarped dunes and active dunes. That is, it is active because during the windy season it is fed with sediment coming from the wide beach in front of the dune (Picture 5 on Figure 22); on the other hand, it is an impeded dune because it is limited by a lagoon, and as a consequence, it is fixed in position by the lack of space to move further landward.

After measuring the transects over the dunes, it was noticed that the least vegetated dunes are those that have been identified previously as active dunes (dunes 5 and 6). These dunes are in areas where there is abundant sand supply and thus burial by sand inhibits the establishment of many of the plants found on the eroding dunes. In fact, scarped dunes have not only more diverse and mature vegetation species, but they are also more vegetated. As reported by Bitton

(2013) for the dunes found in the Florida Panhandle, because usually scarped dunes are the oldest, they have had more time to develop soil and to establish more diverse plant assemblages than embryo dunes and foredunes.

Following the same lines, it was noticed that the Shannon diversity index has larger values in dunes landward from erosive coastlines (scarped dunes) than in dunes landward from accretive coastlines (active dunes). This is due to the fact that these areas next to the shoreline on scarped dunes were originally formed landward from their present location, being therefore less exposed to wind and waves than today. Miot da Silva et al. (2008) and Miot da Silva and Hesp (2013) highlight the contrasting differences in vegetation diversity and zonation between shorelines facing different degrees of wind and wave energy. In this regard, shorelines under high wave/wind energy regimes present wider species zonation and lower diversity, whereas sheltered shorelines have higher species diversity and smaller zonation.

In addition to wave energy, another key aspect influencing vegetation coverage on dunes is the availability of sediment to feed the dunes. In fact, it was found that those dunes with the highest diversity indexes (Dunes 2 and 3 on Table 12) are associated with high erosion rates and vice versa. This finding is in agreement with Hesp (1998), who stated that because only certain species have adaptations to high sand burial, the diversity of the vegetation decreases with a higher sediment supply (i.e., accretive or low erosion shorelines). Accordingly, those species that react positively to sand burial are the most useful in building foredunes (Nordstrom, 2008).

As sand deposition within vegetation is key to the development of embryo dunes and afterwards the foredune complex (Davidson-Arnott, 2010), any attempt to restore dunes and

beaches through planting native species should take into account common pioneer species colonizing the transition zone between beach and dune. Species found in Isla Salamanca that are at some degree salt tolerant as well as psammophitic, and may therefore enhance embryo dune development include *Sesuvium portulacastrum*, *Cyperus ligularis*, and *Batis marítima*. Other species found on and seaward from the stoss face of the studied dunes are *Melochia tormentosa* (also termed *Melochia crenata* – Romero, 1971; Tavera and Gamba, 2001), *Capparis flexuosa*, and *Sporobolus virginicus*. These last three species, although they thrive close to the shoreline, seem to be related to more mature (old) dunes.

Regarding the precipitation analysis, data taken in Santa Marta and Barranquilla show an increasing trend in the rainfall since the early 1960s and 1940s, respectively. These statistically significant increases in rainfall likely sparked the establishment and development of different vegetation communities over the dunes. In that sense, extremely dry/wet periods in the area are coupled with El Niño/La Niña phenomenon. In fact, it was observed that a single La Niña event, such as that which occurred during 2010-2011, abruptly increases the slope of the line associated with the rain trend over time (Figures 15 and 16). To verify the above, the total rainfall values for the period between 2010 and 2012 were eliminated, determining that the slope value from Equation 5 dropped from 6.16 to 4.95, the latter value obtained after dropping the 2010-2012 data.

The above is to say, extreme dry/wet years related to El Niño/La Niña greatly influence the rainfall trend regression line slope. As it is apparent from the slope in equations 5 and 6, the overall increase in rainfall in Santa Marta is larger than is the case in Barranquilla. Assuming that the relative humidity is similar at both meteorological stations, the highest rainfall increase

in Santa Marta may be due to the condensing effect that the SNSM range has over the moisture associated with the off-shore northeasterly winds, a topographic barrier effect that is missing in Barranquilla.

To add to the increasing rainfall, the decreasing strength of wind events of over 6 m/s since the early 1980s have as well accelerated the stabilization of dunes through vegetation coverage (Figure 17). A comparison between Figures 16 and 17, indicates that weaker wind velocities are related to La Niña (wet years), while stronger wind velocities are associated with El Niño (dry years).

Unlike rainfall data, the Shapiro-Wilk (W) and Anderson-Darling (A) tests (Table 6) revealed that the wind data analyzed are not normally distributed. In this case, the modified Mann-Kendall test, a non-parametric test to verify whether or not a trend is statistically significant, is especially meaningful. In so doing, the test confirmed that the decreasing trend in wind strength since the early 1980s are in fact statistically significant at 95% level.

Further studies have found similar trends of increasing rainfall and decreasing wind strength over time. Miot da Silva and Hesp (2013), while working in the Santa Catarina dunefields in Southern Brazil, associated these trends with more water availability, higher water tables, and lower aeolian sediment drift, enabling plants more readily to colonize dunefields along the Southern Brazilian coast, and causing their partial or full stabilization by the late 1970s (Miot da Silva et al., 2013). Similarly, higher precipitation rates and fewer wind events of over 6 m/s may have contributed to increasing the vegetation coverage in ISNP and as a consequence to dune stabilization.

To summarize, a regular pattern of cross-shore spatial distribution in the vegetation was not evident in the study site. Rather, the vegetation profiles made over the dunes indicate that the spatial distribution of species is controlled by the changing relationship between past coastal changes in front of the dune, shoreline orientation, salt spray, and wave energy. Thus, contrary to García-Mora (2000) findings in the Gulf of Cadiz (SE Portugal and SW Spain), where increasing levels of diversity were related to lower vulnerability index, in Isla Salamanca those dunes with the highest diversity indexes are characterized by being highly vulnerable from a beach morphodynamic perspective.

4.3 GEOMORPHOLOGY

The geomorphology of ISNP can be approached through three time scales: (1) the delta barrier formation period, which likely occurred around 2000 years ago (Angulo, 1978; Wiedemann, 1973); (2) a mid-term scale of over two centuries provided by the comparison of the earliest maps with the present morphology; and (3) a third time scale of a few years to six decades that encompasses recent changes taking place in the area.

With regard to the delta barrier formation, despite the lack of data (e.g., cores) preventing a description of the evolution of Isla Salamanca during the Holocene, it is well recognized that barrier genesis and evolution is associated with rising sea-levels (Pilkey and Fraser, 2003). In fact, many barrier island systems initially formed after a rapid sea level rise between 7000 and 5000 BP slowed down and approached present-day sea level (Stutz and Pilkey, 2011). Allegedly, the CGSM lagoon came into existence by a relative sea level rise of about 2 metres during the last 2300 years (Wiedemann, 1973).

On a more recent time scale, historical maps from the seventeenth century pictured the area west from the Magdalena River (Figure 3) as a series of small islands associated with the mouth of the Magdalena River. This former landform configuration fits the delta barrier island landform concept, characterized by having energetic waves, huge supply of sand-size sediment, and a river delta platform (Pilkey, 2003). It has been recognized that the first large human-made modification of the Magdalena River was the Dique Canal construction in 1650 (Alvarado, 2005). Afterwards, the port construction and dredging activities at the river mouth altered even more the flow patterns of the river and its influence over the study site. It is suggested that the evolution from a chain of small islands−delta barrier−to present day single barrier reveals that the decreasing discharge of the Magdalena River has favoured the influence of wave-dominated regimes in detriment of the fluvial processes. Similarly, Stutz and Pilkey (2011) proposed that barrier islands tend to grow longer as the influence of waves relative to tides increases.

The third time scale analysis was based on aerial photographs, satellite images, and fieldwork. From the study of these materials, it is apparent that whereas dunes were key in infilling the seaward border of lagoons in the past, nowadays the main processes reducing the lagoon areas nearby Cuatro Bocas is driven by overwashes. Contrastingly, in the area close to the Magdalena River, where accretive processes are predominant, aeolian activity is still the main cause for reducing the extent of the lagoons. In any case, unless a lagoon breaching occurs enabling some offshore-onshore sediment interchange, the current infilling of lagoons triggered by either aeolian or marine forces implies that sediments that contributed to supplying beaches and dunes in the past are currently being lost from the sediment budget.

In spite of the fact that determining the role of washovers in the coastal evolution of the area is beyond the scope of this work, their importance in providing the initial conditions for dunes scarping and lagoons breaching cannot be underestimated. Furthermore, washovers contribute to net landward migration of barrier islands (Sallenger, 2000; Pilkey and Fraser, 2003). In the field, both runup and inundation overwashes (cf. Donnelly et al., 2006) were observed in the stretch of coast between the 20th km and Cuatro Bocas lagoon. The runup overwash occurs when excessive wave runup level exceeds the beach crest height. Inundation overwashes, on the other hand, are confined to sites of the shore with low elevation such as concave depressions that exist between dunes, or beaches with low slope located seaward of lagoons, where frequent storm surge high levels end forming fans and overwash channels.

An example of an overwash channel within the park is the elongated channel located between La Atascosa and Cuatro Bocas lagoons. This channel, which in the past connected the lagoons known as Manatíes and La Atascosa, has recently been shaped by inundation washovers that have aligned the channel with a direction of S40W. The SW predominant direction in the overwash channels in that sector indicate that they are produced by the added effect of overwashes intruding on the lowest surfaces of the former dunes (see number 2 on Figure 21).

Following the well-known geologic principle of uniformitarianism initially proposed by Hutton, examining present processes may be key to elucidating not only past, but also future geologic events (Hutton, 1970). Indeed, the breaching of El Torno lagoon in the late 1960s was followed by the formation of an ebb tidal delta (Figure 31). Around 18 years passed before the continuous accumulation of sand seaward from the lagoon formed a subaerial sand bar that separated the lagoon from the sea again.

Currently, there is no evidence of either recent or old washover fans in front of El Torno. On the contrary, the beach is being colonized by pioneer species, and rolling mounds or embryo dunes forming over the beach are common (Figure 31d). Conversely, the presence of numerous inlets in the past, as portrayed in Figure 3, may be due to the effect of higher discharge flows coming from the Magdalena River through channels flooding the lagoons. Thus, these currents impeded the complete development of a sand barrier in front of the lagoons. In a similar case of a decreasing number of inlets on the North Carolina Outer Banks since the seventeenth century, Pilkey et al. (1998) suggested that the large number of inlets that existed in the past were a product of increased storminess during the LIA.

Once the actual configuration of Isla Salamanca barrier was developed because the Magdalena River influence was hindered, it underpinned beach and dune development, and afterwards vegetation establishment. The successive repetition of the breaching/closure processes that apparently took over in front of the lagoons through time, ended up enhancing the growth of beaches seaward of the lagoons. Notwithstanding the different space and time scales, the recent breaching and subsequent inlet closure of El Torno Lagoon is probably similar to the whole process that gave place to the current configuration of Isla Salamanca.

Nowadays, under the current worldwide trends of rising temperatures and sea-level, as stated by the 2013 IPCC report, it is likely that natural thresholds will be exceeded more frequently, which in turn will lead to greater occurrences of storm surges overwashing and breaching barriers (FitzGerald et al., 2008). Accordingly, a continuous inland displacement of the coastline–resulting in decreasing sizes of lagoons and beaches–is the expected scenario in the near future (100 years) east of El Torno lagoon.

4.4 FINAL DISCUSSION

As discussed so far, there are a few factors, ranging from regional to local, determining current configuration of Isla Salamanca. On a regional scale, consideration of sea-level changes and climate variability is key to properly depicting the regional history. However, addressing past sea levels leaving aside neotectonic contributions to relative sea-level changes, is not plausible. This is especially the case for areas like the study site, where at least one active fault, the SBFS, is located just few kilometres east from Tasajera. In spite of the importance of these regional influences, it is clear that new data are required to better assess the role that phenomena such as subsidence, fault activity, and wave behavior, have had in relative sea level variations.

Even though dry climate is not a fundamental condition for coastal dune formation, having a long dry season, along with strong persistent onshore winds, and ample sediment supply, may contribute to enhancing dune development (Maun, 2009). Thus, the predominantly dry conditions occurring during the LIA over northern South America (Haug et al., 2001) in conjunction with abundant sediment coming from the former Magdalena channel distribution inside the study site would have been, at that point in time, ideal conditions for dune formation. However, controversy surrounds the starting and ending dates for the LIA in South America (González et al., 2010). In any case, the fact that pieces of pottery made by indigenous communities have been discovered buried in the dunes of Isla Salamanca (National Park employee, personal communication, May 15th, 2014) supports the hypothesis that some of the parabolic dunes were formed prior to the colonial period.

Accordingly with the above, rather that reflecting present day climate conditions,

the large dunefields found in ISNP are composed of dunes reflecting past conditions. The increasing rain and decreasing wind strength trends found in this work are likely mirroring similar conditions to those occurring after the LIA came to an end.

In tandem with regional aspects shaping the study site, local variables (e.g., sediment availability and human-made effects) may greatly influence the shape of the coastline. Indeed, the *Canal del Dique* construction in 1650 (Alvarado, 2005) to some degree reduced the river discharge and as a result the volume of sediments arriving to the former mouths of Magdalena River. More recently, the port construction next to Barranquilla further dampened the river input of sediment into Isla Salamanca.

The increase on the nearshore sea-bottom depths over time discovered after the bathymetry analysis in some of the erosion hotspots within the study site (e.g., the area nearby the 20^{th} km), added to the decreasing sources of sediment, may have resulted in an increase of the nearshore breaker height. As a result, it is likely that waves are distributing most of their energy closer to the shoreline that was the case in the past, and hence, the longshore transport may have been increased as well. Unfortunately, although regional studies for the Caribbean Sea support a growing probability in extreme total mean sea-levels (Losada et al, 2013), neither wave analysis nor longshore rates over time have been examined for the area of interest. That being said, it is not possible to assure that in fact a strengthening the littoral drift has taken place. In any case, local deeper bathymetries with respect to past conditions found on the Danish North sea coast (Aagaard, 2013), and wave-climate changes on the northeast coast of Scotland (Milne et al., 2012), have been associated with a strengthening of the littoral drift. Specifically, the

latter authors proposed that the temporal variations in patterns of longshore drift and the associated morphological variations are likely driven by wave-climate change during the 1980s.

At any rate, retreating coastlines, deflating dunes, dying mangroves with progressively shorter distances to the coastline, reducing lagoon sizes, and numerous washovers, are all indicators that a transgressive phase is taking place in Isla Salamanca where the ever-changing landforms are coping with higher offshore energy inputs and lower sediment availability.

Deterring the current coastal retreat taking place in ISNP through human-made structures such as groins, seawalls or breakwaters is, at the very best, a costly solution. In accordance, the structures recently built in the 20th km may have been accelerating even more the erosion downdrift of the structures. The bedrock (mudstone) that was discovered outcropping under the sea water just ~~a~~ few metres northwest from the sandbag barrier installed in May 2014 (Figure 5) is further evidence of the sand deficit in that area.

Beach-dune systems are a valuable buffer between the coastal hinterland and the sea, with the beach being effective at dissipating wave energy (Milne et al., 2012), while the dune act as a sand storage and natural barrier against overwash, flooding, wind stress, salt spray and sediment transport during small storms (Nordstrom, 2008). Given the importance of the beach-dune system in maintaining the overall integrity of habitats landward and seaward of them, the following mitigation approaches are proposed to promote sediment accumulation in order to ameliorate the erosion at specific sites in the park: (1) sediment nourishment to raise the beach height and to promote embryo dune formation. This strategy may be approached either by restabilising the communication between the Magdalena River and the study site, or by

artificially transporting some of the sediments that are presently dragged from the mouth of the Magdalena River to the erosion hot spots existing along ISNP (2) installing sand trapping fences; and (3) planting pioneer dune species. This latter approach may require installing nurseries for growing species such as *Sesuvium portulacastrum* and *Melochia tormentosa*. However, if beach widths are narrow and the cycles of wave erosion and mechanical deposition are frequent, planting vegetation on scarped dunes may be either counterproductive (Nordstrom, 2008) or useless. In that sense, the areas for restoration within the park must have a buffer space seaward from the selected sites to protect the plants from frequent marine intrusions.

Chapter 5 Conclusions

Characterizing dunes, beaches, and vegetation along the park and explaining their evolution required a thorough understanding of the interplay between the variables acting over the coastal zone. From the many physical factors influencing the coastal evolution of Isla Salamanca, this study focused on investigating landscape evolution, recent climate trends of precipitation and wind, and coastline and bathymetry changes. These variables were related to the vegetation distribution over the dunes.

The evolution of Isla Salamanca from a fluvial-dominated system to a wave-dominated sand barrier has occurred in tandem with the decreasing influence of the Magdalena River over the study site since the early twentieth century. Consequently, within the stretch of coast that extends from Tasajera to El Torno, marine processes are currently either eroding or masking previous landscapes of fluvial or aeolian origin. Along that barrier stretch, washovers, shrinking lagoons, and eroding beaches and dunes are common, suggesting that a landward rollover is taking place along this segment of the barrier. Therefore, had this project taken cores or ground penetrating radar profiles in the backshore of the barrier, coarsening upward sequences (e.g., mangrove mud to beach to overwash) should have been found for at least the last sixty years of the sequence.

Particularly, the observed size-reduction of lagoons through time suggests that these bodies of water are currently being infilled as sand sheets driven by either aeolian or wave

forces (overwashes) migrate into them. When breaching of the barrier system occurs due to intense storms and/or as a result of high water levels in any of the lagoons, the now-dominant marine forces favour the formation of flood-tidal deltas. In a time span that may range from few years to decades, this landscape will evolve into a bar healing the breaching.

In terms of seabed changes, a general trend of surface decrease from 1938 to 2012 for those bathymetry contours close to the coastline was revealed through the extraction of bathymetry surfaces; this pattern of sea-bed sediment loss matches well with the coastline trends for a period beginning in the early 1950s and lasting until today, with retreating coastlines being the most common process. In that sense, the highest erosion rates were found in the stretch of coast between the 20th km and Cuatro Bocas lagoon, where erosive values ranged between 10 m/yr to 14 m/yr for the last 60 years. Although details of the reasons underlying the high erosion rates affecting that area remain speculative, they could be the result of a subsiding paleodelta, a strengthening of the littoral currents, and sediment depletion.

In contrast to the fringe of coast between Tasajera and El Torno lagoon, the study westernmost extreme of the study site, a sediment sink for the sediments transported by the predominant east-west littoral drift, currently presents accretive processes, resulting in abundant embryo dunes and wide beaches. Overall, two different dunes types were observed in ISNP: fixed old parabolic dunes−also termed inactive dunes−on the central and eastern sectors, and mobile recent embryo dunes−also termed active dunes−on the western end of the study area. 500 years old is the suggested minimal age for some of the fixed old dunes. This age is inferred from pieces of ceramic−produced by indigenous communities−that have been found buried in the scarped surface of dunes nearby Kangarú.

The topographic profiles added to the vegetation transects that were made over six dunes along the park illustrated that, in conjunction with physical factors such as coastline and dune orientation, as well as antecedent climate and coastal changes, vegetation species and abundance changed from east to west. In fact, common species found on erosive dunes in Isla Salamanca include *Calatropis procera*, *Lemaireocereous griseus*, *Cnidoscolus urens*, *Capparis flexuosa*, *Pereskia colombiana*, and *Prosopis juliflora*. These climax species are not found on young dunes, but rather are on dunes affected by coastal retreat. These erosive parabolic dunes are not mobile, but instead are fixed in position by vegetation and sometimes by the lack of space to move landward.

In contrast, the embryo dunes found in the westernmost sector are mobile and either unvegetated, or covered only by isolated patches of *Sesuvium portulacastrum* and *Cyperus ligulari*. These latter two species, in addition to *Sporobolus virginicus*, *Capparis flexuosa* and *Melochia tormentosa*, somewhat thrive under windy and sandy regimes, and are adapted to temporal sand burial. Knowing these patterns of vegetation distribution in areas affected by erosion versus accretion would enable decision-makers and park managers to define strategies to promote deposition of sand through establishing dune building plants in areas affected by erosion. The planting of these species added to sand nourishment and sand trapping fences will locally promote the development of embryo dunes and ultimately of the foredune complex.

Chapter 6 Recommendations

In this section, monitoring programs together with pilot projects focused on mitigation practices are proposed. From that standpoint, the following recommendations are suggested to the park managers:

-Monitoring some of the dunes and beaches in the park through profiles and vegetation surveys at least twice yearly (e.g., rainy and dry seasons) would enable the park authorities to precisely assess their trends over time. The six dunes surveyed in this project are a starting point for the future monitoring campaigns.

-Generating awareness between local communities (Tasajera, Pueblo Viejo) of the importance of dunes from an ecological and coastal system perspective is necessary to avoid negative common practices such as beach and dune sand extraction for construction. Correspondingly, an ongoing program of guided visits to the park, specifically to the coastal area, will help to engage communities with goals of the park.

-Regarding the coastal erosion issues affecting Isla Salamanca, they are expected to continue in the near future, likely affecting the road west from the 20^{th} km and next to the Tasajera toll. Even though initially highly expensive, moving sections of the road landward from its current location would probably be cheaper in the long term than protecting it at its present location indefinitely.

-In agreement with the previous recommendation, pilot restoration projects including planting of pioneer dune species to promote sand accumulation are recommended in the following sites: (1) Dune 3 (X=939830/Y=1710253); (2) behind a narrow beach located east from the 20th Km (X=941058/Y=1709837), and (3) in Kangarú, specifically next to the small lagoon located close to the cabin (X=948222/Y=1707552). Depending on the success of these pilot projects, and keeping in mind that this approach is only a mitigation practice, other areas with more narrow beaches such as those in front of Dune 4 (X=938512/Y=1710769) may also be included to pursue restoration.

-From an academic perspective, given the importance of the breaching of lagoons in the coastal evolution, having a logbook of the dates, precise location, and dimensions every time a breaching/closure occurs will contribute to better understanding the cyclic dynamic of this phenomenon and its relation with both storms or rainy seasons. Along the same lines, tracking the development of washovers after storms will help to recognize their role in breachings of lagoons and dismantling of the dunes.

-Coring or ground penetrating radar data in the barrier, added to dating, would provide valuable information to better depict the barrier evolution.

-Temporally installing anemometres during the windy season along beach/dune profiles would enable park managers to precisely define wind directions and wind steering over the dunes. This information is valuable for determining the best location and orientation of sand fences.

- Assessing the sediment budget would provide the necessary information to define the weight that the deficit of sediment has in the coastal retreating trends in the park. Particularly, there

exists a limited understanding of cross-shore transport volumes, time-scales and mechanisms, so it is necessary to quantify cross-shore (and long-shore) processes, so that the hypothesis that some sediment is travelling onshore-offshore may be assessed.

-The lack of knowledge of the spatial pattern and present-day rates of land-surface subsidence in Isla Salamanca make that the predictions of future local sea level rise carry large uncertainties. Developing a monitoring program of surface-elevation change and vertical accretion rates in the floodplain unit using marker horizons and surface elevation tables would enable park authorities to assess the role of land subsidence in the barrier retreat.

Appendix A: Sample of coastal transects after running DSAS

ID	STARTX	STARTY	EPR	AOR
1	973264	1705913	-0.44	-0.44
50	972047	1705767	0.11	0.11
100	970805	1705627	-0.14	-0.35
150	969566	1705464	-0.67	-0.57
200	968317	1705455	-0.40	0.44
250	967067	1705452	-0.71	-0.71
300	965817	1705448	-0.91	-0.91
350	964567	1705445	-1.32	-1.32
400	963317	1705441	-1.59	-1.59
450	962067	1705437	-2.25	-2.24
500	960817	1705434	-1.87	-1.88
550	959567	1705430	-1.74	-1.74
600	958327	1705563	-1.61	-1.61
650	957092	1705755	-2.17	-2.13
700	955858	1705955	-2.12	-2.09
750	954625	1706159	-1.91	-1.87
800	953392	1706368	-2.16	-2.17
850	952164	1706597	-2.39	-2.39
900	950952	1706904	-2.74	-2.83
950	949733	1707180	-3.37	-3.66
1000	948513	1707451	-3.93	-4.27
1050	947317	1707813	-4.20	-4.25
1100	946120	1708176	-4.93	-5.14
1150	944913	1708498	-5.51	-5.65
1200	943709	1708831	-6.78	-7.27
1250	942522	1709223	-7.94	-8.43
1300	941334	1709610	-8.46	-5.53
1350	940162	1710046	-10.14	-12.30
1400	938995	1710492	-10.60	-13.09
1450	937816	1710908	-10.85	-11.09
1500	936644	1711342	-10.83	-11.12
1550	935481	1711801	-10.23	-10.40
1600	934321	1712265	-9.33	-9.87
1650	933162	1712734	-8.05	-8.97
1700	932005	1713206	-11.66	-11.18
1750	930859	1713706	-11.64	-11.03
1800	929723	1714226	-11.15	-8.94
1850	928581	1714736	-10.87	-9.60
1900	927430	1715222	-11.14	-9.69
1950	926278	1715708	-3.10	-4.33
2000	925131	1716204	-3.01	0.00
2050	923983	1716699	-3.76	-2.73
2100	922817	1717148	-3.19	-3.74
2150	921640	1717564	-2.36	-2.74
2200	920396	1717653	0.82	0.82
2250	919177	1717878	4.27	4.02
2300	918047	1718409	5.80	5.28
2350	916971	1719043	0.01	0.01
2380	916430	1719562	9.48	9.48

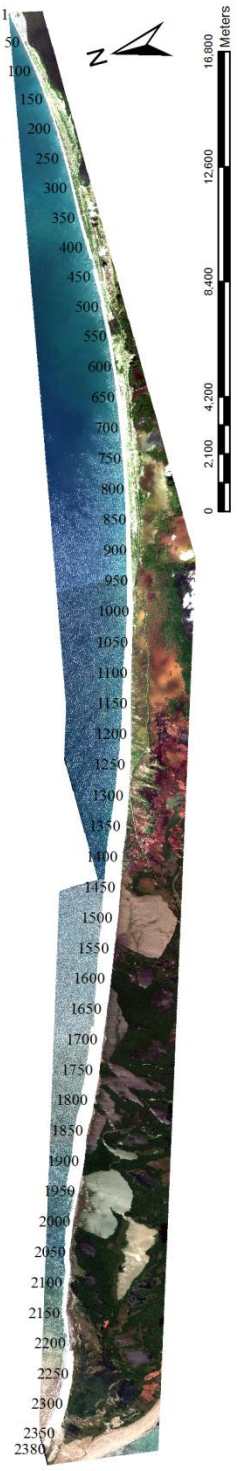

Appendix B: Vegetation identified on dunes

Sesuvium portulacastrum

Sporobolus virginicus

Cyperus ligularis

Cyperus ligularis

Melochia tormentos

Melochia tormentosa

Cnsidoscoulus urens

Lemaireocereous griseous

Matalea sp *rubra*

Calotropis procera

Capparis flexuosa

*Capparis flexuosa and Prosopis juliflora**

Pereskia colombiana

Plumbago sp

Talinum fructicosum

Alternanthera porrigens

Family Euphorbiaceae, sp

Family Euphorbiaceae, sp

Chapter 7 References

Aagaard, T. and Sorensen, P., 2013. Sea level rise and the sediment budget on an eroding barrier on the Danish North Sea coast. *In*: Conley, D.C.; Masselink, G.; Russell, P.E., and O'Hare, T.J. (eds), *Proceedings 12th International Coastal Symposium (Plymouth, England*), Journal of Coastal Research, Special Issue No 65, pp. 434-439.

Aagaard, T.; Davidson-Arnott, R.; Greenwood, B., and Nielsen, J. 2004. Sediment supply from shoreface to dunes: linking sediment transport measurements and long-term morphological evolution. *Geomorphology*, 60, 205-224.

Acevedo, E., 1971. *Atlas de Mapas Antiguos de Colombia siglos XVI a XIX*; Santafé de Bogotá: Arco, 169p.

Allen, J.; LaBash, C.L.; August, P.V., and Psuty, N.P., 2002. *Historical and Recent Shoreline Changes, Impacts of Moriches Inlet, and Relevance to Island Breaching at Fire Island National Seashore, New York*. Boston, Massachusetts, U.S. Geological Survey, Final Report to the National Park Service, Northeast Region, Boston, MA, 76 pp.

Alvarado, M., 2005. Cartagena y el plan de restauración ambiental del canal del Dique y Barranquilla y las obras de profundización del canal navegable de acceso a la zona portuaria: Visión general. *In*: Restrepo, J.D. (eds), *Los sedimentos del río Magdalena: Reflejo de la crisis ambiental*, Medellín: EAFIT, pp. 218-254.

Angulo, C., 1978. *Arqueología de la Ciénaga Grande de Santa Marta*. Santafé de Bogotá, Colombia: Fundación de Investigaciones Arqueológicas Nacionales del Banco de la República, 172p.

Backstrom, J.T.; Jackson, D.W.T., and Cooper, J.A.G., 2007. Shoreface Dynamics of Two High-Energy Beaches in Northern Ireland, *In*: Lemckert, C. (eds), *Proceedings of the 9th International Coastal Symposium (Gold Coast, Australia)*, Journal of Coastal Research, Special Issue No 50, pp. 594-598.

BaMasoud, A. and Byrne, M. L., 2013. The predictive accuracy of shoreline change rate methods in Point Pelee, Canada. *Journal of Great Lakes Research*, 39, 173-181.

Benavente, J.; del Río, L.; Menapace, W., and Plomaritis, P.A., 2013. Impact of Coastal Storms in a Sandy Barrier (Sancti Petri, Spain), *In*: Conley, D.C.; Masselink, G.; Russell, P.E., and O'Hare, T.J. *(*eds*), Proceedings 12th International Coastal Symposium (Plymouth, England*), Journal of Coastal Research, Special Issue No 65, pp. 666-671.

Bernal, G., 1996. Caracterización geomorfológica de la llanura deltáica del río Magdalena con énfasis en el sistema lagunar de la Ciénaga Grande de Santa Marta, Colombia, *Boletín de Investigaciones Marinas y Costeras-Invemar*, 25, 19-48.

Bird, E.C.F., 1985. *Coastline Changes: A Global Review*, Chichester: John Wiley & Sons., 219p.

Bishop, P., 2007. Long-term landscape evolution: linking tectonics and surface processes. *Earth Surface Processes and Landform*, 32, 329-365.

Bitton, M., 2013. Beach-Dune interactions and a new cycle of foredune evolution, Gulf County, Florida: Louisiana State University and Agricultural Mechanical College, Ph.D. Thesis, 250p.

Blanco, J.A.; Viloria, E.A., and Narváez, B., 2006. ENSO and salinity changes in the Ciénaga Grande de Santa Marta coastal lagoon, Colombian Caribbean. *Estuarine Coastal and Shelf Science*, 66, 157-167.

Boorman, L.A., 1977. Sand-dunes. *In*: Barnes, R.S.K. (ed.), *The Coastline*, England: John Wiley & Sons Ltd., pp. 161-197.

Bott, M.H.P., 1979. Subsidence Mechanisms at Passive Continental Margins. *In*: Watkins, J.S.; Montadert, L., and Wood Dickerson, P. (eds.), *Geological and Geophysical Investigations of Continental Margins*, Tulsa, Oklahoma: The American Association of Petroleum Geologists, pp. 3-9.

Campbell, C.J., 1968. The Santa Marta Wrench Fault of Colombia and its Regional Setting, In: Saunders, J.B. (ed.), *4th Caribbean Geology Conference*, pp. 247-261

Campbell, I. A. and Honsaker, J., 1982. Variability in badlands erosion; problems of scale and threshold identification. *In*: Thorn, C.E. (ed.), *Space and Time in Geomorphology*, London: George Allen and Unwin Ltd, pp. 59-79.

Clark, W.A.V. and Hosking, P.L, 1986. *Statistical Methods for Geographers*, USA: John Wiley & Sons, 518p,

Colmenares, P.; Mesa, M.; Roncancio, J.; Pedraza, P.; Contreras, A.; Cardona, A.; Silva, C.; Romero, J.; Alvarado, S.; Romero, O.; Vargas, F., and Santamaría, C., 2007. *Geología de la plancha 18*. Santafé de Bogotá, Colombia: Invemar, Ingeominas, Ecopetrol, ICP, Geosearch LTDA, scale 1:100,000, 1 sheet.

Correa, I.; Alcántara-Carrió, J, and González, D.A., 2005. Historical and Recent Shore Erosion along the Colombian Caribbean Coast. *Proceedings of the 2nd meeting in Marine Sciences (Valencia, España*), Journal of Coastal Research, Special Issue No 49, pp. 52-57.

Crawley, M.J., 2007. *The R book*, London: John Wiley & Sons, 942p.

Curray, J.R., 1964. Transgressions and Regressions. *In*: Miller, R.L. (ed.), *Papers in Marine Geology*. New York: The Macmilan Company, pp. 175-203.

Davidson-Arnott, R., 2010. *Introduction to coastal processes and* geomorphology. New York: Cambridge, 442p.

Dean, G.D. and Dalrymple, R.A., 2004. *Coastal processes with engineering applications.* New York: Cambridge, 475p.

Del Río, L. and Gracia, F. J., 2013. Error determination in the photogrammetric assessment of shoreline changes. *Natural Hazards*, 65, 2385-2397.

Delgado-Fernandez, I., 2010. *Mesoscale measuring and modeling of aeolian sediment input to coastal foredunes*: The University of Guelph, Ph.D. Thesis, 230p.

Demek, J., 1972. *Manual of Detailed Geomorphological Mapping*. Czecjoslovak: International Geographical Union Commission of Geomorphological Survey and Mapping, 344p.

Demek, J. and Embleton, C., 1978. *Guide to Medium Scale Geomorphological Mapping.* Stuttgart: International Geographical Union Commission of Geomorphological Survey and Mapping, 348p.

Dolan, R.; Hayden, P.; May, P., and May, S., 1980. The Reliability of Shoreline Change Measurements from Aerial Photographs. *Shore and Beach*, 48(4), pp. 42-49.

Donnelly, C.; Kraus, N., and Larson, M., 2006. State of Knowledge of Measurement and Modelling of Coastal Overwash. *Journal of Coastal Research,* 22(4), pp. 965-991.

Dramis, F.; Guida, D., and Cestari, A., 2011. Nature and Aims of Geomorphological Mapping. *In*: Smith, M.J.; Paolo, P., and Griffiths, J.S., *Geomorphological Mapping. Methods and Applications*, Oxford, Great Britain: Elsevier, pp. 39-73.

Duque-Caro, H., 1980. Geotectónica y evolución de la región noroccidental colombiana. *Boletín Geológico Ingeominas*, 23(3), 4-37.

Duque-Caro, H., 1979. Major Structural Elements and Evolution of Northwestern Colombia. *In*: Montadert, L. and Wood Dickerson, P. (eds), *Geological and Geophysical Investigations of Continental Margins*, Tulsa, Oklahoma: The American Association of Petroleum Geologists, pp. 329-351.

Elster, C.; Perdomo, L. and Schnetter, M.L., 1999. Impact of ecological factors on the regeneration of mangroves in the Ciénaga Grande de Santa Marta, Colombia , *Hydrobiologia,* 413, 35-46.

Emery, K.O., 1981. Stratigraphy and Structure of Pull-Appart Margins, *Geology of Continiental Margins*(Washington, D.C., AAPG), pp. B1-B20.

Ensminger, I. 1997. *Apoyo de la regeneración natural de una vegetación de manglares degradada. Repercusiones de obras hidráulicas en el Canal Clarín, Ciénaga Grande de Santa Marta, Colombia*. Eschborn, Germany: Deutsche Gesellscahft fur Techische Zusammendarbeit (GTZ), report TÖB F II/4S, 49p.

Etayo, F. 1983, *Mapa de Terrenos Geológicos de Colombia*. Santafé de Bogotá: Colombia, Publicación Geológica Especial de INGEOMINAS No14, scale 1:5,000000, 1 sheet.

FitzGerald, D. M.; Fenster, M. S.; Argow, B. A., and Buynevich, I. V., 2008. Coastal Impacts Due to Sea-Level Rise. *Annual Review of Earth and Planetary Sciences,* [Online], 38, 601-647. http://earth.annualreviews.org.

Flinch, J.F., 2003. Structural Evolution of the Sinú-Lower Magdalena Area (Northern Colombia). *In*: Bartolini, C.; Buffler, R.T., and Blickwede, J.F. (eds.), *The Circum-Gulf of Mexico and the Caribbean: Hydrocarbon Habitats, Basin Formation and Plate Tectonics*, Tulsa, Oklahoma: The American Association of Petroleum Geologists Memoir 79, pp. 141-144.

Frihy, O.E.; Lofty, M.F., and Komar, P.D., 1995. Spatial variations in heavy minerals and patterns of sediment sorting along the Nile Delta, Egypt. *Sedimentary Geology,* 97, 33-41.

García-Mora, M.R.; Gallego-Fernández, J.B., and García-Novo, F., 2000. Plant Diversity as a Suitable Tool for Coastal Dune Vulnerability Assessment. *Journal of Coastal Research,* 16(4), 990-995.

Gellert, J.F., 1972. Conception and Content of Detailed Geomorphological Maps. *In*: Demek, J. (ed.), *Manual of Detailed Geomorphological Mapping*. Czecjoslovak: International Geographical Union Commission of Geomorphological Survey and Mapping, pp. 18-37.

González, C.; Urrego, L.E.; Martínez, J.I.; Polanía, J., and Yokoyama, Y., 2010. Mangrove Dynamics in the Northwestern Caribbean since the "LIA": A History of Human and Natural Disturbances. *The Holocene,* 20(6), 849-861.

Hamed, K. H. and Ramanchandra Rao, A., 1998. A modified Mann-Kendall trend test for autocorrelated data. *Journal of Hidrology*, 204, 182-196.

Harris, R. and Jarvis, C., 2011. *Statistics for Geography and Environmental Science*, Harlow, England: Pearson, p262

Hatfield, R.G.; Cioppa, M.T., and Trenhaile, A.S., 2010. Sediment sorting and beach erosion along a coastal foreland: Magnetic measurements in Point Pelee National Park, Ontario. *Sedimentary Geology*, 231, 63-73.

Haug, G.H.; Hughen, K.A.; Sigman, D.M.; Peterson, L. C., and Röhl, U., 2001. Southward migration of the Intertropical Convergence Zone through the Holocene. *Science,* 293(5533), 1304-1308.

Heathfield, D.K. and Walker, I.J, 2011. Analysis of coastal dune dynamics, coastline position, and large woody debris at Wickaninnish Bay, Pacific Rim National Park, British Columbia . *Canadian Journal of Earth Sciences*, 48(7),1185-1198.

Heezen, B.C., 1956. Corrientes de turbidez del río Magdalena. *Boletín de la Sociedad Geográfica de Colombia,* 14(51-52), 135-143.

Hesp, P.A., 2013. Conceptual Models of the Evolution of Transgressive Dune Systems. *Geomorphology*, 199, 138-149.

Hesp, P.; Martínez, M.; Miot da Silva, G.; Rodríguez-Revelo, N.; Gutiérrez, E.; Humanes, A.; Laínez, D.; Montaño, I.; Palacios, V.; Quesada, A.; Storero, L.; González-Trilla, G., and Trochine, C., 2011. Transgressive dunefield landforms and vegetation associations, Doña Juana, Veracruz, Mexico. *Earth Surface Processes and Landforms*, 36, 285-295.

Hesp, P.A., 1981. The Formation of Shadow Dunes. *Journal of Sedimentary Petrology*, 51(1), 101-111.

Hesp, P.A.; Dillenburg, S.R.; Barboza, E.G.; Tomazelli, L.J.; Ayup-Zouain, N.P.; Esteves, L.S.; Gruver, N.L.S.; Toldo, E.E; Tabajara, L.L.C., and Clerot, L.C.P., 2005. Beach ridges, foredunes or transgressive dunefields? Definitions and an examination of the Torres to Tramandair barrier system, southern Brazil. *Annals of the Brazilian Academy of Sciences*, 77(3), 493-508.

Hutton, J., 1970. Theory of the Earth. *In*: White, G.W. (ed.), *Contributions to the History of Geology Volume 5*. Darien, Connecticut: Hafner Publishing Company, pp. 33-131.

Hydrographic Office of the United Kingdom's Royal Navy, 1944. *Cabo de San Juan de Guia to Punta Galera, Charts of 1938*. London:, scale 1:200,000, 1 sheet. Original edition, United States Government Charts, 1938.

Idárraga-García, J, 2008. Actividad neotectónica en tres sectores del sistema de fallas de Santa Marta, piedemomente occidental de la Sierra Nevada de Santa Marta. Medellín, Colombia: Universidad EAFIT, Master's thesis, 133p.

Idárraga-García, J. and Romero, J., 2010. Neotectonic Study of the Santa Marta Fault System, Western foothills of the Sierra Nevada de Santa Marta, Colombia. *Journal of South American Earth Sciences*, 29, 849-860.

Inman, D.L. and Dolan, L., 1989. The Outher Banks of North Carolina: budget of sediment and inlet dynamic along a Migrating Barrier System. *Journal of Coastal Research*, 5(2), 193-237.

International Hydrographic Organization, 2008. *IHO Standards for Hydrographic Surveys*. Monaco: International Hydrographic Bureau, 27p.

Instituto Geográfico Agustín Codazzi, 1977. *Plano topográfico del río de la Magdalena*. Santafé de Bogotá, Colombia: Atlas de Colombia. Original Edition Unknown, 1803.

Jewell, S.A.; Walker, D.J., and Fortunato, A.B., 2012. Tidal asymmetry in a coastal lagoon subject to a mixed tidal regime. *Geomorphology*, 138, 171-180.

Kellogg, J.N.; Godley, V.M.; Ropain, C., and Bermudez, A., 1983. Gravity anomalies and tectonic evolution of northwestern South America. *In*: Duque-Caro, H. (ed.), *10th Caribbean Geological Conference* (Cartagena, Colombia), pp. 18-31

Laslett, G.M., 1994. Kriging and Splines: An empirical comparison of Their Predictive Performance in Some Applications. *Journal of the American Association,* 89(426), 406-409.

Longobardi, A. and Villani, P., 2009. Trend analysis of annual and seasonal rainfall time series in the Mediterranean area [Online]. *International Journal of Climatology*. DOI: 10.1002/joc.2001.

Losada, I.J.; Reguero, B.G.; Méndez, F.J.; Castanedos, S.; Abuscal, A. J., and Mínguez, R., 2013. Long-term changes in sea-level components in Latin America and the Caribbean. *Global and Planetary Change,* 104, 34-50.

Martínez, J.O.; González, L.; Pilkey, H., and Neal, W.J., 2000. Barrier island evolution on the subsiding Central Pacific Coast, Colombia, S.A. *Journal of Coastal Research,* 16(3), 663-674.

Masselink, G.; Hughes, M.G., and Knight, J., 2011. *Coastal Processes & Geomorphology*, London: Hodder Education, 416p.

Maun, M.A., 2009. *The biology of coastal sand dunes.* New York: Oxford, 265p.

McCurdy, P.G., 1947. *Manual of Coastal Delineation from Aerial Photographs*. Hydrographic Office U.S. Navy, Washington D.C., 143p.

Mckee, K.; Cahoon, D.R., and Feller, I.C., 2007. Caribbean mangroves adjust to rising sea levels through biotic controls on change in soil elevation. *Global Ecology and Biogeography*, 16, 545-556.

McKenney Black and Steward Engineers, 1921. *The Boca de Ceniza and Magdalena River to Barranquilla, Colombia, South America: Report and Recommendations*, Washinghton: McKenney Black and Steward Engineers, 22p.

Medina, E.; Cram, W.J.; Lee, H.S.J.; Lüttge, U.; Popp, M., Smith, J.A.C., and Diaz, M., 1989. Ecophysiology of xerophytic and halophytic vegetation in a coastal alluvial plain in northern Venezuela, I: site description and plant communities. *New Phytologist*, 111, 233-243.

Milliman, J.D. and Haq, B.U. Sea-Level Rise and Coastal Subsidence-Towards Meaningful Strategies. *In*: Milliman, J.D. and Haq, B.U. (eds) *Sea-level Rise and Coastal Subsidence*. the Netherlands: Kluwer Academic Publishers, pp 1-9.

Milne, F. D.; Don, P., and Davidson, M., 2012. Natural Variability and Anthropogenic Effects on the Morphodynamics of a Beach-Dune System at Montrose Bay, Scotland. *Journal of Coastal Research*, 28(2), 375-388.

Miot da Silva, G; Martinho, C. T.; Hesp, P.; Keim, B. D., and Ferligoj, Y., 2013. Changes in dunefield geomorphology and vegetation cover as a response to local and regional climate variations. *In*: Conley, D.C.; Masselink, G.; Russell, P.E., and O'Hare, T.J. (eds.), *Proceedings 12th International Coastal Symposium (Plymouth, England*), Journal of Coastal Research, Special Issue No 65, pp 1307-1312

Miot da Silva, G. and Hesp, P., 2013. Increasing Rainfall, Decreasing Winds, and Historical Changes in Santa Catarina Dunefields, Southern Brazil. *Earth Surface Processes and Landforms*, 38,1036-1045.

Moore, L.J., 2000. Shoreline Mapping Techniques. *Journal of Coastal Research*, 16(1), 111-124.

Múnera, J.C.; Velez, J.; Poveda, G.; Posada, J.; Montoya, J.D., and Cardona, J.M., 2005. Dinámica Hidrológica de la Ciénaga Grande de Santa Marta. *Avances en Recursos Hidráulicos*, 10, 47-62.

Murray-Wallace, C.V. and Woodroffe, C.D., 2014. *Quaternary Sea-Level Changes. A global Perspective*. New York: Cambridge University Press, 484p.

National Oceanic and Atmospheric Administration, *SOI Index 2012*. http://www.esrl.noaa.gov/psd/data/correlation/soi.data.

Nickling, W. G. and Neuman, C. M., 1999. Recent investigations of airflow and sediment transport over desert dunes. *In*: Goudie, A. S.; Livingstone, I., and Stokes, S. (eds.), *Aeolian environments, Sediments and Landforms*, New York: John Wiley & Sons, pp. 15-47.

Nordstrom, K.F., 2008. *Beach and Dune Restoration.* Cambridge, United Kingdom: Cambridge University Press, 187p.

Numedal, D., 1982. River Delta Morphodynamics. *In*: Numedal G. (ed.), *Deltaic Sedimentation on the Louisiana Coast*, Louisiana: Society of Economic Paleontologists and Mineralogists, pp. 71-91.

Ojeda, J.; Vallejo, I., and Malvarez, G.C., 2005. Morphometric evolution of the active dune system of the Doñana National Park (1977-1998), Southern Spain. *Journal of Coastal Research*, Special Issue 49, pp. 40-45.

Ordóñez, C.I., 2008. Controle Neotectonico do Diapirismo de Lama na Regiao de Cartagena, Colombia. Brazil: Universidad Federal Fluminense, Master's thesis, 201p.

Ortiz, J.C.; Salcedo, V., and Otero, L.J., 2014. Investigating the Collapse of the Puerto Colombia Pier (Colombian Caribbean Coast) in March 2009: Methodology for the reconstruction of Extreme Events and the Evaluation of their Impact on the Coastal Infraestrcture. *Journal of Coastal Research*, 30(2), 291-300.

Pabón, J.D, 2012. Cambio climático en Colombia: tendencias en la segunda mitad del siglo XX y escenarios posibles para el siglo XXI. *Revista Academia Colombiana de Ciencias,* 36(139), 261-278.

Paris, G.; Machette, M.N.; Dart, R.L., and Haller, K.M., 2000. *Maps and Database of Quaternary Folds and Faults in Colombia and its Offshore Regions*. Denver, Colorado: U.S. Geological Survey, Open-File Report 00-0284, 61p.

Penland, S. and Boyd, R., 1982. Mississippi Delta Barrier Systems: An Overview. *In*: Numedal G. (ed.), *Deltaic Sedimentation on the Louisiana Coast*, Louisiana: Society of Economic Paleontologists and Mineralogists, pp. 71-91.

Pethick, J., 1988. *An Introduction to Coastal Geomorphology*. London: Edward Arnold, 260p.

Pfeffer, W.T.; Harper, J.T., and O'neel, S., 2008. Kinematic Constraints on Glacier Contributions to 21st-Century Sea-Level Rise. *Science*, 321(5894), 1340-1342.

Pilkey, O. H. and Cooper, J.A., 2005. Society and Sea Level Rise. *Science*, 303(5665), 1781 1782.

Pilkey, O.H. and Fraser, M.E., 2003. *A Celebration of the World's Barrier Islands.* New York: Columbia University Press, 309p.

Pilkey, O.H.; Neal, W.J.; Webb, C.A.; Bush, D.M.; Pilkey, D.F.; Bullock, J., and Cowan, B.A. 1998. *The North Carolina Shore and Its Barrier Islands. Restless Ribbons of Sand*. Durham, North Carolina: Duke University Press, 318p.

Poveda, G. and Mesa, O.J., 1997. Feedback between hydrological processes in tropical South America and large-scale ocean-atmospheric phenomena. *Journal of Climate* 10, 2690-2702.

Raasveldt, H.C. and Tomic, A., 1958. Lagunas colombianas. *Revista Academia Colombiana de Ciencias Exactas, Físicas y Naturales,* 10(40), 16-198.

Restrepo, J.D. and López, S., 2008. Morphodynamics of the Pacific and Caribbean deltas of Colombia, South America. *Journal of South American Earth Sciences,* 25, 1-21.

Restrepo, J.D. and Kjerfve, B., 2000. Magdalena River: Interannual variability (1975-1995) and revised water discharge and sediment load estimates. *Journal of Hydrology,* 235, 137-149.

Restrepo, J.D.; Kjerfve, B.; Hermelin, M., and Restrepo, J.C., 2006. Factors controlling sediment yield in a major South America drainage basin: the Magdalena River, Colombia. *Journal of Hydrology*, 316, 213-232.

Richling, A., 1999. On the Universal Natural Unit. *In*: Moss, M.R. and Milne, R.J (eds.), *Landscape Synthesis Concepts and Applications*. Warsaw, Poland: University of Guelph and University of Warsaw, pp. 67-81.

Rico, E., 1967. *Las obras de Bocas de Ceniza*. Barranquilla: Colpuertos, 100p.

Robertson, K. and Martínez, N., 1999. Cambios del Nivel del Mar Durante el Holoceno en el Litoral Caribe Colombiano. *Cuadernos de Geografía,* 8(1), 168-198.

Sallenger, A.H., 2000. Storm Impact Scale for Barrier Islands. *Journal of Coastal Research*, 16(3), 890-895.

Shepard, F.P., 1973. Sea Floor Off Magdalena Delta and Santa Marta Area, Colombia. *Geological Society of America Bulletin,* 83, 1955-1972.

Shepard, F.P. and Dill, R.F., 1966. *Submarine Canyons and Other Sea Valleys.* Chicago*:* Rand Mc.Nally & Company, 381p.

Smith, J.M., 2011. Digital Mapping: Visualization, Interpretation and Quantification of Landforms. *In*: Smith, J.M.; Paron; P., and Griffiths, J.S. (eds.), *Geomorphological mapping methods and applications*. Great Britain: Elsevier, pp. 225-251.

Stutz, M.L. and Pilkey, O.R., 2011. Open Oceanic Barrier Islands: Global Influence of Climatic, Oceanographic, and Depositional Settings. *Journal of Coastal Research,* 27(2), 207-222.

Swales, A., 2002. Geostatistical Estimation of Short-Term Changes in Morphology and Sand Budget. *Journal of Coastal Research,* 18(2), 338-351.

Taboada, A.; Rivera, L.A.; Fuenzalida, A.; Cisternas, A.; Philip, H.; Bijwaa, H.; Olaya, J., and Rivera, C., 2000. Geodynamics of the northern Andes' subductions and intracontinental deformation (Colombia). *Tectonics,* 19(5), 787-813.

Tavera, H.A. and Gamba, N.J., 2001. Caracterización de la vegetación de la vía Parque Isla Salamanca. Magdalena, Colombia. Santafé de Bogotá, Colombia: Universidad Distrital Francisco José de Caldas, Bachelor's Thesis, 310p.

Thieler, E.R.; Martin, D, and Ergul, A., 2003. *The Digital Shoreline Analysis System, Version 2.0: Shoreline Change Measurement Software Extension for ArcView*. Woods Hole, Massachusetts: U.S. Geological Survey Open-File Report 03-076.

Thieler, R.E.; O'connell, J.F., and Schupp, C.A., 2001. *The Massachusetts Shoreline Change Project: 1800s to 1994*. Massachusetts: U.S. Geological Survey, 60p. http://www.mass.gov/czm.

Timmons, E. A.; Rodriguez, A. B.; Mattheus, C. R., and DeWitt, R., 2010. Transition of a regressive to a transgressive barrier island due to back-barrier erosion, increased storminess, and low sediment supply: Bogue Banks, North Carolina, USA. *Marine Geology,* 278, 100-114.

Tinley, K.L., 1985. *Coastal Dunes of South Africa*. Pretoria, South Africa: South African National Scientific Programmes, *Report No 109*, 300p.

Urbano, C.P.; Otero, L.J., and Lonin, S., 2013. Influencia de las corrientes en los campos de oleaje en el área de Bocas de Ceniza, Caribe Colombiano. *Boletín Científico CIOH*, 31, 191-206.

Van Zuidam, R.A., 1986. *Aerial photo-interpretation in terrain analysis and geomorphologic mapping.* The Hague: Smits Publishers, 442p.

Vernette, G., 1986. *La platerforme continentale de Colombie (di debouche du Magdalena au Golfe de Morrosquillo). Importance du diapirisme argileaux sur la morphologie e la sédimentation*. Bordeaux, France: Memoires del' Insitut de geologie du bassin d' Aquitaine No 20, 387p.

Villegas, B.; Sesana, L., and Dromgold, M., 2006. *Colombia Natural Parks*. Santafé de Bogotá, Colombia: Villegas Editores, 447p.

Vinnels, J.M.; Butler, R.W.H.; McCaffrey, W.D., and Patton, D.A., 2010. Depositional Processes across the Sinú Accretionary Prism, Offshore Colombia. *Marine and Petroleum Geology*, 27, 794-809.

Von Erffa, A.F., 1972. Sedimentation, transport und erosion an der nordkuste kolumbiens zwischen Barranquilla und der Sierra Nevada de Santa Marta, Berlin: Justus Liebig University.

Walford, N., 2011. *Practical Statistics for Geographers and Earth Scientists*. Singapore: John Wiley & Sons Ltd, 416p.

Walker, I.J.; Eamer, J.B.R., and Darke, I., 2013. Assessing significance geomorphic changes and effectiveness of dynamic restoration in a coastal dune ecosystem. *Geomorphology*, 199, 192-204.

Wiedemann, H.U., 1973. Reconnaissance of the Ciénaga Grande de Santa Marta, Colombia: Physical Paremetres and Geologic History. *Boletín de Investigaciones Marinas y Costeras-Invemar,* 7, 85-119.

Woodroffe, C.D., 2003. *Coasts: Form, Process, and Evolution*. Cambridge: University Press, 623p.

Wu, J., 1999. Hierarchy and Scaling: Extrapolating Information along a scaling ladder. *Canadian Journal of Remote Sensing*, 25, 367-380.

Zhang, C.; Douglas, B., and Leatherman, S., 2004. Global Warming and Coastal Erosion. *Climatic Change*, 64, 41-58.